

Task 4.1.2

Future evolution of the
geological and geohydrological
properties of the geosphere

Radioactive substances and ionizing radiation are used in medicine, industry, agriculture, research, education and electricity production. This generates radioactive waste. In the Netherlands, this waste is collected, treated and stored by COVRA (Centrale Organisatie Voor Radioactief Afval). After interim storage for a period of at least 100 years radioactive waste is intended for disposal. There is a world-wide scientific and technical consensus that geological disposal represents the safest long-term option for radioactive waste. Geological disposal is emplacement of radioactive waste in deep underground formations. The goal of geological disposal is long-term isolation of radioactive waste from our living environment in order to avoid exposure of future generations to ionising radiation from the waste. OPERA (OnderzoeksProgramma Eindberging Radioactief Afval) is the Dutch research programme on geological disposal of radioactive waste. Within OPERA, researchers of different organisations in different areas of expertise will cooperate on the initial, conditional Safety Cases for the host rocks Boom Clay and Zechstein rock salt. As the radioactive waste disposal process in the Netherlands is at an early, conceptual phase and the previous research programme has ended more than a decade ago, in OPERA a first preliminary or initial safety case will be developed to structure the research necessary for the eventual development of a repository in the Netherlands. The safety case is conditional since only the long-term safety of a generic repository will be assessed. OPERA is financed by the Dutch Ministry of Economic Affairs and the public limited liability company Electriciteits-Produktiemaatschappij Zuid-Nederland (EPZ) and coordinated by COVRA. Further details on OPERA and its outcomes can be accessed at www.covra.nl.

This report concerns a study conducted in the framework of OPERA. The conclusions and viewpoints presented in the report are those of the author(s). COVRA may draw modified conclusions, based on additional literature sources and expert opinions. A .pdf version of this document can be downloaded from www.covra.nl

OPERA-PU-TNO412

Title: Future evolution of the geological and geohydrological properties of the geosphere

Authors: Johan ten Veen (TNO)

Contributors: Joan Govaerts (SCK-CEN), Koen Beerten (SCK-CEN), Dario Ventra (TNO), Geert-Jan Vis (TNO)

Date of publication: 17-07-2015

Keywords: future evolution, driving forces, processes, effects, Boom Clay
predictive modeling, long-term safety assessment



Summary	7
Samenvatting	7
1. Introduction	9
1.1. Background	9
1.1.1. Isolation	9
1.1.2. Delay & attenuation of the releases	9
1.1.3. Engineered containment	10
1.2. Objectives	10
1.3. Realization	11
1.4. Explanation of contents	11
2. Driving forces	13
2.1. Introduction	13
2.2. Future Climate	14
2.2.1. Climate change mechanisms and timescales (BIOCLIM)	14
2.2.2. The role of climate change	15
2.2.3. Understanding past climate change	16
2.2.4. Predicting future climate change	17
2.2.1. Possible future climate types	18
2.2.2. Present-day Temperate Climate	20
2.2.3. Boreal climate - Dfc - ZB VIII	22
2.2.4. Periglacial - ZB IX - ET	23
2.2.5. Glacial - EF	25
2.2.6. Mediterranean, warm/dry summer climate - Csb	26
2.3. Future Tectonic processes	28
2.3.1. Origin of tectonic movements	28
2.3.2. The role of tectonics	28
2.3.3. Prediction of tectonic movements	29
CLIMATE SECTION	31
3. Glacial erosion and -deformation processes	33
3.1. Introduction	33
3.2. Current state of knowledge	33
3.3. Physical erosion and sediment production by ice sheets	34
3.3.1. Landscape analyses	35
3.3.2. Sediment fluxes	36
3.3.3. Stratigraphic analysis	37
3.4. Glaciotectonic structures	38
3.4.1. Origin	38
3.4.2. Classification	38
3.4.3. Depth of deformation	38
3.5. Tunnel valleys: generalities and erosive potential	39
3.6. Discussion	42
3.6.1. Depth of the Boom Clay	42
3.6.2. Erosion potential	42
3.7. Relevance and synthesis for the safety case:	44
4. Effects of glacial loading and unloading	45
4.1. Coupled mechanical-hydraulic effects	45
4.1.1. Isostasy vs. hydrology	47
4.2. Seismicity during deglaciation	48
4.2.1. Deglaciation effects below ice sheets	48
4.2.2. Far field effects	50
4.3. Assessment of glacio isostasy and -seismicity in the Netherlands	51
4.4. Summary of Dutch ice cover scenarios	52

4.4.1.	Ice sheet extent	52
4.4.2.	Ice sheet thickness	53
4.5.	Relevance and synthesis for the safety case.....	55
5.	Permafrost	57
5.1.	Literature study on permafrost in NW Europe during the last ice age	57
5.1.1.	Motivation	57
5.1.2.	New data on the stability of permafrost in Europe.....	57
5.1.3.	Comparison of permafrost depth modeling results for NW Europe.....	60
5.1.4.	Implications for potential geological waste repositories in Belgium and the Netherlands	60
5.2.	Assessment of input parameters for Permafrost modeling	60
5.2.1.	Porosity prediction	60
5.2.1.	Thermal parameters	61
5.2.2.	Area selection and data delivery.....	63
5.3.	Permafrost depth modeling	65
5.3.1.	Results	65
5.3.2.	Comparison with Boom Clay depth.....	65
5.1.	Relevance and synthesis for the safety case:.....	67
6.	Accommodation changes (sea level vs. supply).....	69
6.1.	Periodicities of global sealevel change	69
6.2.	Waterdepth change effects	69
6.3.	Water loading effects	70
6.4.	Interplay between eustatic sea-level change and sediment budget	71
6.5.	Relevance and synthesis for the safety case:.....	74
	GEOLOGY SECTION.....	75
7.	Effects of seismicity and faulting	77
7.1.	First assessment of effects	77
7.2.	Relevance and synthesis for the safety case:.....	77
8.	Salt tectonics	79
8.1.	Introduction.....	79
8.2.	Ice-sheet loading and salt structures	79
8.3.	Quantifying growth rates from Dutch subsurface data	81
8.3.1.	Average external growth rate	81
8.3.1.	Average internal growth rate	81
8.4.	Suggestion for alternative approach to estimate salt induced uplift.....	82
8.5.	Relevance and synthesis for the safety case.....	83
9.	Compaction and subsidence	85
9.1.	Introduction.....	85
9.2.	Relevance and synthesis for the safety case:.....	86
10.	Fluid migration pathways.....	87
10.1.	Introduction	87
10.2.	Shallow gas accumulations.....	87
10.3.	Seabed pockmarks	89
10.4.	Acoustic Chimneys	91
10.5.	Combination of explosive methane venting and deglaciation	92
10.6.	Relevance and synthesis for the safety case:	93
11.	Combined scenarios - a synthesis	95
11.1.	Introduction.....	95
11.2.	Periglacial conditions.....	95
11.2.1.	Sea-level change	95
11.2.2.	Sediment budget.....	95
11.2.3.	Glaciotectonic effects	96
11.2.4.	Permafrost	96
11.2.5.	Hydrogeological and geochemical changes	96

11.2.6.	Scenario synthesis	96
11.3.	Glacial conditions	97
11.3.1.	Sea level	97
11.3.2.	Sediment budget.....	97
11.3.3.	Glaciotectonic effects	97
11.3.4.	Glaciotectonic deformation and erosion	97
11.4.	Present Temperate - Interglacial conditions	98
11.4.1.	Sea level (change)	98
11.4.2.	Glaciotectonic effects	98
11.4.3.	Sediment budget.....	98
11.5.	Global warming related sea-level rise - Mediterranean type	98
11.5.1.	Sea level	98
11.5.1.	Sediment budget.....	99
11.5.2.	Glaciotectonic effects	100
11.6.	Boreal Climate.....	100
11.6.1.	Sea level	100
11.6.2.	Sediment budget.....	100
11.6.3.	Glaciotectonic effects	100
12.	Concluding Remarks.....	101
13.	Recommendations	103
14.	Acknowledgements	105
15.	References.....	107
Appendix 1	116

|

Summary

This report describes how geological and geohydrological properties of the geosphere are controlled by earth's processes over a time span of 1 million years. In particular it was studied how these processes might affect the long-term safety assessment of radioactive waste disposal facilities in the Boom Clay in the Netherlands. This study focuses on the processes that are instigated by two natural driving forces - tectonics and climate - whereas human activity is regarded a modulator of both forces. This report is based on the huge number of previous studies that address the effects of single processes, either in academic- or applied context (radioactive waste disposal, CO₂ and/or gas storage, hydrocarbon exploration). Emphasize, however, lies on the interaction of geological and geohydrological future processes by defining five future scenarios that are significantly driven by the predicted climate evolution. These scenarios range from a warmer Mediterranean climate setting with higher sea-level to a glacial setting where the Netherlands are ice-covered and sea-level is comparably low. For all scenarios it is shown that the physical isolation of radioactive waste containment only locally affects the Boom Clay. Most future processes mainly affect the transport of radionuclides through the Boom Clay and overlying sediments due to changing vertical or horizontal stress conditions that affect fluid flow conditions. The boundary conditions for the future scenarios under which these postulated future changes will occur serve as input for further research questions including hydrological modeling.

Samenvatting

Dit rapport geeft een overzicht van het verloop van aardse processen over een tijdspanne van een miljoen jaar. In het bijzonder wordt beschouwd hoe deze processen de veiligheid van opslag van radioactief afval in de Boomse Klei in Nederland beïnvloeden. Dit onderzoek richt zich op de processen die gerelateerd zijn aan de twee natuurlijke krachten, tektoniek en klimaat, terwijl menselijke invloed wordt beschouwd als een modulator van de eerste twee. Dit rapport verwijst naar het grote aantal studies van individuele processen, hetzij in academische dan wel toegepast-wetenschappelijke context (radioactief afval berging, CO₂ en / of opslag van gas, hydrocarbon exploratie), maar tracht deze niet te verbeteren. Daarentegen ligt de nadruk op de interactie van geologische en geohydrologische toekomstige processen door het definiëren van vijf toekomstscenario's die voornamelijk bepaald worden door toekomstige klimaat verandering. Deze scenario's variëren van een warmer Mediterraan klimaat en met een hogere zeespiegel en bijbehorende landvorm tot een glaciële klimaat waarbij de zeespiegel extreem is verlaagd en Nederland met ijs is bedekt. Voor alle scenario's blijkt dat de fysieke isolatie van de Boomse Klei (en het mogelijk opgeslagen radioactief afval) alleen lokaal beïnvloed wordt daar waar begravingstoepte te gering is. De meeste toekomstige processen hebben vooral invloed op het transport van radionucliden door de Boomse Klei en de bovenliggende sedimenten door middel van veranderingen in de verticale of horizontale stresscondities en de daarmee gepaard gaande vloeistofstromingen. De randvoorwaarden voor de toekomstscenario's waaronder deze gepostuleerde toekomstige veranderingen zullen optreden dienen als input voor verder onderzoek, waaronder hydrologische modelering.

1. Introduction

1.1. Background

The five-year research programme for the geological disposal of radioactive waste - OPERA- started on 7 July 2011 with an open invitation for research proposals. In these proposals, research was proposed for the tasks described in the OPERA Research Plan. In this report, the results of the research task 4.1.2 - *Future evolution of the geological and geohydrological properties of the geosphere* - are described. The main aim of this study was to describe how geological and geohydrological properties of the geosphere are controlled by various earth forming processes over a time span of 1 million years, and particularly how this might affect the long-term safety functions of radioactive waste disposal facilities in the Boom Clay^a in the Netherlands.

The safety functions isolation, delay & attenuation of the releases, and engineered containment are defined in report NIRON-TR-2009-12E - *The Long-term Safety strategy for the geological disposal of radioactive waste*. The safety functions provided by the Boom Clay and other components of the disposal system and by the geological coverage, together with the time frames over which they are expected to be fulfilled, are illustrated in Figure 1-1 and described below.

1.1.1. Isolation

The Boom Clay and its geological coverage provide the safety function of isolation. Because of the stability and thickness of the geological coverage, the radioactive waste and the repository as a whole will remain well-isolated from the biosphere for a period extending into the far future. Commonly, 1 million years is taken as the time frame to be covered by modeling in many recent safety assessments. Furthermore, the repository is located far enough from underground areas of mineral resources to reduce the likelihood of inadvertent human intrusion, and the self-sealing capacity of the Boom Clay contributes to reducing the possible consequences of such intrusions.

1.1.2. Delay & attenuation of the releases

The host formation, together with the engineered components of the disposal system and the waste forms is considered to have low hydraulic conductivity and low hydraulic gradient and a high fixation capacity for radionuclides and other contaminants. It also performs the function of delay & attenuation of the releases of category C waste following a period of engineered containment by the supercontainers. This safety function is again expected to be performed into the far future, because of the stability of the physical and chemical properties of the host formation; the properties of the Boom Clay limit the water flow, ensuring a diffusion dominated transport, and are expected to be effective in retarding and spreading in time the migration of radionuclides and other contaminants within the system for a prolonged period. According to current understanding, any contaminants released from the repository will be contained virtually completely within the Boom Clay for a period of at least several tens of thousands of years, and the many contaminants that are subject to significant geochemical retardation will be contained even longer.

^a Throughout this report the term Boom Clay is often used. However, Boom Clay is not an official stratigraphic unit in the Netherlands where it is referred to as the Rupel Clay Member. The latter is, together with the Rupel Sand Member, part of the Rupel Formation.

1.1.3. Engineered containment

The safety function ‘engineered containment’ describes the isolation of the radionuclides from their immediate environment (i.e. water) by the waste container (supercontainer). According to the safety strategy chosen in the disposal concept, the design should ensure that this function applies throughout the thermal phase. The buffered physicochemical environment of the repository – the Boom Clay – also provides stable and predictable conditions for the disposed wastes and the engineered repository components. Furthermore, the emphasis on the geological setting in the safety concept also reduces the safety-relevance of some of the uncertainties in the characteristics and evolution of the engineered repository components, including implementation procedures (for example, uncertainties in sorption coefficients for backfill material and non-centered emplacement of supercontainers). Quality assurance procedures will nevertheless be implemented for the manufacture and emplacement of engineered components, in order to ensure, as far as possible, that they are implemented according to design specifications, thus avoiding or reducing potential uncertainties. Some engineered repository components are also intentionally “over-designed”, so as to provide robustness in the event, for example, that degradation processes affecting these components are more rapid than expected. Thus, for example, the expected containment period provided by the supercontainer in the current design extends significantly beyond the thermal phase.

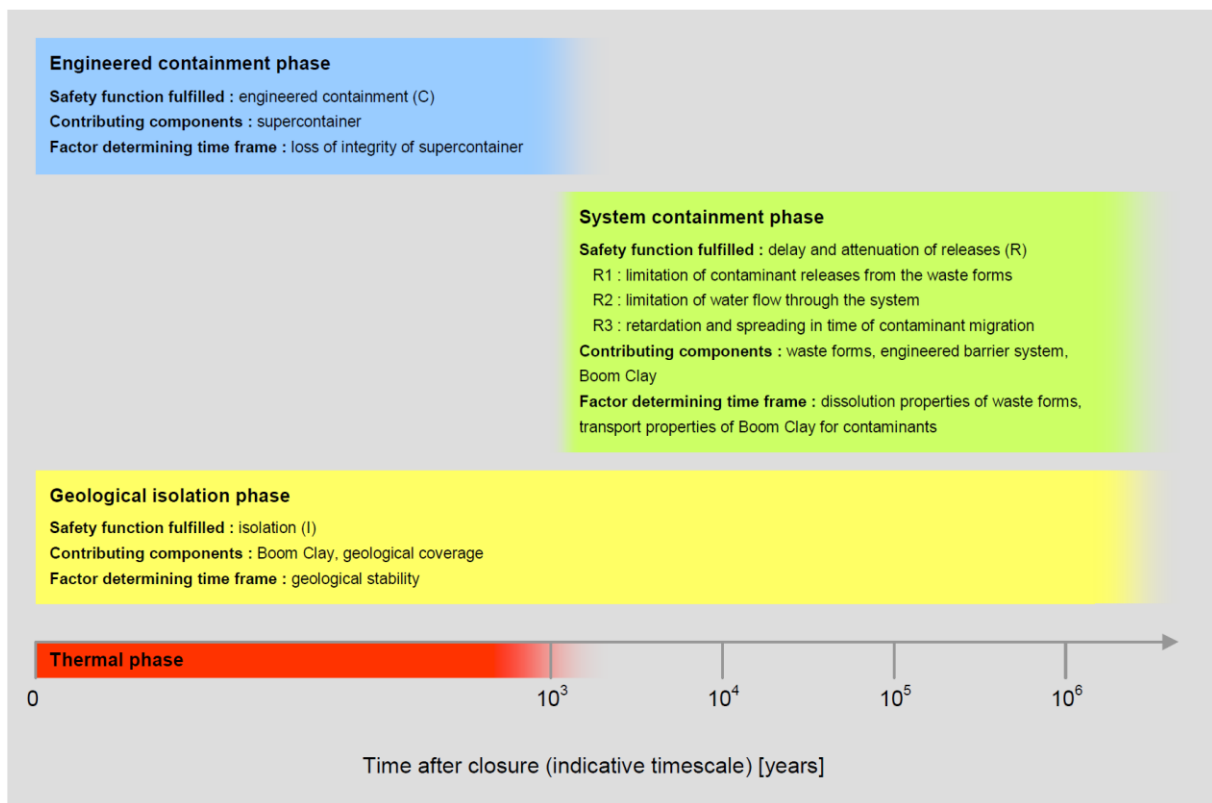


Figure 1-1 Safety functions provided by the main components of the disposal system in Boom Clay and its geological coverage and the time frames over which they are expected to be fulfilled. The engineered containment phase is specific to heat-generating waste (category C waste, that is, vitrified high-level waste and spent fuel).

1.2. Objectives

This research focuses on the three main driving forces, i.e. geology, climate and human activity, and describes their future evolution by assessing the complex interaction of processes and ensuing effects on geological and geohydrological processes. Rather than

focusing on individual processes, which are thoroughly addressed in a large number of studies over the past three decades, this study attempts to cope with the complex interaction of processes by presenting a description of several possible future evolution scenarios. For each scenario an indication of individual and/or combined effects is given that should serve as the basis for defining boundary conditions for geohydrological modeling exercises and test-scenarios for radioactive waste storage. Key in this assessment is the question whether or not these effects and processes are relevant with respect to the safety functions.

1.3. Realization

This study is a multidisciplinary study in nature and presents an overview of well-documented (state-of-the-art), though conceptual, scenarios that are based on workshops, literature studies and predictive modeling of climatic evolution. This, finally, results in a summary of all possible future scenarios (qualitative) with clear indication of possible ranges (semi-quantitative) that should serve as the basis for defining boundary conditions for geohydrological modeling exercises and test-scenarios for radioactive waste disposal. The largest part of the presented research is based on literature studies performed by TNO and SCK-CEN. Model simulations for future permafrost development are performed by SCK-CEN, based on input data provided by TNO.

1.4. Explanation of contents

This report is divided in three sections. The first section describes the three main driving forces acting within the geosphere: tectonics, climate and human activity. In the second section, potential geological and geohydrological processes that are affected by or follow from changes in the driving forces are described independently. With each process, the plausible effects on the safety functions 'isolation', 'delay & attenuation', and 'engineered containment' of a possible geological disposal facility in the Boom Clay are described. The interrelationship of many of these processes is dealt with in the synthesis section that proposes five scenarios for the future evolution and summarizes the stress on safety functions for the particular scenario.

2. Driving forces

2.1. Introduction

In establishing a safety-case for the Boom Clay Formation as geo-repository for radioactive waste, an assessment is needed of geological and geomorphological boundary conditions which would influence the formation's mechanical and compositional integrity in the long-term (~1 Myr). Three external driving forces capture the main processes that will be relevant for the future evolution of the geological and geohydrological properties of the geosphere: Climate, Geology and Human actions. "Climate" describes processes that ensue from projected future changes in climatic conditions, whereas, "Geology" mainly concerns (plate) tectonic processes. It should be noted that some processes and sub processes may evolve from more than one of the steering features (e.g. sea-level change). Also, processes ensuing from one steering feature may induce other processes (e.g. uplift or subsidence in relations to ice-sheet loading). Although the effects of "Human" activities might be manifold, in this report the focus will be on human influences on future climate and will therefore be incorporated in the "Climate" section of this report. Induced seismicity is integrated with the "Geology" processes. The processes acting under a certain future change in driving forces mainly have hydrological or hydrogeological.

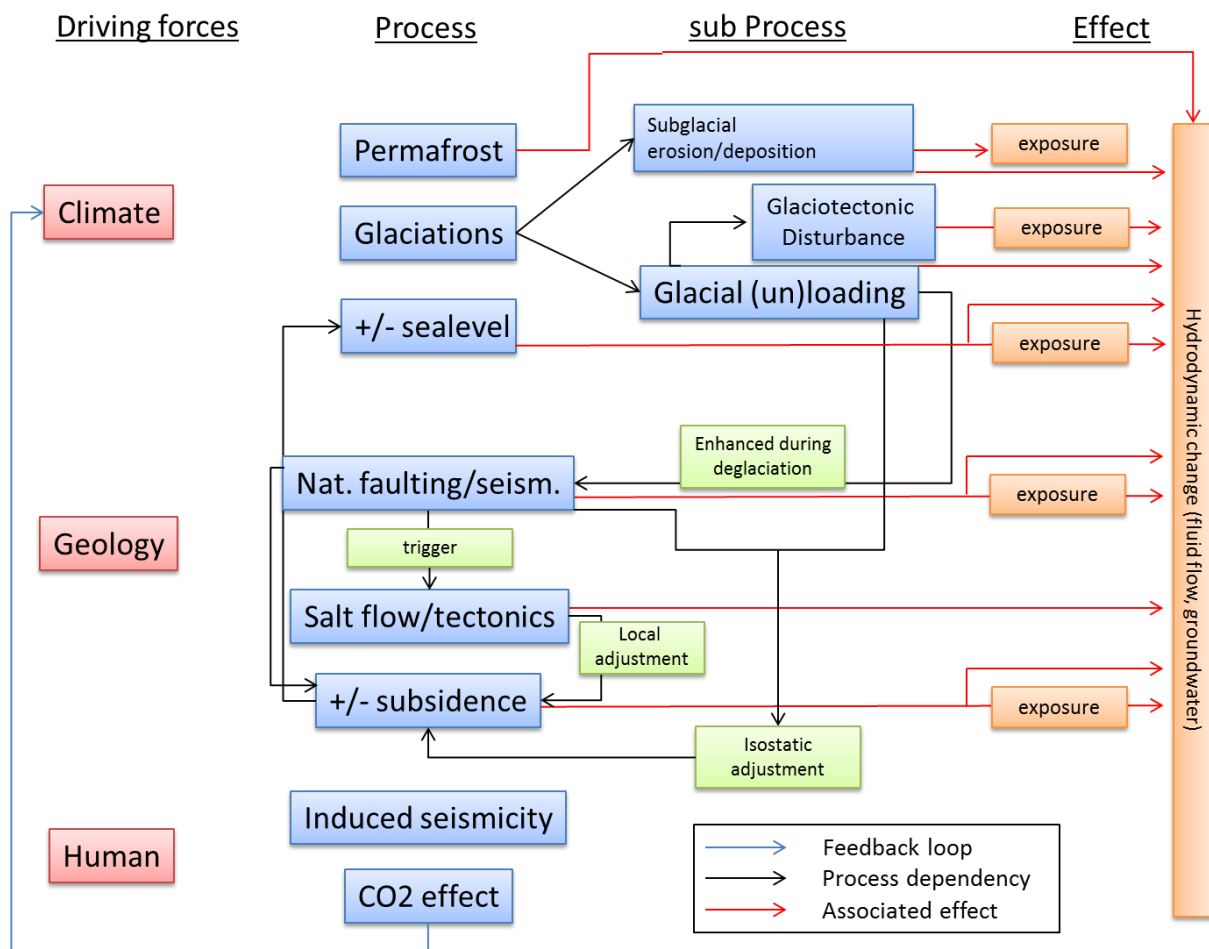


Figure 2-1 Relationships between steering features (sub) processes and effects.

2.2. Future Climate

2.2.1. Climate change mechanisms and timescales (BIOCLIM)

Climate changes on a wide variety of spatial and temporal scales and is affected by many mechanisms that operate on timescales of up to, and beyond one million years.

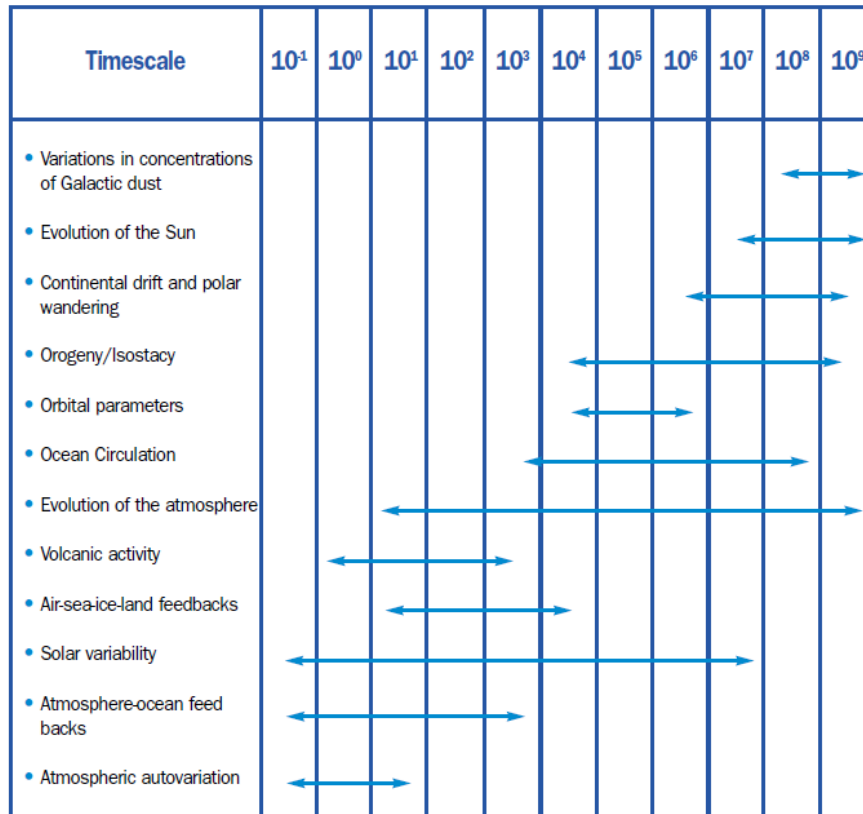


Figure 2-2 Characteristic Timescales of Factors Affecting Climate Change (modified from BIOCLIM, 2001).

As depicted in Figure 2-2, climate change mechanisms operate over four main timescales up to 1 million years:

Less than 10 years: On this scale, mainly astronomical variations in irradiance and atmospheric autovariation drive the annual and seasonal variations in climate that will lead to regionally limited episodes of higher temperatures or heavy run-off of precipitation and consequently influence hydrological recharge and discharge.

10 to 1000 years: Modifications of the solar constant and in the composition of the atmosphere (thermic pollution, greenhouse gases, aerosols), atmospheric autovariation, and periods of intense volcanism, appear to dominate climatic variations in this timeframe. Random meteorological events explain abnormal rates of precipitation or regional overheating. The increase of greenhouse gas concentrations due to anthropogenically increased release of CO₂ to the atmosphere (some 20 thousand million tons per year) is causing major climatic effects in the next decades and centuries.

10³ to 10⁴ years: This time frame includes the (partial) melting of the polar ice-caps, an example of which is the last deglaciation which occurred between 18,000 and 9,000 years Before Present (BP). The transition from a glacial state to interglacial conditions appears to be controlled by the period of time necessary for the ice-sheet to melt under conditions of increased irradiance slightly below a given critical value and from ice feedback mechanisms. This transition from glacial to interglacial phases is accompanied by other changes including the restructuring of ocean currents, which might be the missing element

for understanding the enormous significance of the Atlantic Ocean on the overall climate of the planet. The change from glacial conditions to interglacial climate states has also been accompanied by a strong variation in the concentration of atmospheric CO₂ and methane, as shown in the studied Vostok ice cores from Antarctica (Petit et al., 1999; Figure 2-3). This study of the Vostok ice cores and several other ice core records from the northern and southern hemisphere demonstrate the strong correlation between air temperature and CO₂ atmospheric concentrations over the past hundreds of thousands and even millions of years.

10⁴ to >10⁶ years: The most important climatic phenomenon in this timeframe is the transition to glacial climatic states from non-glacial states (and vice versa) controlled by astronomical forcing mechanism frequencies (19 ka, 23 ka, 41 ka and 100 ka). The astronomical forcing mechanisms account for about 60 % of the variance recorded in the past 780,000 years between 19 ka and 100 ka BP, and up to 85 % of the variance if the 'windows' are four narrow bands around the orbital cycles. There is now substantial evidence of interglacial-glacial changes in oceanic circulation, its chemistry and vertical structure. The impact of glacial climates on the geosphere-biosphere system needs to be calculated by specific models to estimate the impacts originating from these special conditions. For time frames longer than 1 Mio years, the continental drift and plate tectonics activity appear to dominate. Structural changes in oceanic currents are also important since they modify the efficiency and form of transport of oceanic heat between upper and lower latitudes. But the main forcing mechanisms have a tectonic origin.

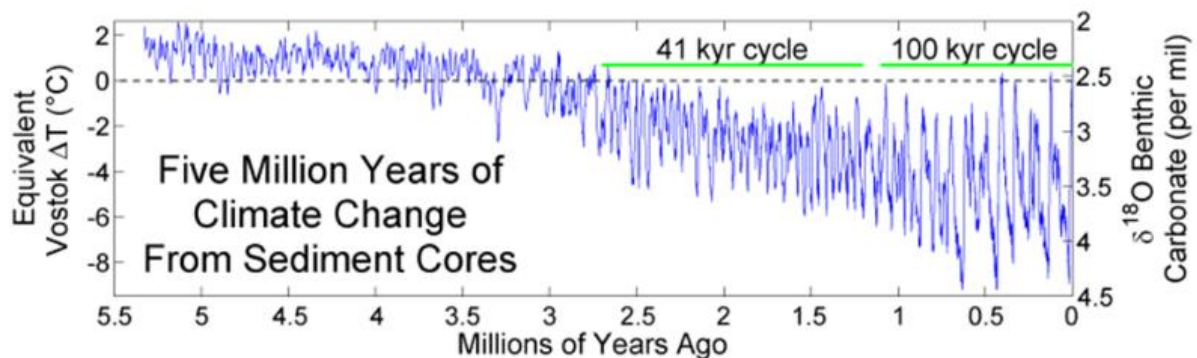


Figure 2-3 Correlation between air temperature and CO₂ atmospheric concentrations in Vostok ice cores from Antarctica. Changes in δ¹⁸O isotope concentrations point at a periodic sea-level change and temperature lowering in the past 5.5 Myrs. From Lisiecki and Raymo (2005).

2.2.2. The role of climate change

Future climate predictions (<1 Myr) should be based on understanding of the mechanisms affecting climate change as well as its possible effects. This can be achieved by combining theoretical predictions with an understanding of past climate change. For instance, the fact that the Netherlands are located near two centres of Pleistocene glaciation (Scandinavia and the British isles) that expanded during several glacial/interglacial cycles, helps to define the expected effects of predicted future ice-sheet advance. Next to an analogy with the past, climate predictions should also consider the human contribution to rapid global climate warming and the associated melting of glaciers. Following a binary approach, climate may change to warmer or colder conditions and associated humidity either increases or decreases, depending on precipitation and evapotranspiration. In analogy with knowledge of past climate deterioration e.g., in the Pleistocene, a change towards colder climate in the Netherlands will be related to an increase in northern hemisphere glaciation and may be associated with permafrost and sea-level low stand.

In the most extreme case, incursions of ice sheets over Dutch territory would have the following potential effects (Figure 2-1):

- 1) surface erosion (see following section for an evaluation), may affect the isolation function by exposing the Boom Clay and its associated nuclear waste;
- 2) altered stress fields and glaciotectonic/glacio-isostatic perturbations that might locally compromise hydrogeological properties of the Boom Clay;
- 3) loading/unloading effects that alter subsurface pressure fields and permeability, which would modify patterns of fluid flow and the geohydrological prerequisites for radioactive waste containment.

The development of permafrost and its depth would have great impact on the hydrological properties and (rates of) geochemical processes and affect several of the safety functions of both the host rock and the geosphere. The effects of contributions to sea-level change are multiple and often difficult to disentangle. Sea-level lowering associated with the growth of northern hemisphere glaciers may endanger the isolation function of the host rock through the incision of deep river valleys and submarine canyons.

A change to warmer climate conditions, on the contrary, will be associated with or even caused by melting of glaciers and sea-level rise. Potential sea-level rise will undoubtedly affect the accessibility of repository sites and will lead to a repositioning of depositional systems, particularly in the delta's. The change of the salt/fresh water interface, loading effects due to either water or sediments (or both) will ultimately lead to a change in hydrological charging conditions. A such, climatic change and associated (sub)processes will have their impact on a large number of geological processes, as will be discussed elsewhere in this report.

2.2.3. Understanding past climate change

After the very warm global climatic conditions which existed during the Cretaceous and early Cenozoic periods, temperatures began to drop around 35 to 40 million years ago, giving rise to the first glaciation on the Antarctic continent. Glaciation of the northern hemisphere began much later, approximately 3 million years ago (Figure 2-3). It can therefore be assumed for the northern hemisphere that it was first necessary that reinforcement mechanisms (plate tectonic processes, changes in oceanic circulation patterns, ice-albedo-temperature-feedback, natural fluctuations in atmospheric CO₂ concentrations) created the right conditions to reach these low temperatures. These conditions, when modulated by the Milanković cycles, finally initiated the typical fluctuations between glacial and interglacial periods that the Netherlands experienced (Figure 2-4).

The changes in reinforcement mechanisms which are largely related to distribution of landmasses (and thus plate tectonic processes), act on a larger time scale, i.e. >10⁶ years. Therefore, first-order predictions on the duration of the present (Holocene) interglacial and on the inception of future glaciation phases can be based on the orbital theory of cyclic climate change (Hays et al., 1976; Berger, 1978) and on its implications for the ongoing Quaternary ice age. The initiation of northern hemisphere ice sheets in the last 800 kyr appears to be closely (for 85 %) controlled by minima in summer insolation forcing at 65°N.

The three components of orbital variation that affect the magnitude and distribution of solar insolation are: precession at periods of 19 and 23 kyr, obliquity at about 40 kyr period, and eccentricity at 400 and 100 kyr periods (Berger, 1978). The last ~800 kyr of the Quaternary have been characterised by relatively regular alternations between long glacial phases and much shorter, warmer interglacials, with a quasi-periodicity of ~100 kyr related to the short eccentricity cycle of the Earth's orbit (Imbrie et al., 1993; Lang and Wolff, 2011).

Various feedbacks inherent to the climate system probably assume a fundamental role in amplifying or buffering the direct effect of radiative forcing (insolation). Of these, CO₂ as a greenhouse gas may have particular relevance because: 1) past variations in its atmospheric concentration closely tracked orbitally-paced glacial-interglacial cycles (e.g. Lorius et al., 1993; Berger et al., 1993; Loutre and Berger, 2000); 2) the enhanced concentration of CO₂ and other greenhouse gases related to human activities has the potential to interfere with the dynamics of interglacial-glacial transitions, and thus possibly with the onset of a future glacial cycle (e.g. Loutre and Berger 2000; Archer and Ganopolski 2005; Kidder and Worsley, 2012; Berger and Yin, 2012). During the Last Glacial Maximum pCO₂ was at about 200 ppm, whereas it has been measured at ~280 ppm for the pre-industrial era and has passed 360 ppm in the current industrial era. Recent climate models indicate that in the current orbital configuration, with a weak minimum in summer insolation (i.e., a lesser probability for the climate system to switch into a glacial mode), CO₂ concentrations well below the pre-industrial 280 ppm would be needed to allow natural inception of a new glaciation (Vettoretti and Peltier, 2004; Archer and Ganopolski, 2005; Cochelin et al., 2006; Tzedakis et al., 2012; Berger and Yin, 2012).

Important to note is that the human contributions to CO₂ will not dissipate for a geologically long period. Archer and Ganopolski's (2005) carbon cycle models indicate that 25 % of CO₂ from fossil fuel combustion will remain in the atmosphere for thousands of years, and 7 % will remain beyond one hundred thousand years. They predict that a carbon release from fossil fuels or methane hydrate deposits of 5000 Gton could prevent glaciation for the next 500,000 years. The duration and intensity of the projected interglacial period includes two 400 kyr eccentricity minima and is longer than has been modelled for the last 2.6 million years.

In fact, average global temperatures and latitude-averaged global temperature gradients today suggest that the Earth has reached a thermal state extremely close to those of early Pliocene pre-glacial times and of the Eemian (Hansen and Sato, 2012), although the ocean-atmosphere dynamics of those past times must have been sufficiently different from today to caution against direct comparisons of temperature as a single parameter representative of a general climate state.

For time frames over 10⁶ years, continental drift and plate tectonic activity would appear to dominate. Structural changes in oceanic currents are also important since they modify the efficiency and form of transport of oceanic heat between upper and lower latitudes.

2.2.1. Possible future climate types

Although a consensus on long-term future climate change has not been attained in the scientific community, the most recent data bring authors to a consistent conclusion that the combination of present orbital forcing and high concentrations (and long lifetimes) of anthropogenic greenhouse gases will stabilize the climate system within a prolonged interglacial over the next tens of thousands of years. The implication for the study at hand is that ice-sheet advances over the Dutch territory should not be a likely factor in evaluating the feasibility of nuclear waste disposal in the Boom Clay over geologically intermediate timescales (~100 kyr). For the further future, the range of likely future climate types (Table 4-1) are directly linked to the range of possible future temperatures, which includes both natural scenarios and those incorporating the effects of anthropogenic carbon emission as suggested by Archer and Ganopolski (2005). The shifts in temperature (ΔT 's) calculated by the latter authors are between -8 and +4 °C.

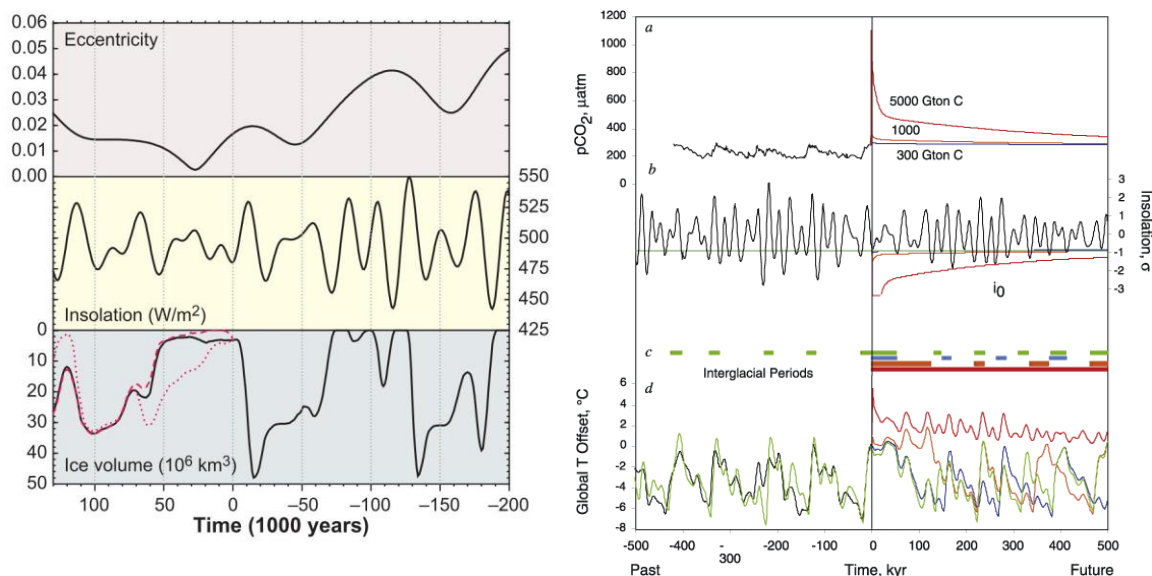


Figure 2-5 Natural vs. anthropogenetically influenced ice volume predictions (resp. Berger and Loutre, 2002 and Archer and Ganopolski, 2005). Left: Following a natural evolution of climate the next glacial would coincide with a 400 kyr eccentricity minimum and will begin in about 55 kyr and has a duration of ~120 kyr. Right: Blue, orange and red represent critical insolation values (i_0) that are needed to trigger glacial inception with different contributions of anthropogenic carbon, respectively 300, 1000 and 5000 Gton. In all modelled CO_2 scenarios the predicted “natural” glaciation at 55 kyr will be skipped.

As a matter of simplicity, it is here assumed that this temperature change will lead to a latitudinal shift of climate, i.e. the Netherlands keeps an Atlantic-influenced maritime climate and no increased continentality (expressed as warmer summers and colder winters) is expected to occur. In order to select present day analogues for the projected future climate types, the BIOCLIM approach (Bioclim, 2003) is applied by describing the climate characteristics of several type localities. These characteristics are then linked to vegetation to describe “biomes”. As such, distinctive lifeform association (Figure 2-6) are coupled to a climate class with estimates for average annual precipitation and average annual temperature (Figure 2-7).

Table 4-1 Future climate and vegetation types

Climate class used here	Walter climate type classification (IAEA 2003)	Köppen-Geiger (see Figure 2-6)	Vegetation (biomes)
Present-day : Typical maritime temperate with a short period of frost (nemoral)	ZB VI	Cfb: continental, fully humid, warm summer	Deciduous Forest Biome
Boreal (cold continental climate)	ZB VIII	Dfc: snow, fully humid, cool summer	Taiga
Periglacial (permafrost in near glaciated areas -tundra)	ZB IX	ET: polar tundra	Tundra
Subglacial (Arctic/ Antarctic, polar) or paraglacial	ZB IX:	EF: polar frost	none
Mediterranean (Winter rain and summer drought, arid-humid)	ZB IV	Csa: continental, dry summer, hot summer	Chaparral

To assess the biosphere change expected under the Normal Evolution Scenario (NES), four constant biosphere systems, reflecting the first four climate states mentioned will be considered. The last biome (glacial) will be considered as Alternative Evolution Scenario (AES).

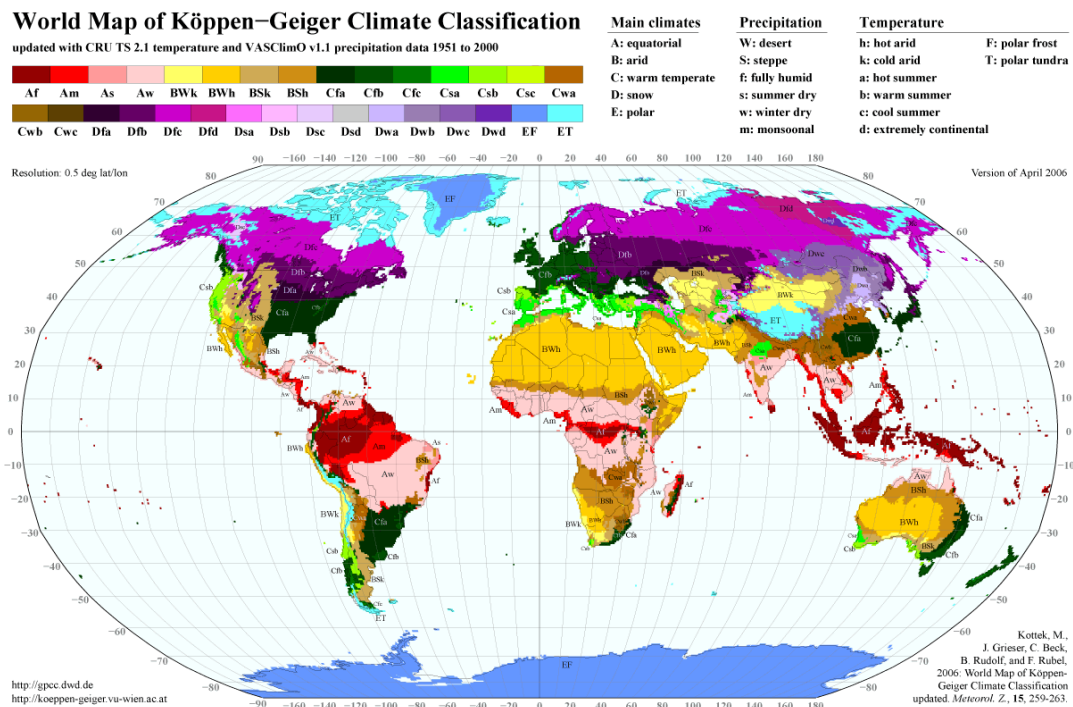


Figure 2-6 World map of the Köppen–Geiger climate classification (from Rubel and Kottek, 2010).

2.2.2. Present-day Temperate Climate

General

The temperate climate is a rather broad zone since it includes those latitudes of the Earth that lie between the tropics and the polar regions. The temperatures in these regions are generally relatively moderate, rather than extremely hot or cold, and the changes between summer and winter are usually moderate.

There are two types of temperate climate: **maritime and continental**. The maritime climate is strongly influenced by the oceans, which maintain fairly steady temperatures across the seasons. Since the prevailing winds are westerly in the temperate zones, the western edges of continents in these areas experience most commonly the maritime climate. Such regions include Western Europe, in particular the UK, and western North America at latitudes between 40° and 60° north.

Continentality increases inland, with warmer summers and colder winters as the effect of land on heat receipt and loss increases. This is particularly true in North America, where the north-south aligned Rocky Mountains act as a climate barrier to the mild maritime air blowing from the west. Maritime climate, on the other hand, penetrates further into Europe where the major mountain range - the Alps - is orientated east-west.

For the Netherlands, the maritime temperate climate is most representative, assuming the sea will never be so far away that a full continental climate will develop. Below the temperate climate for the Netherlands at present is summarized. Variations in the climate are also considered.

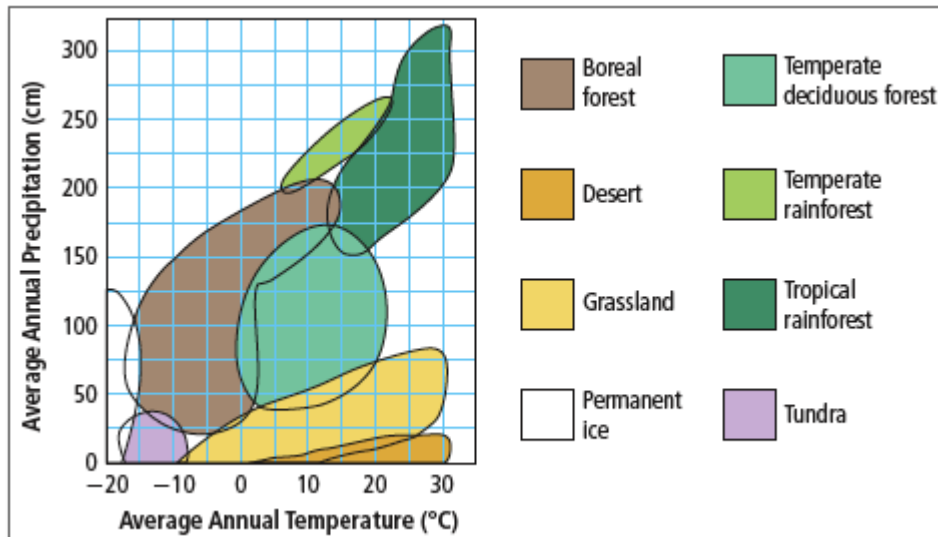


Figure 2-7 Biomes as defined by mean annual precipitation and mean annual temperature, Note the overlap in biomes (source: <http://sciencebitz.com>).

Temperature

An annual average temperature (AAT) of 9.43°C is calculated based on the so-called CNT-series (http://www.knmi.nl/klimatologie/onderzoeksgegevens/CNT/tg_CNT.txt) of the KNMI covering the years 1906-2013 and are representative for de Bilt, i.e., the center of the Netherlands. Over the time period measured, the AAT shows an increase of $1.5 \pm 0.5^\circ\text{C}$, which is considered statistically significant. This increase appears to be strongest in spring and summer seasons.

Precipitation

The average annual precipitation (AAP) for the Netherlands amounts to 766 mm/yr and is based on measurements from de Bilt collected over the past ~100 years. It has been strongly variable over this time period. For example in 1921, the AAP was 425 mm, whereas in 1998 it was 1109 mm. A statistically significant linear increase of 160 mm/yr (23 %) can be deduced over the period 1906-2011 (Visser, 2005). The causes for this increase can be multiple and may be linked to variations in wind speed and -direction, temperature and humidity or a combination.

Processes and Landforms

The ratio between groundwater recharge and surface runoff is strongly variable and depends among other factors on the presence of rivers, polders and soil type.

Vegetation

Based on the AAP and AAT, the Netherlands predominantly represents a temperate deciduous forest biome, but also overlaps with the temperate grassland biome (Figure 2-6). This explains the multitude of landscape existing in the Netherlands: forests, wetlands, marshlands and waterways, each with its typical vegetation.

2.2.3. Boreal climate - Dfc - ZB VIII

General

A subarctic (or subpolar) climate is characterized by long winters and short, cool to mild summers. It is usually found on large landmasses, away from the moderating effects of an ocean, generally at latitudes from 50°N to 70°N poleward of the humid continental climates. However, coastal regions may experience higher precipitation and milder winters. A future boreal climate in the Netherlands would exist close to oceans and would have milder winters and no permafrost. It should be noted that such a situation might occur during colder/glacial periods when sea level will be lower. This sea-level drop would only change the relative height of the country and no alpine (mountainous) conditions would be expected.

Temperature

These climates have an average temperature above 10 C in their warmest months, and a coldest month average below -3 C. This type of climate offers some of the most extreme seasonal temperature variations found on the planet: In winter, temperatures can drop to -40°C and in summer, the temperature may exceed 30°C. However, the summers are short; no more than three months of the year (but at least one month) must have a 24 hour average temperature of at least 10°C to fall into this category of climate.

Precipitation

Although precipitation occurs throughout the year, most subarctic climates away from coasts have very little precipitation, typically no more than 15 inches (380 mm) in the warmer months. In coastal areas with subarctic climates, the heaviest precipitation usually falls during the autumn months. In combination with the very low evapotranspiration there would be a water-logged terrain in many areas of subarctic climate with snow cover during winter.

Processes and landforms

The taiga is the dominant landform under boreal climate conditions. Some taigas in northern areas with subarctic climates located near oceans (southern Alaska, the northern fringe of Europe, Sakhalin Oblast and Kamchatka Oblast), have milder winters and no or discontinuous permafrost (see Figure 2-8), and are more suited for farming unless precipitation is excessive. The frost-free season is very short, varying from about 45 to 100 days at most, and frost can occur during any month in many areas.

Vegetation

The forests of the taiga are largely coniferous, dominated by larch, spruce, fir and pine. The woodland mix varies according to geography and climate.

Analogue - Murmansk

The Murmansk climate^b is cold and temperate with moderate rainfall and even in the driest month there rain. The climate here is classified as Dfc by the Köppen-Geiger system. Based on 107 years monitoring, the AAT is -1.6°C and average annual precipitation (AAP) is 606 mm. The evapotranspiration is 365 mm annually. Altitude: 51 m.

^b Climate data provided by CRU TS 3.1 - University of East Anglia Climate Research Unit (CRU; Phil Jones, Ian Harris). CRU Time Series (TS) high resolution gridded datasets (NCAS British Atmospheric Data Centre, 2008).

2.2.4. Periglacial - ZB IX - ET

General

Periglacial climates occur principally in areas of permafrost with intense freezing with an active layer of freeze/thaw near the surface, which thaws briefly in summer. These areas are also known as tundras. Periglaciation occurs near mountain glaciers (alpine tundras) and at lower levels where it forms a zone of coldness around continental glaciers in areas of high latitudes (arctic tundras), covering perhaps 20 % of the Earth's land surface.

Temperature

The average winter temperature is -34°C but the average summer temperature is $3-12^{\circ}\text{C}$ which enables this biome to sustain life.

Precipitation

Most areas under periglaciation have relatively **low precipitation** (if not the areas would likely be glaciated and become biome EF in the Köppen-Geiger classification) and **low evapotranspiration**, which makes average river discharge rates low. Rainfall may vary in different regions of the Arctic. Yearly precipitation, including melting snow, is 150 to 250 mm. Soil is formed slowly. A layer of permanently frozen subsoil called permafrost exists, consisting mostly of gravel and finer material. When water saturates the upper surface, bogs and ponds may form, providing moisture for plants. There are no deep root systems in the vegetation of the Arctic tundra, however, there are still a wide variety of plants that are able to resist the cold climate.

Many rivers flowing into the Arctic Sea of northern Canada, Alaska and Siberia have despite this a very strong erosive capacity due to the fact that thaw occurs first in the upper part of the drainage basin leading to large areas being flooded further down (north) because of obstructing river ice. When these dams melt or break large amounts of water are released with destructive and erosive power.

Processes and landforms

With 5-7 consecutive months where the average temperature is below freezing, all moisture in the soil and subsoil freezes solidly to depths of several meters. Summer warmth is insufficient to thaw more than a few surface meters, so continuous permafrost prevails (Figure 2-8). The landform is characterised by:

- Mechanical weathering
- Low T, sparse vegetation cover and poorly developed soils exclude the likelihood of chemical and biological weathering
- Lack of vegetation increases wind (aeolian) action
- Further erosion occurs as the wind-blown sand grains abrade rock outcrops
- Wind action building dunes of loess

Surface runoff

- Amount of transport and erosion by rivers is huge
- High load comes from rivers flowing over areas covered by loose debris from glaciers
- High discharge from melting ice (1-2 months a year)

Vegetation

There are about 1,700 kinds of plants in the Arctic and Subarctic, and these include:

- low shrubs, sedges, reindeer mosses, liverworts, and grasses
- 400 varieties of flowers

- crustose and foliose lichens

All of these plants are adapted to sweeping winds and disturbances of the soil. Plants are short and group together to resist the cold temperatures and are protected by the snow during the winter. They can carry out photosynthesis at low temperatures and low light intensities. The growing seasons are short and most plants reproduce by budding and division rather than sexually by flowering.

Analogues

For the Netherlands, periglacial phenomena with continuous permafrost are known from the Last Glacial Maximum (LGM) of the Weichselian glacial period (Table 2-2; Figure 2-9). This past situation forms the best analogue for predictions of future scenarios and has also been used in permafrost prediction studies (see chapter 5). Rationale is that landform, influence of oceans and river drainage of this past situation are better analogues for a future periglacial scenario than present-day periglacial settings. A more thorough assessment of permafrost phenomena and permafrost depths across the Netherlands is presented in chapter 5.

Table 2-2 Estimated of temperature and approximations of wind action and precipitation during specific time windows in the lowland of northwest and central Europe based on proxy data. Modified from Huijzer and Vandenberghe (1998). The 20-13 ka period corresponds to the LGM.

Time-window (ka)	Temperature of warmest month (°C)	Mean annual temperature (°C)	Temperature of coldest month (°C)	Annual amplitude (°C)	Climate gradient	Wind activity	Precipitation
74-59	10 to 13	-8 to -4	-26 to -20	30 to 39	North to south	++	-
50-41	≥ 7 to ≥ 10	≤ -4 to ≤ -1	≤ -20 to ≤ -13	23 to 27	West to east	-	+
Upton Warren	16 to 18	4 to 9	-7.5 to 0.5	15 to 26	(?) West to east	-	+
41-38	10 to 11	-9 to -4	-27 to -20	30 to 37	North to south	+	-
36-32	10	-7 to -2	-20 to -16	26 to 30	-	-	+
27-20	4 to 8	-8 to -4	-25 to -20	28 to 33	North to south	+	±
20-13	7 to 11	-9 to -4	-26 to -20	28 to 36	North to south	++	-

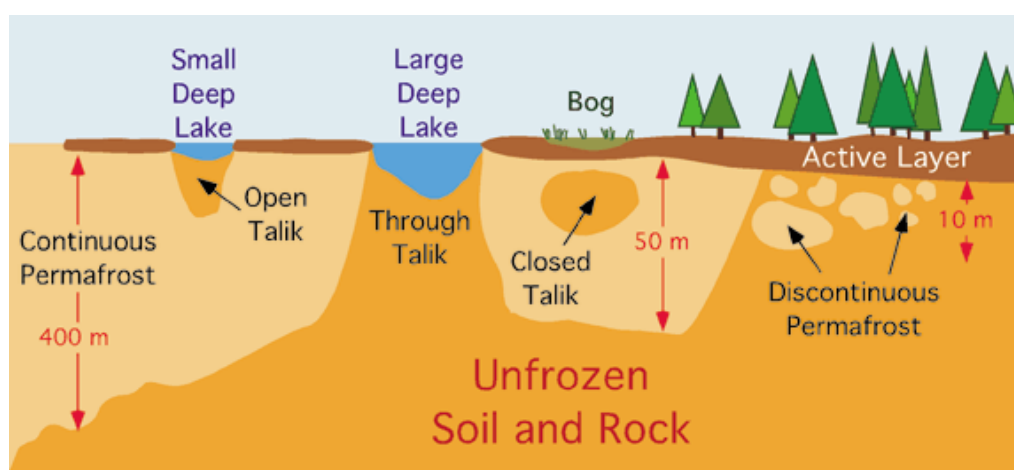


Figure 2-8 Vertical cross section of the transition zone between continuous and discontinuous permafrost. The graphic also shows the various types of talik or unfrozen ground. Open talik is an area of unfrozen ground that is open to the ground surface but otherwise enclosed in permafrost. Through talik is unfrozen ground that is exposed to the ground surface and to a larger mass of unfrozen ground beneath it. Unfrozen ground encased in permafrost is known as a closed talik. (source:www.physicalgeography.net/fundamentals/10ag.html).

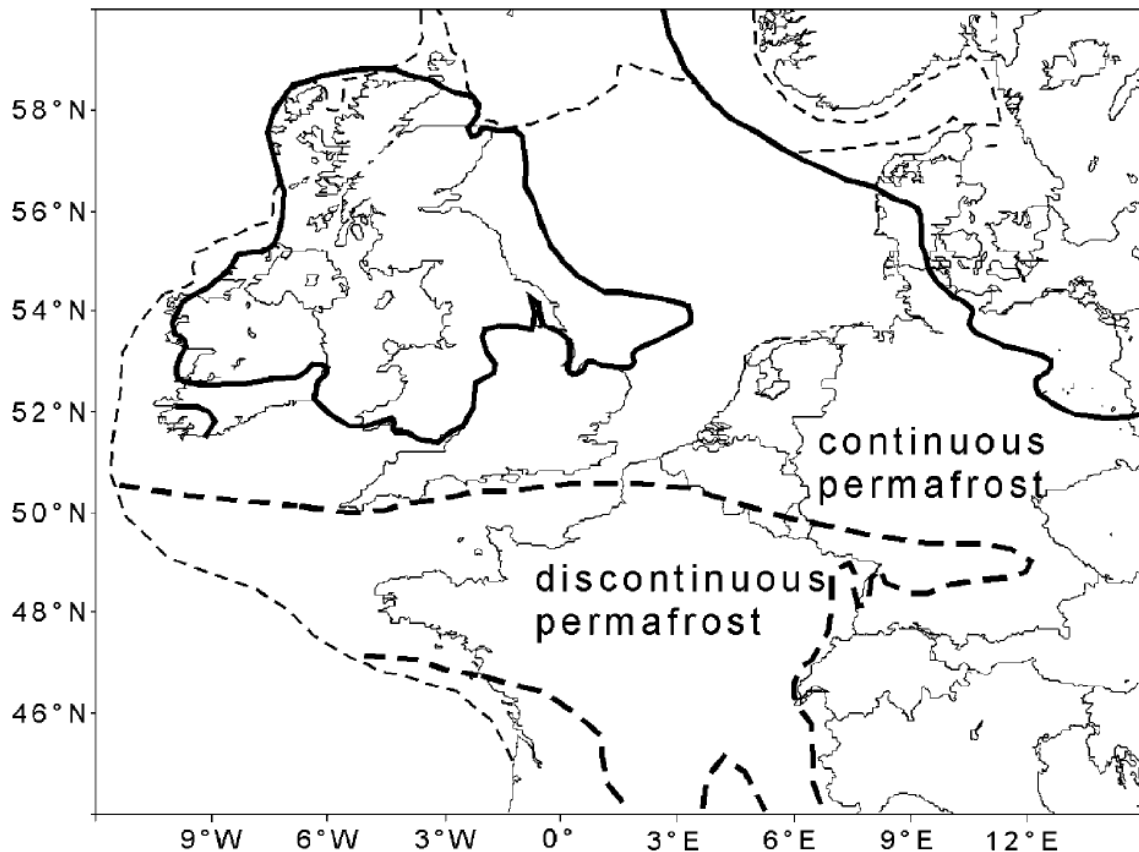


Figure 2-9 Spatial distribution of permafrost during the last glacial maximum (from Rensen and Vandenberghe, 2003).

2.2.5. Glacial - EF

General

The northern polar ice cap in fact represents the frozen part of that Arctic ocean's surface. The only large landmass in the extreme northern latitudes bearing an ice cap is Greenland, but several smaller islands near the Arctic Ocean also have permanent ice caps. Under the Köppen climate classification, the ice-cap climate is denoted as EF. Such areas are found around the north and south pole, and on the top of the highest mountains.

Temperature

The glacial climate is defined as a climate with no months above 0 C.

Precipitation

Precipitation is very low with annual averages of 3-4 mm. Estimates of evaporation over the Arctic Ocean are scarce. The one-year Surface Heat Budget of the Arctic Ocean (SHEBA) project collected some of the best measurements during 1997 and 1998 in the Beaufort Sea. These observations showed that evaporation was nearly zero between October and April, and peaked in July at about 7 mm/month (Persson et al., 2002). Since the temperature never exceeds the melting point of water, any snow or ice that accumulates remains there permanently, over time forming a large ice sheet.

Processes and Landforms

Glaciers and ice sheets are extraordinary effective structures of landform generation and especially, of landscape erosion. Ice bodies with different configurations and physical properties variously modify the Earth's surface eroding their substrates (bedrock and regolith) and depositing debris at their margins. Physical processes of substrate erosion and debris entrainment are of much greater impact than chemical weathering in glacial environments (Kump and Alley, 1994). See Chapter 3 for a more thorough inventory of processes and landforms associate with glaciers.

Vegetation

Glaciated terrains are not covered by vegetation.

Analogues

Greenland.

2.2.6. Mediterranean, warm/dry summer climate - Csb

General

The Mediterranean climate is characterized by warm to hot, dry summers and mild to cool, wet winters. These climates usually occur on the western sides of continents between the latitudes of 30°C and 50°C. Mediterranean climate zones are associated with the five large subtropical high pressure cells of the oceans: the Azores High, South Atlantic High, North Pacific High, South Pacific High, and Indian Ocean High. These climatological high pressure cells shift towards the poles in summer and towards the equator in winter, playing a major role in the formation of the world's subtropical and tropical deserts as well as the Mediterranean Basin's climate.

Temperature

Because most regions with a Mediterranean climate are located near large bodies of water, temperatures are generally moderate with a comparatively small range of temperatures between the winter low and summer high (although the daily range of temperature during the summer is large due to dry and clear conditions, except along the immediate coasts). Temperatures during winter only occasionally fall below the freezing point and snow is generally seldom seen. Under the Köppen-Geiger system, "C" zones have an average temperature above 10°C in their warmest months and an average in the coldest month between 18°C to -3°C. The third letter indicates the degree of summer heat: "a" represents an average temperature in the warmest month above 22°C, with at least four months averaging above 10°C; "b", an average temperature in the warmest month below 22°C, and again with at least two months averaging above 10°C. Under this classification, dry-summer subtropical climates (Csa, Csb) usually occur on the western sides of continents. Csb zones include areas normally associated with Oceanic climates, not Mediterranean, such as much of the Pacific Northwest, much of southern Chile, parts of west-central Argentina, western Portugal and northwestern Spain.

Precipitation

The second letter indicates the precipitation pattern: "s" represents dry summers: first, Köppen has defined a dry month as a month with less than one-third that of the wettest winter month, and with less than 30 mm of precipitation in a summer month. Some, however, use a 40 mm level. During summer, regions of Mediterranean climate are dominated by subtropical high pressure cells, with dry sinking air capping a surface marine layer of varying humidity and making rainfall impossible or unlikely except for the occasional thunderstorm, while during winter the polar jet stream and associated periodic storms reach into the lower latitudes of the Mediterranean zones, bringing rain, with snow

at higher elevations. As a result, areas with this climate receive almost all of their precipitation during winter, autumn and spring seasons, and may have between 4 and 6 months during summer without any significant precipitation.

Processes and landforms

Not one specific landform type can be assigned to this climate type. Typical are both low land and hilly terrains in near-coastal regions, drained by non-perennial rivers (semi-permanent and ephemeral rivers).

Vegetation

Mediterranean vegetation examples include the following:

- Evergreen trees: such as Pines, Cypresses, and Oaks
- Deciduous trees: such as Sycamores, Oaks, and Buckeyes
- Fruit trees such as Olives, Figs, Citrus, Walnuts and Grapes
- Shrubs: Bay laurel, Ericas, Banksias, and Chamise
- Sub-shrubs: such as Sages, Artemisias, and Sagebrush
- Grasses: Grassland types, Themeda triandra, Bunchgrasses; Sedges, and Rushes
- Herbs: such as fragrant Rosemary, Thyme, and Lavender.

Analogue

South of Porto (Portugal) a lowland area exists as part of the Lusitanian Basin that has an oceanic setting and may serve as a “warmer analogue” to the Netherlands. AAT is 15.4°C and AAP is 1236 mm/yr, which is remarkably higher than the present-day AAP of the Netherlands. Average evapotranspiration is 600-700 mm/year.

Table 2-3 Summary of climate data for the 5 climate zones described.

		min	max	average	period
<i>source: KNMI</i>					
NL	Annual rainfall (mm)	425	1109	766	1906-2011
Present-day, maritime temperate	Annual evapotranspiration (mm)	541	607	578	1981-2014
	Annual Runoff (mm)	120	400	?	
	Mean annual ambient air temperature (°C)	7,89	11,52	9,43	1906-2015
	Air temperature of warmest month (°C)	13,82	22,59	17,1	1906-2015
	Air temperature of coldest month (°C)	-7,02	7,41	2,13	1906-2015
<i>source: CRU TS 3.1</i>					
Murmansk, Boreal	Annual rainfall (mm)	-	-	606,2	109 years
	Annual evapotranspiration (mm)	-	-	365,4	5 years
	Annual Runoff (mm)	-	-	-	
	Mean annual ambient air temperature (°C)	-	-	-1,55	109 years
	Air temperature of warmest month (°C)	-	-	12,7	109 years
	Air temperature of coldest month (°C)	-	-	-17,8	109 years
<i>Source: Instituto de Meteorologia Hong Kong Observatory</i>					
south of Porto Mediterranean	Annual rainfall (mm)	-	-	1237	?
	Annual evapotranspiration (mm)	-	-	650	
	Annual Runoff (mm)	-	-	?	
	Mean annual ambient air temperature (°C)	-	-	15,2	
	Air temperature of warmest month (°C)	-	-	20,8	
	Air temperature of coldest month (°C)	-	-	9,5	
<i>Huizer & Vandenberghe, 1998</i>					
Periglacial, LGM	Annual rainfall (mm)	-	-	?	
	Annual evapotranspiration (mm)	-	-	0	
	Annual Runoff (mm)	-	-	-	
	Mean annual ambient air temperature (°C)	-9	-4	-6,5	
	Air temperature of warmest month (°C)	7	11	9	
	Air temperature of coldest month (°C)	-26	-20	-23	
<i>source: CRU TS 3.1</i>					
subglacial, paraglacial Greenland	Annual rainfall (mm)	-	-	40	
	Annual evapotranspiration (mm)	-	-	3,5	
	Annual Runoff (mm)	-	-	-	
	Mean annual ambient air temperature (°C)	-	-	-17	1900-2009
	Air temperature of warmest month (°C)	-	-	-2	1900-2009
	Air temperature of coldest month (°C)	-	-	-28	1900-2009

2.3. Future Tectonic processes

2.3.1. Origin of tectonic movements

Tectonic movement is defined as a horizontal or vertical movement of the earth crust (including the sedimentary overburden) that occurs in response to stresses applied to the crust. These stresses can be of various origin and include both natural and anthropogenic sources. Most of the natural tectonic forces are directly or indirectly related to plate-tectonics although the role of ice-sheet or sediment loading are important as well. Changes of the stress state induced by human activities, though at a completely different time scale and magnitude, may impose the same effects (e.g. induced seismicity). The natural tectonic processes include regional uplift/subsidence, movement along faults and associated seismicity, glaciotectonic movement, tsunamis and salt movement (halokinetics).

2.3.2. The role of tectonics

In assessing the role of tectonic movements it is first of all important to consider how and if the long-term safety assessment of radioactive waste disposal facilities in the Boom Clay in the Netherlands will be affected. There are three modes in which tectonic movements can have an effect (Figure 2-1):

1. Exposure/exhumation of the unit under scrutiny, such that the isolation function will be affected by exposure of radionuclides to surface waters/air.
2. Hydrological changes through changes in pore water pressure induced by tectonic stress.
3. Fluid flow effects along faults and discontinuities, affecting transport, dilution and dispersion functions

These effects can be induced by the following processes and sub-processes (Figure 2-1):

Regional uplift

- Compressional tectonic, i.e. the formation of anticlinal structures
- Local uplift along faults and rift systems (shoulders)
- Isostatic compensation in response to unloading (ice, sediment or water)
- Salt tectonics (salt flow, doming)

Regional subsidence

- Compressional tectonics, i.e. the formation of synclinal structures
- Extensional tectonics, i.e. the formation of rift systems
- Isostatic compensation in response to loading (ice, sediment or water)
- Salt tectonics (dome collapse and subsidence)
- Subsidence due to depletion of gas fields

2.3.3. Prediction of tectonic movements

Effects of active tectonics and associated natural seismicity are rarely observed in the Netherlands, although the occurrence of several moderate earthquakes in both the historic and instrumental periods suggest that natural earthquake hazards exist (

Figure 2-10). Best-known example is the earthquake that hit the city of Roermond on April 13, 1992, which has a magnitude of 5.8 on the Richter scale ($ML=5.8$). Natural seismicity is mainly confined to large faults in the south of the Netherlands, which are part of the Ruhr Valley Rift System (Figure 2-11). The effects of natural seismicity, as reported for the last three centuries, have been moderate on the whole, and in epicentral areas include structural damage to buildings and small fault offsets affecting the surface topography. Instrumentally recorded natural seismicity onshore, outside the region discussed above, is limited to a few locations near Nijmegen, ca. 70 km north of Roermond, where three events of magnitude $ML=3.2$, 3.0 and 4.6 have been recorded in 1972, 1979 and 2011, respectively. It is unclear whether they can be associated with the Viersen Fault of the Roer Valley Rift System. In the area south of Bergen op Zoom, close to the Belgian-Dutch border, a small event of magnitude $ML=2.1$, possibly connected to the Antwerpen Fault, took place on June 15, 1988.

De Crook (1996) presented first rough estimates of expected horizontal peak ground accelerations, based on empirical intensity-peak ground acceleration relations used in Germany. This hazard analysis based on historical seismicity shows a maximum expected magnitude of $ML=6.3$. Paleoseismological investigations (Demanet et al., 2001; Van den Berg et al., 2002), however, indicate events that may reach one magnitude higher, at an average recurrence interval in the order of 2 to 3 kyrs along the major fault zones.

Also remote seismic events occurring under the ocean at the continental shelf can be of importance, for instance by triggering tsunamis. Tsunamis can travel over distances of hundreds of kilometers before reaching land and it is not necessary for such events to take place close to the region of interest in order to have an impact on a given landscape. Especially coastal areas are sensitive to such short-lived marine transgressions that may produce salinity contamination with consequent impacts on water resources. In Rotterdam, sediments related to a tsunami around 8000 years ago have been identified that are possibly linked to the Storegga-tsunami (Hijma and Cohen, 2008).

In the north of the Netherlands, no significant natural seismic activity has been detected, but since 1986 induced events were recorded, of which the locations coincide with producing gas fields. Deep tectonic activity, below the Zechstein salt, is mostly accommodated by flow and deformation of the plastically behaving Zechstein salt layer. Especially, salt domes up to 8 km height penetrate deposits of the Middle and Upper North Sea Group, i.e. those levels where the Boom Clay (or Rupel Clay Mb) resides. Subtle anticlinal dome structures in Quaternary deposits are located above salt pillars and attest to (sub)recent halokinetic activity. Associated fluid flow (brine water, gas) is shown both onshore and offshore and locally affects storage potential. To date, no seismicity

associated with this halokinetic activity was recorded. The contributing role of salt in induced seismic events is currently under investigation.

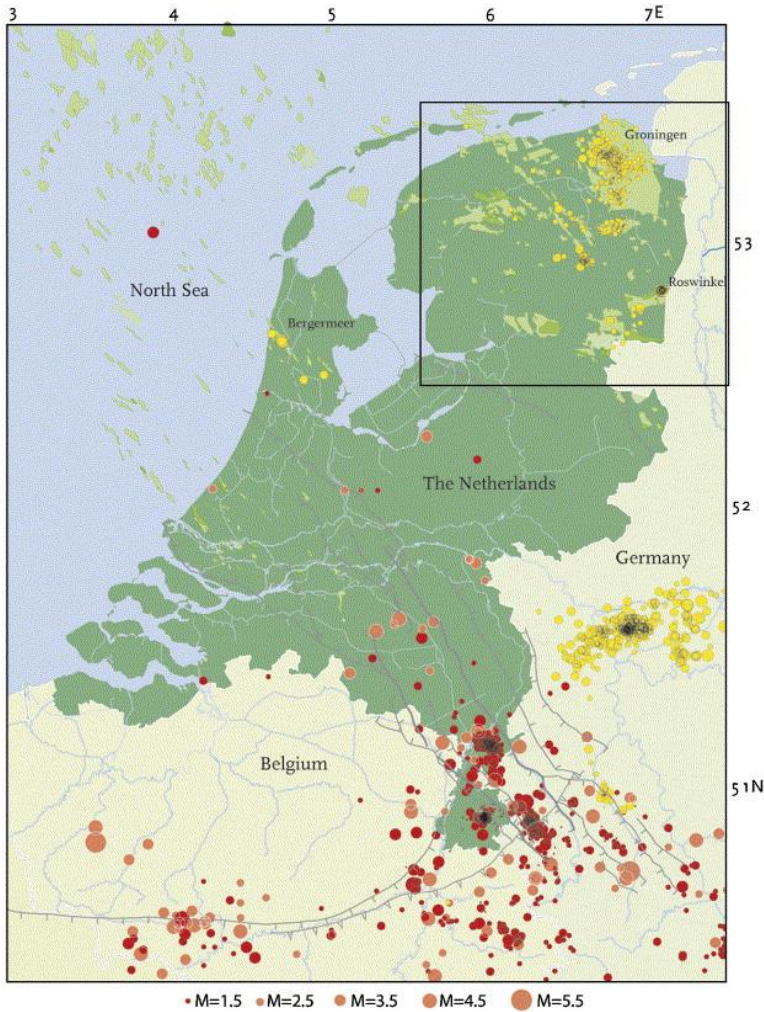


Figure 2-10 General overview of the seismicity in The Netherlands and its immediate surroundings since 1900. Red circles indicate natural tectonic earthquakes. Yellow circles indicate induced earthquakes. The earthquakes are scaled according to magnitude (M). Grey solid lines indicate mapped faults in the upper-north-sea formation according to the TNO. Light green indicates the approximate contours of the gasfields. Modified after Van Eck et al, (2006)

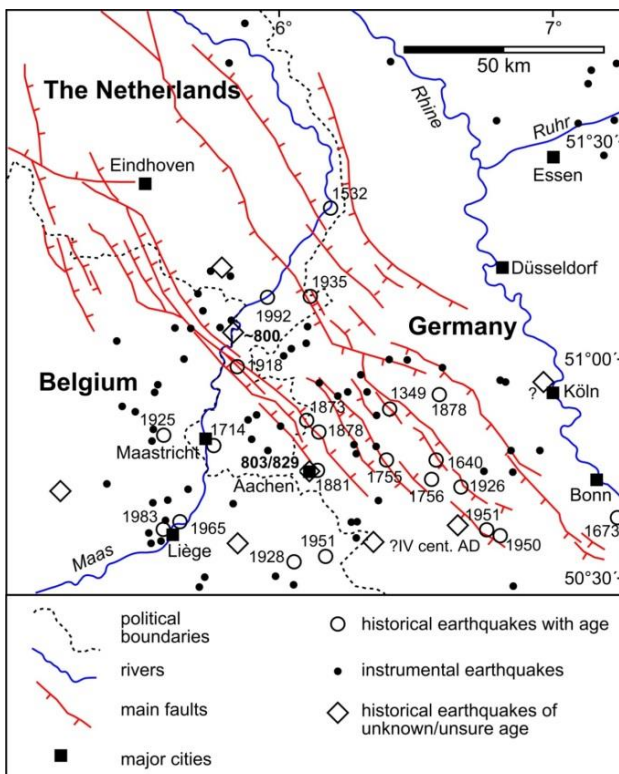


Figure 2-11 Instrumental- and historical earthquakes in the Ruhr Valley Graben (source: Klaus Reicherter, RWTH Aachen).

CLIMATE SECTION

3. Glacial erosion and -deformation processes

3.1. *Introduction*

In the aim of assessing potential for the Boom Clay Formation to act as long-term subsurface repository for radioactive waste in the Netherlands, scenarios of future climatic and geomorphic change must evaluate any possible erosional processes which may lower the topographic surface too close to the host rocks's subcrop depths. Considering the geographic position of the country and its tectonic context, the most likely agent for drastic modification of the Dutch territory could be represented by a possible climate transition from the present interglacial state to a new glacial one. The encroachment of ice sheets and/or proglacial domains over Dutch territory would be accompanied by processes of erosion and sedimentation, and glacio-tectonics, respectively. The impact of these processes is related to the dynamics and extent of the ice mass. This section aims to provide a concise, geologically informed rationale to assess the risk for glacial erosion and glacio-tectonics to affect the Boom Clay.

3.2. *Current state of knowledge*

Glaciers and ice sheets are extraordinarily effective agents of landform generation, and especially of landscape erosion. Ice bodies with different configurations and physical properties variously modify the Earth's surface, eroding their substrates (bedrock and regolith) and depositing debris at their margins. Physical processes of substrate erosion and debris entrainment are of much greater impact than chemical weathering in glacial environments (Kump and Alley, 1994). Although, there are still numerous unsolved issues in this field of research mainly due to the difficulty to examine active processes underneath and in proximity to glaciers (as exceptions, see Boulton, 1974, and Cohen et al., 2005, 2006).

Processes of physical erosion are traditionally grouped as abrasion, quarrying or meltwater action. Effects by subglacial meltwater can be of local importance over unconsolidated substrates and its relevance is most probably limited to the ice-margin domain, in correspondence of subglacial and proglacial drainage systems fed by ablation which tend to transport sediment away from the ice mass. At the scale of entire ice sheets, the action of glacial meltwater is considered of minor impact compared to the mechanisms of abrasion and quarrying. However, exceptionally high discharge and turbulence along particularly large subglacial drainage systems (tunnel valleys) recently gained much interest (see chapter 3.5).

Patterns of glacial erosion generally depend on the basal thermal regime of the ice which is the first-order control on glacial dynamics, and more specifically on rates of ice movement, influenced by the availability of basal meltwater. In 'cold-based glaciers' or 'polar glaciers' of cold arid climates, ice temperatures are below the pressure-melting point throughout the glacier's vertical profile. Meltwater is scarce or absent in such glaciers, inhibiting glacier movement and thus substrate erosion. By contrast, basal temperatures for 'warm-based glaciers' (or 'temperate glaciers') in milder maritime or alpine climates with significant precipitation persist long enough around the pressure-melting point to consent substantial sliding and erosion. For further details on glacier/ice-sheet mobility and erosion, the reader is referred to recent textbooks and review articles (e.g., Paterson, 1994; Martini et al., 2001; Glasser and Bennett, 2004; Bennett and Glasser, 2009; Benn and Evans, 2010; Hambrey and Glasser, 2012).

3.3. *Physical erosion and sediment production by ice sheets*

First research questions on large-scale patterns of glacial erosion and sediment production were directed at the continent-wide effects of Quaternary ice sheets. Geomorphic, stratigraphic and geophysical evidence led some authors to postulate pervasive stripping of regolith and sediment cover from recently glaciated cratonic interiors down to the Precambrian metamorphic basement (e.g., White, 1972; Dent, 1973; Boulton, 1974). Based on analogies between the mega-geomorphology of Scandinavia and northern North America, general models envisioned deeper scouring below ice-sheet centres, and progressively lesser erosion toward ice margins. The present depressions of the Gulf of Bothnia and Hudson Bay are typical examples of ice-centre excavation. Estimates of average depths of erosion ranged from several hundreds of metres (White, 1972) to more conservative values of 50-120 m (Laine, 1980; Bell and Laine, 1985; Hall and Sugden, 1987). By contrast, several studies propose much shallower depths for glacial action, limited to a few tens of metres of removed material (e.g. Gravenor, 1975; Sugden, 1976; Higgs, 1978). The latter group suggest that the central Precambrian shield had been fully exposed well in advance of Quaternary glaciations based on compositional evidence from overlying glacial deposits (Gravenor, 1975). At that time, the Hudson Bay was still underlain by Paleozoic rocks and preserved evidence of an extensive drainage system consistent with North American mega-geomorphology, thus not significantly modified by ice sheets (Sugden, 1976). A fundamental result of such observations was that major erosive action had been focussed on the peripheral regions of ice sheets rather than around their centres (Gravenor, 1975).

A contribution to the debate came from studies of shallow-marine stratigraphy along the northern seaboard of North America, aiming to calculate volumes of Quaternary sediments produced by erosion of the glaciated continental interior. Such studies probably were the first attempts to estimate large-scale, source-to-sink sediment budgets of glaciated basins, linking sediment packages to specific phases of ice-sheet advance and retreat. Whereas Flint (1947) asserted that the thinness of glacial 'drift' in most of the North American interior evidenced scarce erosion by ice sheets, White (1972) argued that most glacially produced sediments would be fine-grained, and thus amenable to long-distance transport and preferential deposition in distal (marine) settings. The major source of uncertainty was thus represented by the inability to estimate volumes of submarine glaciogenic debris (White, 1972). Through the combined analysis of Deep Sea Drilling Project data and seismic lines from the offshore of eastern North America and southern Greenland, Laine (1980) reported that probably over 90 % of sediment produced by glacial erosion accumulated in shallow to deep-marine environments along the continental margins. Most notably, Laine (1980) calculated that such an estimate would differ by a factor of ~20 from volumes calculated solely on the basis of glacial deposits preserved on land. This validates White's (1972) hypothesis that most ice-age sediments of terrestrial origin might be preferentially preserved in marine environments. These inferences were successively integrated with provenance studies and chronologically refined to suggest that early phases of ice-sheet advance would be the most effective in sediment production over yet undisturbed land. Moreover, cyclically expanding and retreating ice sheets are probably more effective in erosion and sediment production than more permanent ice sheets (e.g., Bell and Laine, 1985; Andrews, 1982). Such analyses of large-scale stratigraphic datasets from glaciated margins were to be integrated by more accurate methods over the successive decade (e.g., Piper et al., 1994; Elverhøi et al., 1995; Jaeger et al., 1998; Dowdeswell and Siegert, 1999).

Over the last two decades, more quantitative research has been devoted to glacial erosion and sediment production and to their variability in different climatic stages and geological settings, corroborating the widespread assumption that erosion by glaciers and ice sheets is more effective than erosion by 'common' fluvial/alluvial processes (Molnar and England, 1990; Nesje et al., 1992; Hallet et al., 1996; Glasser and Hall, 1997; Kuhlemann et al.,

2002; Montgomery, 2002). Indeed, several studies have shown that rates of erosion and sediment production from regional (e.g., Rea and Snoeckx, 1995; Glasser and Hall, 1997; Shuster et al., 2005; Anell et al., 2010; Dowdeswell et al., 2010; Charreau et al., 2011; Hjelstuen et al., 2012) to global scales (Peizhen et al., 2001; Molnar, 2004) increase drastically from the pre-glacial Neogene and early Quaternary to the extensively glaciated Late Quaternary. However, a fundamental role in regulating the total volume of debris shed from glaciated areas is evidently played by pre-existing basement lithology (Hallet et al., 1996; Delmas et al., 2009) and by sustained bedrock exhumation in high-relief, active orogenic settings (Jaeger et al., 1998; Tomkin, 2007; Kleman et al., 2008; Koppes and Montgomery, 2009). The principal approaches to quantify glacial erosion can be categorized as: 1) landscape analyses at regional to continental scales; 2) direct measurement of sediment fluxes from present-day glaciers and glaciated basins; 3) integrated analyses of stratigraphic successions within, or sourced by, Quaternary glaciated terrains.

3.3.1. Landscape analyses

The first, process-oriented line of research is of more direct interest in the context of this report, and is thus discussed in more depth here. Pioneered in its modern form by Sugden (1978), landscape analyses has provided a rationale to link the large-scale geomorphology of glaciated regions with the internal dynamics and long-term evolution of ice-sheets. It has been demonstrated that patterns of glacial erosion and sediment production are controlled primarily by feedbacks between subglacial topography and the geometric and thermo-mechanical configuration of the ice mass. These latter properties, in turn, are controlled by regional and temporal climate variations and directly affect the deformation and dynamics of ice (Boulton et al., 1985; Glasser, 1995). Intensely scoured landscapes have been recognized in areas associated with basal melting of Quaternary ice sheets and where subglacial topography favoured ice-flow convergence (i.e. ice thickening). Conversely, relatively little erosion has been observed in areas of formerly cold-based glaciers and in correspondence of highlands, which would force a divergence of ice flow (i.e. ice thinning; Sugden, 1978; Kleman, 1994; Glasser, 1995; Kleman and Glasser, 2007). In view of the link between the glacial thermal regime and erosive processes (see previous section), elevated ice thickness has insulating effects upon geothermal heat and elevates the melting point of ice under pressure. Consequently, it favours basal ice melting, associated higher sliding rates, and consequently greater impact upon the substrate. However, a positive thermal balance at the ice base is favoured also by frictional heating in the presence of fast flow due to internal strain within the ice mass and to its mechanical work on the substrate. A similar role is played by subglacial topography, driving ice-flow convergence and divergence, associated thickness changes of the ice mass, and consequently patterns of melting and erosion (Hall and Sugden, 1987). For example, protracted high rates of erosion and sediment transport over geological times at locations of ice streams suggest a positive feedback by which large pre-glacial valleys may have focussed ice flow during early ice-sheet development, being further scoured by enhanced glacial action, and thus remaining sites of particularly high sliding rates and sediment transfer over successive cycles of glaciation (Glasser, 1995; Glasser and Hall, 1997; Kessler et al., 2008; Jamieson et al., 2010). Generalized spatial models for ice-substrate interactions have been based on the zonation of thermomechanical conditions within ice sheets (Dyke, 1993; Kleman, 1994; Kleman et al., 2008; Bennett and Glasser, 2009). These models mathematically synthesize the above-mentioned concepts into idealized belts of thermal and dynamic balance within an ice sheet. They show that there are ideally three regions can be identified: 1) an interior region of cold, low-mobility basal ice with little or no erosion, 2) an intermediate belt of partly to mostly warm-based ice with net erosion, and 3) an outer margin of prevalent erosion and deposition. Obviously, many potential combinations of paleogeography, subglacial topography and regional climate gradients will result in actual thermo-mechanical configurations for ice sheets which differ from

idealized models. One of the main generalizations drawn from the several studies (e.g., Atkins et al., 2002; Lloyd Davies et al., 2009; Hambrey & Fitzsimons, 2010; Hambrey & Glasser, 2012) is that reduced erosion occurred below cold-based portions of former ice sheets, and that actually landscapes are mostly preserved with little modification by the long-term permanence of ice sheets. In correspondence, minor sediment production takes place (Hall and Sugden, 1987; Sugden et al., 1991; Kleman, 1994; Näslund, 1997; Siegert, 2001; Hättestrand and Stroeven, 2002; Sugden and Denton, 2004; Stroeven et al., 2006; Kleman and Glasser, 2007; Jamieson et al., 2010). However, most active sediment production and transfer should take place associated with formerly active ice streams, presently recognizable by linear erosional troughs of regional extent and by the presence of large 'trough-mouth fans' at their distal outlets (Vorren and Laberg, 1997; Stokes and Clark, 1999; Ó Cofaigh et al., 2003; Kleman and Glasser, 2007). Such inferences have been recently supported by the recognition and the cosmogenic-nuclide dating of negligibly eroded relict surfaces in areas occupied by cold-based portions of late Quaternary ice sheets (e.g., Fabel et al., 2002; Hättestrand and Stroeven, 2002; Harbor et al., 2006; Briner et al., 2006).

A fundamental problem for the quantification of erosion through landform analysis is the difficulty to constrain the variability of erosion rates in space and time through different glacial cycles and within a single glacial cycle, as modulated by long-term changes in glaciological and topographic conditions (Porter, 1989; Glasser and Hall, 1997; Kleman et al., 2008). In other words, large-scale landscapes observable today are the end product of a complex succession of events that cannot easily be reconstructed in its progressive steps through time. To this aim, the chronological resolution of processes and events on geological timescales may be better examined by means of stratigraphic studies, although these still provide only rough estimates. On the other hand, the likelihood of reduced sediment yield from glaciated basins being related to insufficient surface hydrological activity in post-/interglacial phases is rather scarce, since large glaciated regions occur in climate belts which necessarily have high enough precipitation rates to feed ice-sheet growth in the first place. The generalization that sediment yields from glaciated basins is higher than yields from colluvial-alluvial basins is thus not always valid, and subject to reassessment after a sufficient body of research will have provided the necessary quantitative data.

3.3.2. Sediment fluxes

The second, more direct research approach consists of measuring sediment yields from present proglacial (fluvial, glaciofluvial and fjord) systems and at the outlets of glaciated highland basins. Systematic monitoring of water discharge and sediment transport in meltwaters is carried out over protracted times or at specific time intervals, to quantify local sediment yields. Average erosion rates are commonly obtained by dividing annual to decadal sediment volumes by the area of the source basin. The technical challenges and costs of such endeavours have resulted in relatively few published data so far. Various authors and data compilations recorded sediment yields ranging over several orders of magnitude, both as bedload and suspended load, showing on one hand the involved environmental variables are not clear yet, and that glaciers cannot always be assumed to be extremely efficient erosive agents (Østrem, 1975; Parks and Madison, 1984; Bogen, 1989, 1996; Andrews et al., 1994; Hasholt, 1996; Rihimaki et al., 2005; Swift et al., 2005; Knudsen et al., 2007; Koppes et al., 2009; Cowton et al., 2012; see reviews by Hallet et al., 1996; Gurnell et al., 1996; Koppes and Montgomery, 2009). Methodologically, the basic assumption of these works is that bedload and suspended-load measurements in water courses fed solely or mostly by ablation should closely reflect the clastic output of glacial systems to the sediment cascade basinward. While this is probably justified at short temporal scales of up to a few decades at most, depending on available data coverage, it cannot be automatically extrapolated to changing rates of glacial sediment production on

longer time scales (Harbor and Warburton, 1993; Delmas et al., 2009). Especially since the 'snapshot' perspective of present observations is not representative of the variability of processes and process intensities that accompanies the development of glaciated basins over thousands to millions of years. Koppes and Hallet (2002, 2006) convincingly demonstrated that calculations of denudation rates in glaciated catchments based on stratigraphic evidence provide lower average values by up to two orders of magnitude than obtained from direct sediment yield measurements extended over just a few decades. Furthermore, such studies suffer from uncertainties related to the inherent variability of sediment output in glacial systems characterized by different properties and of different areal extent (Hallet et al., 1996). For example, studies of non-glaciated portions of presently glaciated basins (e.g., Meigs, 1998; Owen et al., 2003; O'Farrell et al., 2009) demonstrate that paraglacial highlands also undergo relatively high rates of erosion and their specific sediment yield adds a positive contribution to the sediment budget of glaciated basins. However, its origin is physically unrelated to the direct action of glaciers. Bogen (1996) demonstrated great interannual variability in sediment yields from four Norwegian glaciers; the broad range of values was probably related to unpredictable adjustments in the position and hydraulics of subglacial drainage conduits. The number of systems subject to direct measurements over long enough timespans is not yet sufficient to assess major factors and biases controlling the variability of sediment output.

3.3.3. Stratigraphic analysis

The third line of research is to quantify sediment production rates from glaciated basins with thick, Neogene to Quaternary stratigraphic successions at the margins of glaciated terrains. Recent progress in dating and provenance analysis has increased the time-resolution of these projects. These stratigraphic studies address both shallow-marine successions along formerly glaciated shelves (e.g., Piper et al., 1994; Jaeger et al., 1998; Dowdeswell et al., 2010; Hjelstuen et al., 2012), terrestrial basins in proximity of mountain chains (Hinderer, 2001; Kuhlemann et al., 2002; Delmas et al., 2009; Charreau et al., 2011; Dehnert et al., 2012) and proglacial lake basins (Desloges and Gilbert, 1995; Leonard, 1997; Hinderer, 2001; Loso et al., 2004). Fjord basins have received particular attention due to their bathymetric configuration, which offers excellent potential to trap sediments supplied by land-bound glacial sources and reduces bypass toward the more distal marine realm, thus preventing sediment-budget underestimates (e.g., Andrews et al., 1994; Elverhøj et al., 1995, 1998; Jaeger and Nittrouer, 1999; Koppes and Hallet, 2006). Calculation of sediment-volume repartitioning between different stratigraphic intervals provides estimates of variable sediment output through time for a given source area. Several authors have pointed out that the results of such studies are inevitably subject to a number of uncertainties (Harbor and Warburton, 1993; Leonard, 1997; Hinderer, 2001; Koppes and Hallet, 2006; Delmas et al., 2009). These uncertainties are due to the lack of knowledge on whether and how the original source area and denudation mechanisms changed through time, and on whether and how much sediment could be stored in periglacial and paraglacial conditions within basins. Although doubts on absolute volumes of sediment output may be hard to dispel, estimates of the relative variability of such values with time are valid to a first approximation to inform stratigraphic prediction. Major studies and reviews (e.g., Elverhøj et al., 1995; Hallet et al., 1996; Leonard, 1997; Hinderer, 2001; Delmas et al., 2009) have recognized that maximum sediment evacuation from glaciated environments does not correspond to glacial and stadial maxima (i.e. maximal surface extent of glaciers and ice-sheets), but to the following interglacial/interstadial phases of glacial retreat. That is, most available debris can be mobilized by a combination of reactivated surface hydrology, exposure of broad expanses of loose regolith, and still scarce pedo-vegetative cover. Subsequent phases of glacial (re)advance however push a great volume of sediment toward distal depositional settings, such as slope basins in continental shelf settings (Elverhøj et al., 1995; Diekmann et al., 2000; Dowdeswell et al., 2010). The evidence from long-term records (e.g., Leonard, 1997;

Delmas et al., 2009; Norton et al., 2010; Hjelstuen et al., 2012) confirms the importance of a 'paraglacial' peak in sediment shedding from deglaciated basins, as alluvial and slope systems adjust to the excess of relict regolith (Church and Ryder, 1979; Church and Slaymaker, 1989). On the other hand, the contrasting conceptual model envisaging an initial wave of enhanced erosion over previously undisturbed terrains at an ice-age inception has been confirmed in some case studies (e.g., Shuster et al., 2005; Charreau et al., 2011).

3.4. *Glaciotectonic structures*

3.4.1. Origin

Glaciotectonic structures originate from the advance of an ice front. Superimposed glaciotectonic deformation leads to glaciotectonic complexes that occur when ice sheets periodically re-advance and retreat. In fact, the majority of preserved glaciotectonic complexes from the Pleistocene were truncated by the advancing ice that created the complex, or by a subsequent advance/re-advance, or even contemporaneous erosion during the deposition of contemporary outwash sequences. At the base of the translating ice, shear deformation creates drag folds which are superimposed by a cataclastic breccia—the glacitectorite. Nearly all hilly areas in the Netherlands were created or at least affected by glaciotectonic deformations, and the features are included in the mapping of near-surface deposits. Glaciotectonic structures have the following characteristics:

- Very diverse and from micro- to macro-scale, i.e. from mm to more than 100 m.
- Strong glaciotectonic deformation common around ice-sheet margins
- Shear stress concentrated along weaker strata
- Thrust depth varies between 50-500 m
- Structures disrupt seal integrity and may be zones of high permeability

3.4.2. Classification

Pedersen (2014), based on phenomena observed in Denmark, proposes a classification of the architecture of glaciotectonic complexes based on four orders of surfaces that define the structure:

1. First-order surfaces include décollement surfaces and glaciotectonic unconformities. The décollement surface limits the glaciotectonic complex.
2. Second-order surfaces are related to the thrust faults including ramps and flats and form the boundaries of the individual segments building up a complex.
3. Third-order surfaces describe folded beds, including anticlines and synclines
4. Fourth-order surfaces comprise all small-scale folds and faults: kink bands, conjugate faults, box folds.

Below the first-order surface, ordinary flat lying planar bedding occurs and above this, structures of second- to fourth-order elements are present. The top of the glaciotectonic complex is a first-order surface as well and eventually may be replaced by an erosional unconformity associated with younger glaciotectonic complexes.

3.4.3. Depth of deformation

Høyer et al. (2013) use airborne electromagnetic data, high-resolution seismic data and borehole information to document the complexity of deeply rooted thrust sheets of the Varde hill-island (Denmark) that comprises Miocene to Middle Pleistocene deposits. The deformation spans at least 150 m of sediment thickness, placing this complex among the largest glaciotectonic features. For this site it is interesting to see how various glacial

phenomena are superposed: (1) erosion of Miocene deposits by subglacial tunnel valleys and infill of these valleys occurred in pre-Elsterian and Elsterian time, (2) two phases of glaciotectonic thrusting during the Saalian glaciation, (3) erosion by the Saalian ice sheet removing a significant part of the thrust complex and (4) periglacial and postglacial erosion of the hill-island excavating the glaciotectonic elements. Palaeoglaciological calculations suggest that the Saalian ice sheet that caused the thrusting was thick, had a steep profile, rested on a permafrost wedge and moved slowly, which contrasts with the highly mobile, thin ice lobes of the Last Glaciation.

The ice pushed ridges in the central part of the Netherlands were formed at the southernmost extent of the Saalian glaciers. Based on the height of the ridges and the depth of the glacial basin formed by glacial erosion, the thickness of the ice sheet can be estimated. The highest ridge at de Veluwe amounts to 110 m and the deepest glacial basin, the IJsseldal, is over 125 m deep. This means that the ice sheet thickness was approximately 235 m (source: <http://www.geologievannederland.nl>) relative to the ridge top. This gives a rough estimation of the maximum depth of deformation for the Netherlands.

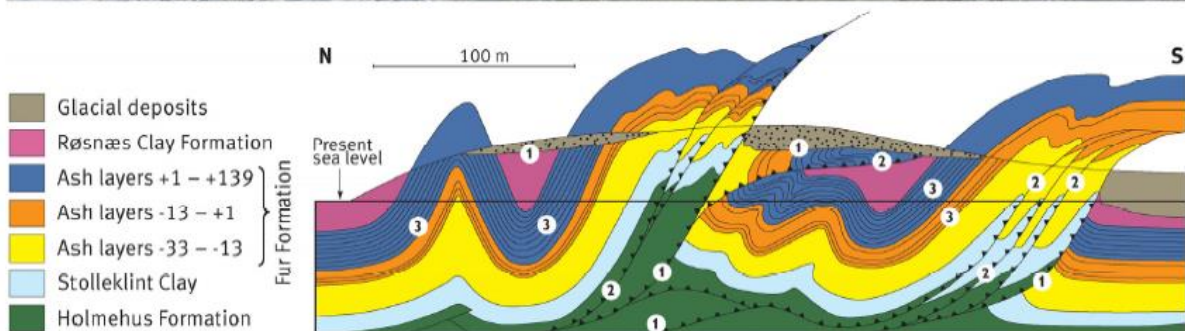


Figure 3-1 Example of three orders (encircled numbers) of glaciotectonic surfaces at Fur Knudeklint (Denmark; from Pedersen 2014).

3.5. Tunnel valleys: generalities and erosive potential

Tunnel valleys represent probably the most extreme landforms related to direct erosion of ice-sheet substrates. As implied by the name, they consist of long and variably deep depressions with linear to moderately sinuous development in plan-view, ranging in length from a few kilometres to over 100 km. Their size commonly ranges from a few tens of metres up to a few hundreds of metres depth and up to a few kilometres in width. The occurrence of these features over the substrate of glaciated basins, their trends commonly

being oblique to those of prevalent regional drainage patterns, their association with glacial and glaciofluvial deposits, and more convincingly their association with Pleistocene late-glacial landscape elements, point to an origin strictly related to subglacial processes of erosion and sediment transport (Booth and Hallet, 1993; O’Cofaigh, 1996; Van der Vegt et al., 2012). In fact, the geographic distribution of the numerous recognized examples of such landforms is strictly tied to the locations of Pleistocene and late-Palaeozoic continental-scale ice sheet margins. This includes the present territory of the northern Netherlands and the southern Dutch offshore. Currently or very recently formed valleys have been identified at the margins of the Antarctic ice sheet and of Icelandic ice caps (Lowe & Anderson, 2003; Björnsson, 1996). The exact mechanisms producing tunnel valleys are currently still an object of debate in scientific literature. Three main hypotheses are currently under consideration to explain most erosional and depositional traits of tunnel valleys:

- Local mobilization of loose subglacial substrates by enhanced creep in correspondence of particularly active basal-ice streams.
- Regular discharge of subglacial meltwaters in proximity to ice-sheets margins that gradually relocate in time (time-transgressive excavation of tunnel valleys).
- Occasional, catastrophic action of extreme discharge events related to subglacial megafloods (O’Cofaigh, 1996; Kehew et al., 2012).

The third hypothesis recently gained much attention in the literature, although consensus is reached that different processes may combine in time to produce the final landform. Depositional processes occurring beyond the ice margins well after ice-sheet retreat also contribute to this. In addition, Quaternary case studies point to the possibility that some tunnel valleys may actually be related to strongly time-transgressive subglacial and proglacial process sets, taking place during separate phases of glaciation. The hypothesis that genesis of tunnel valleys takes place mostly during terminal phases of stagnation and retreat of ice sheets, however, is confirmed by the common observation that the clastic infills of these depressions generally present an upward-decreasing evidence of ice-related depositional processes. The topmost units present a distinctly glaciofluvial/ alluvial proglacial facies and the largest valleys are actually partially left unfilled.

Of particular relevance here are substrate properties which enhance the formation and enlargement of tunnel valleys. Soft substrates consisting of unconsolidated sediment/regolith or poorly cemented sedimentary rocks have been repeatedly observed to be favourable to tunnel-valley formation (e.g. Wingfield, 1990; Eyles and De Broekert, 2001; Boulton et al., 2009; Van der Vegt et al., 2012). This differs for example from hard bedrock, which commonly forms a barrier to the establishment of protracted subglacial linear erosion and favours mostly accumulation (i.e. eskers). In regions where tunnel valleys are widespread, the presence of eskers can be a reliable indicator of specific locations where subglacial meltwaters encountered resistance to erosion, and were forced to a depositional regime (Kehew & Kozlowski, 2007; Kehew et al., 2012). However, other kinds of ice-marginal deposits, such as outwash fans and proglacial lacustrine deltas, can be associated with the distal termini of tunnel valleys and function as efficient pathways for subglacial drainage and sediment routing during early deglacial stages. Beside consolidation, heterogeneity in substrate permeability (and thus texture, age and pedogenic state) is probably the main control for the occurrence and enhanced development of valleys. Partial drainage and percolation of subglacial meltwater through the substrate has been noticed to reduce the effectiveness of erosion and locally form a barrier to longitudinal extension of the valleys (e.g. Glasser and Sambrook-Smith, 1999; Jørgensen and Sandersen, 2006; Van der Vegt et al., 2012).

One final consideration of particular relevance is that available subglacial drainage pathways inherited from previously active tunnel valleys, formed during preceding glacial phases, are likely to focus the location of new valleys systems. Recycling of subglacial aquifers has been recognized especially by sedimentological studies of Quaternary composite tunnel-valley fills at various locations worldwide (e.g. Piotrowski, 1994; Jørgensen and Sandersen, 2006; Kehew et al., 2012). Focussed activity over multiple glacial cycles has produced particularly deep erosional troughs, although more commonly the expansion of such mega-conduits occurs horizontally. Studies converge toward the conclusion that the aggradation of such complex valley fills is not only related to time-transgressive deposition, but also to repeated large-scale erosional events at the same location. For example, at the southern margin of the Scandinavian Ice Sheet during the Elsterian deglaciation (Marine Isotope Stage 12), particularly deep tunnel valleys were formed in the northern Netherlands, reaching down to about 500 m below the present surface, probably in connection with favourably warm paleoclimatic conditions (Van Dijke and Veldkamp, 1996).

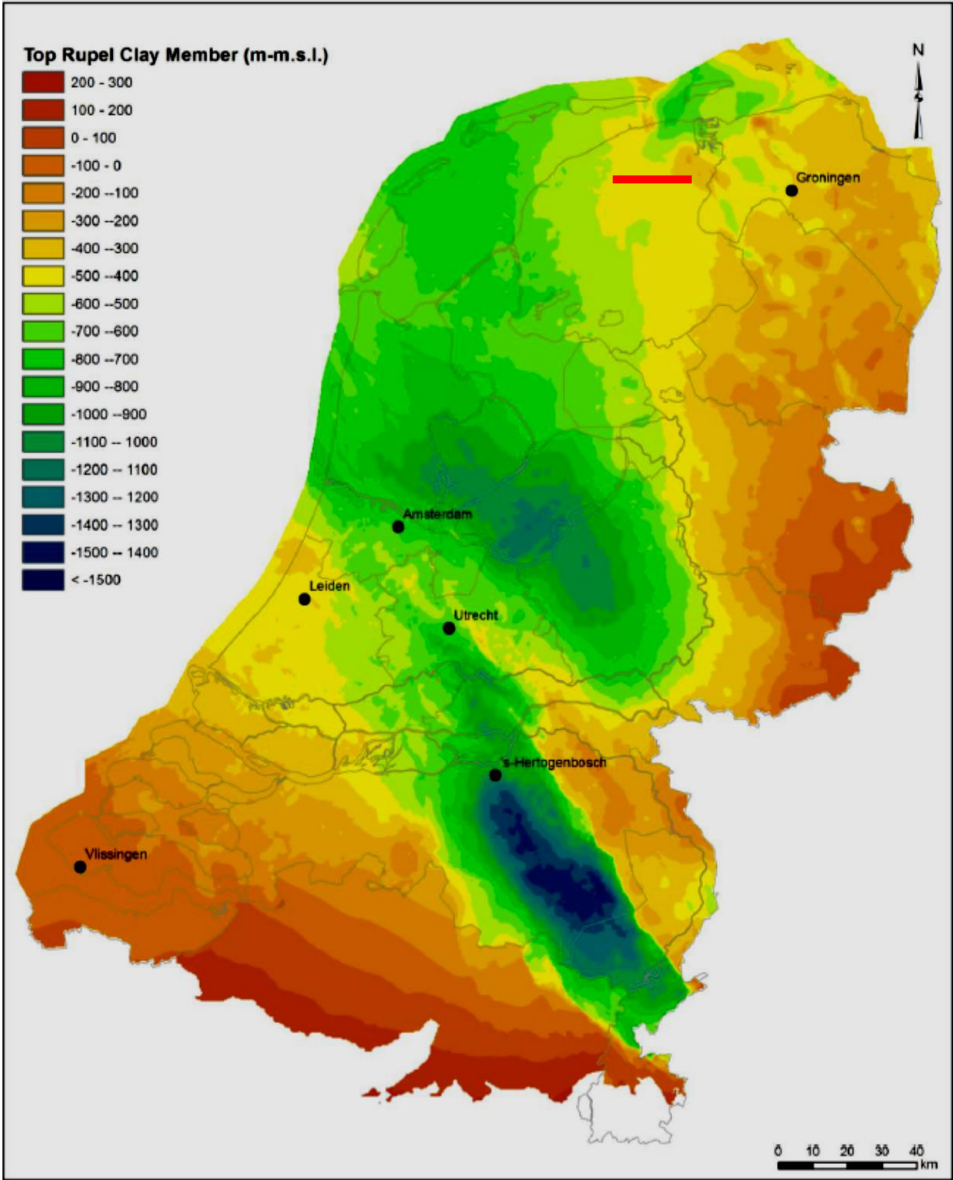


Figure 3-2 Depth of the Top Rupel Clay Member (from Vis and Verweij, 2014). Red line in northern part of the Netherlands indicates locality of Figure 3-4).

3.6. Discussion

3.6.1. Depth of the Boom Clay

In view of a possible ice-sheet incursion over the Netherlands during a future glacial cycle it is necessary to evaluate the likelihood for the Boom Clay (Rupel Clay Member according Dutch Stratigraphic Nomenclature) to be affected by glacial erosion. In particular scouring underneath deep tunnel valleys, which would compromise its viability for long-term storage of radioactive waste, should be considered. According to recent datasets (Vis and Verweij, 2014; Figure 3-2), the Boom Clay crops out at low altitudes in Belgium and in few small outcrops along the central Dutch-German border. Over essentially all of the Dutch territory, the unit's top occurs below the surface, at depths greater than ~500 m below sea level along a central belt oriented approximately NNW-SSE through the country. The deepest burial for the unit's top (over 1000 m below sea level) is registered along a NW-SE belt crossing Noord Brabant and northern Limburg, approximately in correspondence of the Ruhr Valley Graben, and in a similarly oriented depocentre underlying the provinces of Noord Holland, Utrecht, Flevoland and Overijssel (the Central Netherlands Basin). In the northeastern and southwestern parts of the Dutch territory the unit's top is at depths shallower than 400-500 m, with a clear shallowing trend towards the Belgian and German borders. Over most of the Dutch territory, the Boom Clay varies in thickness from a few tens of metres up to ~100 m. It attains its minimum local thickness below the province of Zeeland (<~25 m, whereas maximum thickness (mostly >70 m and up to ~200 m) is reached in the Ruhr Valley Graben.

3.6.2. Erosion potential

Considering the available geological knowledge and generalized conceptual models of ice-sheet erosion (see previous sections), it is not to be expected that the onshore Dutch territory will be subject to major subglacial erosion during a single postulated cycle of glaciation. More specifically, it is very unlikely that the Boom Clay will be affected by subglacial erosional processes. The main points leading to this inference are the following:

- Both paleo-geomorphic evidence and latitudinal considerations suggest that previous glacial occupation of the Netherlands and neighbouring countries was mostly by 'warm-based' (i.e. temperate) ice-sheet margins and associated proglacial belts. As briefly discussed above, the outermost belts of ice sheets are commonly subject to a relatively less effective erosional regime compared to inner areas leading to the ice-sheet spreading centre/core. Commonly, the long-term balance of geomorphic activity at these marginal positions leads to associations of depositional landforms, rather than dominantly erosional landscapes. This is clearly evidenced by the so-called Elsterian Peelo valleys, which are tunnel valleys in the northern part of the Netherlands with depths up to ~600 m, which are completely filled by proglacial deposits (Figure 3-4). Depending on the intensity of glaciation and on the extent of a future Scandinavian ice-sheet advance, such evidence from previous glacial cycles confidently suggests that the location of the Netherlands should maintain the country that can obtain a proglacial to outer marginal setting.
- A complex subglacial topography is a prerequisite for channeling basal ice-sheet flow into convergent patterns which may locally enhance erosion; this prerequisite is missing over the essentially flat, unconsolidated surface of the Dutch territory. Furthermore, basal-ice sliding rates directly control mechanical erosion, and are strongly modulated by subglacial water pressure; the essentially unconsolidated and permeable nature of the Dutch surface imply scarce possibility to develop subglacial overpressured aquifers, and thus reduced erosive action.

- The most intense erosive action by tunnel valleys has been recorded in correspondence of drainage pathways which were active over different (successive?) glacial cycles; given the present-day evidence of recent tunnel-valley formation in the Netherlands, it is to be excluded that future erosional depths in below the top of the Boom Clay can be attained anywhere on the Dutch onshore.

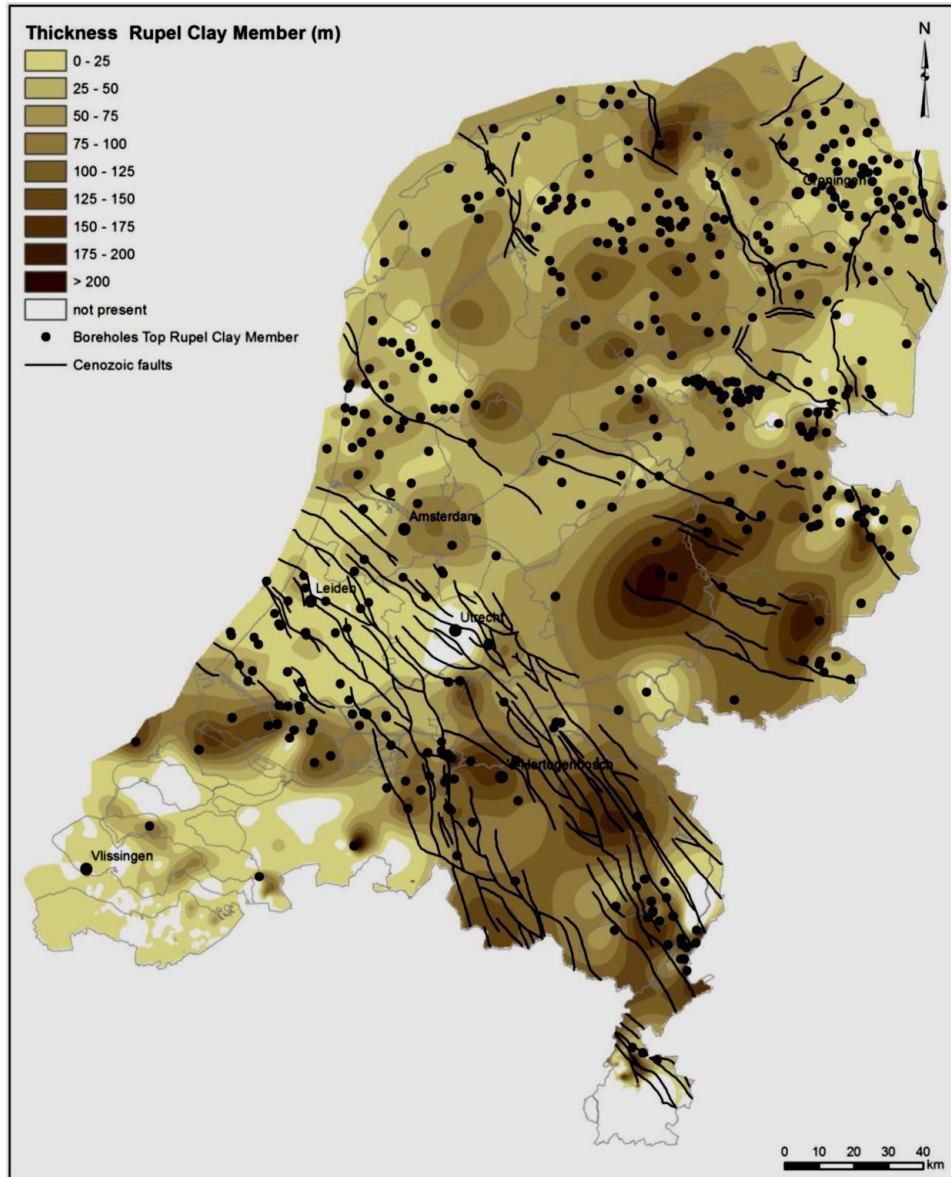


Figure 3-3 The thickness of the Rupel Clay Member (from Vis and Verweij, 2014).

3.7. Relevance and synthesis for the safety case:

Isolation

Cycles of ice-sheet advance and retreat can exert considerable erosive action over the Earth's surface, especially in the temperate high latitudes of northern Europe, where wet-based ice sheets are expected to be more mobile and thus more effective in acting on the substrate.

The geographic position of the Netherlands implies that the country should lie outside the range of maximum potential erosion operated by an ice sheet nucleating over Scandinavia. Additional factors contributing to this evaluation are the lack of a hard substrate and complex topography over Dutch territory, which would prevent focusing (sub)glacial erosion along local ice streams, and the fact that long-term sedimentation budgets at and beyond ice-sheet margins commonly attain a positive balance, owing to marginal glaciofluvial, glaciolacustrine and distal subglacial deposition.

Development of subglacial tunnel valleys has the maximum potential for localized erosion; however, the probability for such major systems to occur on Dutch territory is moderate over the northern onshore and southern offshore portions of the country, and negligible over the central and southern Dutch onshore.

Subcrop depths for the top of the Boom Clay Formation are mostly beyond reach by subglacial erosive processes that may reasonably be expected in the frame of a possible oncoming glacial cycle. Nevertheless, the maximum observed depth of tunnel valleys of ~500 m in the Netherlands is locally within reach of the Boom Clay depth. Although tunnel valleys may scour down to several hundred metres below the surface, this extreme erosive potential is attained generally in composite valley systems developed over successive glacial cycles, and should thus not represent a reasonable problem on the Dutch onshore.

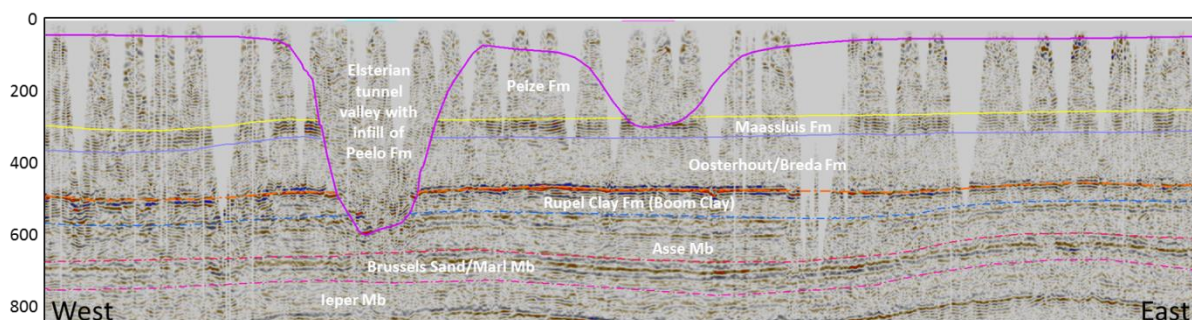


Figure 3-4 Seismic profile showing an Elsterian tunnel valley incised into the Boom Clay (for locality see Figure 3-2). Width is ~25 km, depths are approximately.

Delay & attenuation

It should be considered that development of subglacial tunnel valleys is more likely to affect the host rocks overburden (geosphere). Erosion and/or the formation of subglacial tunnel valleys may interfere with dilution and dispersion of radionuclides. The subglacial drainage may bring radionuclides into the hydrosphere as well.

Engineered containment

The integrity of the engineered containment (the waste containers) only can be affected during the thermal stage (<~10 kyr). Anticipated future glaciations will not occur in the next ~55 kyr and therefore their predicted effects are irrelevant.

4. Effects of glacial loading and unloading

Associated with glacial loading and unloading, two types of processes play a role:

1. Coupled thermal, mechanical and hydrological processes.
2. Clustering of seismic events after or during unloading (neotectonics vs glacial rebound).

4.1. *Coupled mechanical-hydraulic effects*

Small changes in pore water volume that occur when a porous medium is mechanically compressed (loaded) or expanded (unloaded) both result in changes in pore water pressure (e.g., van Weert et al., 1997; Domenico and Schwartz, 1998). In groundwater flow modeling, it is important that not only the timing, duration and extent of glaciations are considered but also the direction of glacial forcing, equivalent to the direction of ice flow (Boulton and Curle, 1997). In highly permeable rock these transient changes in fluid pressure will quickly dissipate. However, in low-permeability units like shales, clay, or crystalline rocks, the effects of loading and unloading can induce anomalous fluid pressures that require thousands of years to return to equilibrium conditions (e.g., Neuzil, 1993). Although clay is less porous, it is highly water-saturated and mechanically compressible. Consequently, a mechanical load, such as an ice sheet, may force the water out of the clay. The release of this consolidation water is likely to enhance the transport of radionuclides into shallower groundwater systems (Figure 4-1; e.g. Boulton et al., 1993; Boulton and Curle, 1997)).

Simultaneously with the mechanical loading, melted ice will infiltrate underneath the ice sheet, which will increase the hydraulic pressure and gradient. Melt waters at the base of the ice sheets will inject water into subglacial permeable beds under a maximum head equivalent to the total ice pressure. As such, the mechanical and hydraulic pressures are coupled and affect the expulsion of formation waters, both from aquitards and through aquifers, respectively. The thickness of the ice sheet (the load) is thus coupled to the hydraulic head and the depth to which this is elevated.

Using numerical models, Boulton and Curle (1997) simulated melting beneath the European ice sheet for the last two glacial cycles and the consequences for groundwater flow. Their results show that the thick Mesozoic and Cenozoic aquifers of the Netherlands and Germany had sufficient transmissivity to drain all subglacial meltwater. During these glacials groundwater heads, potential gradients and fluxes were very much larger than during interglacials. Also the role of proglacial permafrost is important in sustaining fluid overpressures in the ice sheet terminal zone. The protruding-retreating behavior of ice-sheets during a glacial cycle would have induced major pressure pulses that were driven through aquifer systems leading to a complete reorganization of the groundwater system.

Klemann and Wolf, (1998; Figure 4-2) showed that stress anomalies may propagate to depths of >50 km depending on the load and the increased horizontal stresses remain even after 10 kyr after ice sheet retreat. During the most recent North American glaciation, during the latter part of the Wisconsin Stage (26 to 13,3 kyr ago), ice sheets extended to about 45 degrees northern latitude with thicknesses up to 3 to 4 km (Richmond and Fullerton, 1986). In the model scenarios of Bense and Person (2008) a maximum ice sheet thickness of 3200 m during this Last Glacial Maximum (LGM) was applied, a scenario that predicts an elevated hydraulic head down to 5 km.

For the Dutch case: there is a wide range of scenarios for the geometry of the northern European ice sheets during the LGM as well as for the ensuing glacio-eustatic and isostatic responses. Ice sheet models by Grollmund and Zoback (2003) infer a maximum thickness of ~1700 m over Norway, based on published information on temporal and spatial ice thickness changes from Mangerud et al. (1979), Andersen (1981) and Lundqvist (1986).

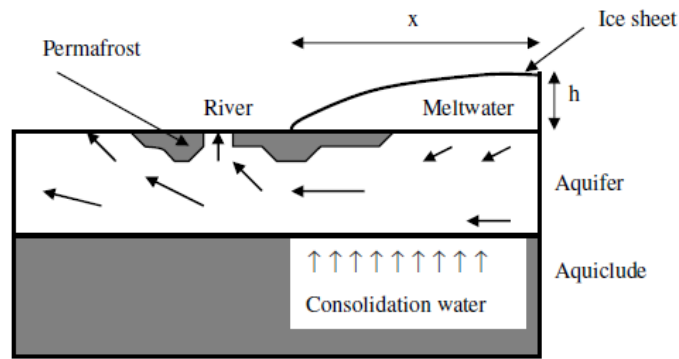


Figure 4-1 Schematic cross-section showing the groundwater flow patterns during glaciation (modified after Boulton et al., 1993).

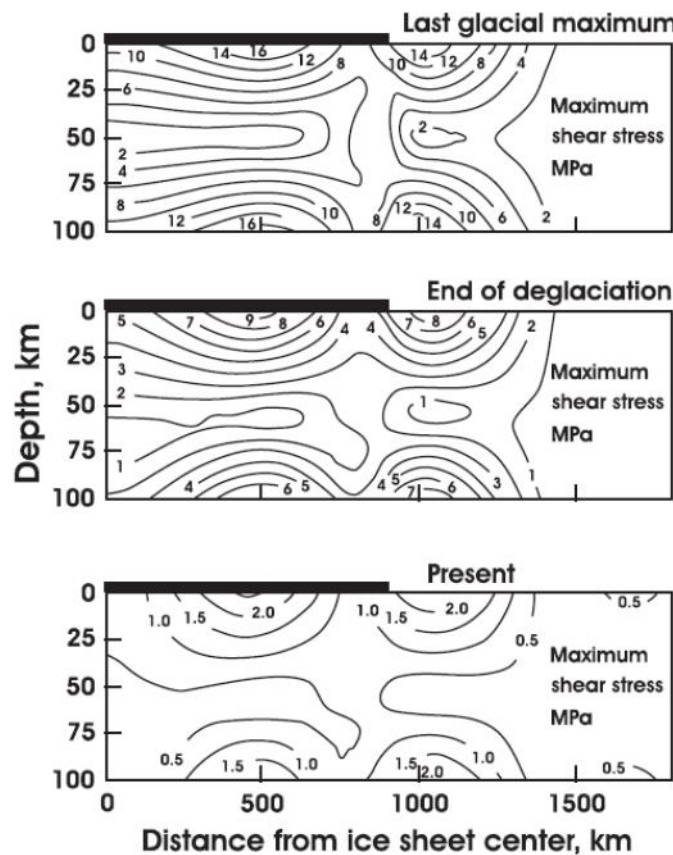


Figure 4-2 Vertical and horizontal effects of ice sheet loading during different stages of the a glacial cycle (from Kleman and Wolf, 1998).

The hydrodynamic consequences of a glaciation/deglaciation cycle within an intercratonic sedimentary basin on subsurface transport processes is assessed using numerical models by Bense and Person (2008). In their analysis the effects of mechanical ice sheet loading, permafrost formation, variable density fluids, and lithospheric flexure on solute/isotope transport, groundwater residence times, and transient hydraulic head (100 m = 1 MPa) distributions are considered. This study was specifically centered around improving the management of groundwater resources in formerly glaciated basins and evaluating the viability on geological timescales of nuclear waste repositories located in intracratonic basins at high latitudes. Although this study concerns the advance and retreat of the

Northern American Laurentide Ice Sheet during the Last Glacial Maximum (20 ka B.P.), the insights gained are applicable for the Dutch case (past, present and future) as well.

The main findings of this study are that:

- Fluid flow and recharge rates are strongly elevated during glaciation as compared to non-glacial periods.
- Steady-state hydrodynamic conditions in these basins are probably never reached during a 32.5 kyr cycle of advance and retreat of a wet-based ice sheet.
- Therefore, present-day hydrogeological conditions across formerly glaciated areas are likely to still reflect the impact of the last glaciation and associated processes that ended locally before 10 ka B.P.
- Characteristic spatial patterns of underpressure and overpressure occur in aquitards and aquifers, respectively, as a result of recent glaciation.
- The calculated emplacement of low salinity, isotopically light glacial meltwater along basin margins is roughly consistent with observations from formerly glaciated basins in North America.

Whereas Bense and Person (2007) focus on the increased flow and recharge rates during ice loading, Grollmund and Zoback (2003) state that deglaciation-induced stress changes on pore pressure are such that they affect the leaking behavior of reservoir faults. An induced horizontal stress increase caused by lithospheric bending resulting from deglaciation can cause a pore pressure increase (as discussed in section 4.2).

4.1.1. Isostasy vs. hydrology

The movement of water on the surface of the Earth, both as water and as ice, during a glacial cycle acts as a load upon the lithosphere. The Earth deforms in response to this force, subsiding under the load of an ice sheet or full oceanic basin, and rebounds once the ice sheets melt or water is removed from the oceanic basins (Figure 4-3). The maximum isostatic deflection of the lithosphere by an ice load should be about 30 % of the ice sheet thickness (e.g., Brevik and Reid, 2000; Howell et al., 2000). Thus, lithospheric flexure by ice loading results in lowering the ice sheet and land surface elevation. Field studies indicate that during ice sheet retreat the great majority of the isostatic rebound (e.g., 75 % of the maximum deflection) happens while the ice is thinning during retreat (e.g., Brevik and Reid, 2000). After this phase of 'restrained' rebound, the remaining topographic depression (now about 25 % of the maximum deflection) will be reduced through "postglacial" rebound (see Table 4-1). Today, typical northern European uplift rates are of the order of 1 cm per year or less. This is clearly shown by the GPS data obtained by the BIFROST GPS network (Johansson et al., 2002). Studies suggest that rebound will continue for about at least another 10,000 years. The total uplift from the end of deglaciation depends on the local ice load (thickness) and could be several hundred meters near the center of rebound.

The surface elevation effect imposed by the flexural response to ice loading is expected to have a strong effect on hydrogeology and will reduce the effective hydraulic head imposed by the ice sheet (Bense & Person, 2008). The isostatic rebound during and after ice retreat will result in a surface elevation rise, which will enhance the topographic gradient to drive groundwater flow.

Table 4-1 - Ice thickness, loading and unloading effects (vertical only) based on estimates discussed in text.

Maximum ice thickness (m)	Subsidence (m) - loading effect at maximum	Deglaciation uplift (m) - <i>elastic</i>	Postglacial rebound (m) Slow viscous flow	Far field (flexural) forebulge uplift
1000	300	225	75	12
2000	600	450	150	24
3000	900	675	225	36
4000	1200	900	300	48

4.2. Seismicity during deglaciation

Deglaciation could be a possible candidate to trigger a sudden increase in fault activity due to its relatively rapid (on a geological time scale) unloading of the crust. Mörner (1978) was the first to describe such link between deglaciation and faulting in Scandinavia. In various publications, e.g. Mörner (2013), 59 seismic events were reported in the Swedish Paleoseismic Catalogue that are related to ice retreat. Figure 4-4 shows that the maximum earthquake magnitude in Sweden increases dramatically back in time. The magnitude was below 4.8 during the last century, >5.5 in historical records of the last 600 years, ~7 in paleoseismic records of the last 5000 years and well above 8 in multiple paleoseismic records of the last 11,000 years. This implies that a meaningful long-term hazard assessment can only be achieved if the paleoseismic records of past earthquakes are included.

Following the proposed link between deglaciation and faulting, many studies of seismicity in areas that are undergoing post-glacial rebound were carried out (e.g. Stein et al., 1989; Dehls et al., 2000; Firth and Stewart, 2000; Fjeldskaar et al., 2000). Most studies focused on the interplay of deglaciation and neotectonics (e.g. Knight, 1999; Mörner et al., 2000; Muir-Wood, 2000), both at active margins (Thorson, 1996) as well as in intraplate settings (Grollimund and Zoback, 2001). Only since the last decade, numerical simulations also allowed analyses of the far field effects of glacial loading on the regional stress field (e.g. Wu and Hasegawa, 1996). Brandes et al., (2011) illustrate how advancing ice-sheets can cause far field extension, which might trigger reactivation of pre-existing normal faults. Geomechanical glacial rebound models predict that significant influence of the ice-sheet (un)loading on stresses in the crust can extend as far as 300-500 km from the ice-sheet margins (Johnston et al., 1998; MuirWood, 2000). The largest effects are located in the forebulge 150 km from the margin of the former ice-sheet (Figure 4-3).

4.2.1. Deglaciation effects below ice sheets

Numerical modeling of the retreat of the Laurentide ice sheet that covered large parts of the northern United States until ca. 20 ka, shows a change in the stress field south of the maximum ice extent. This caused seismic strain rates to increase by about three orders of magnitude and may explain activity of the New Madrid Fault (Grollimund and Zoback, 2001). This study also predicts that the high rate of seismic energy release observed during late Holocene time is likely to remain essentially unchanged for the next few thousand years.

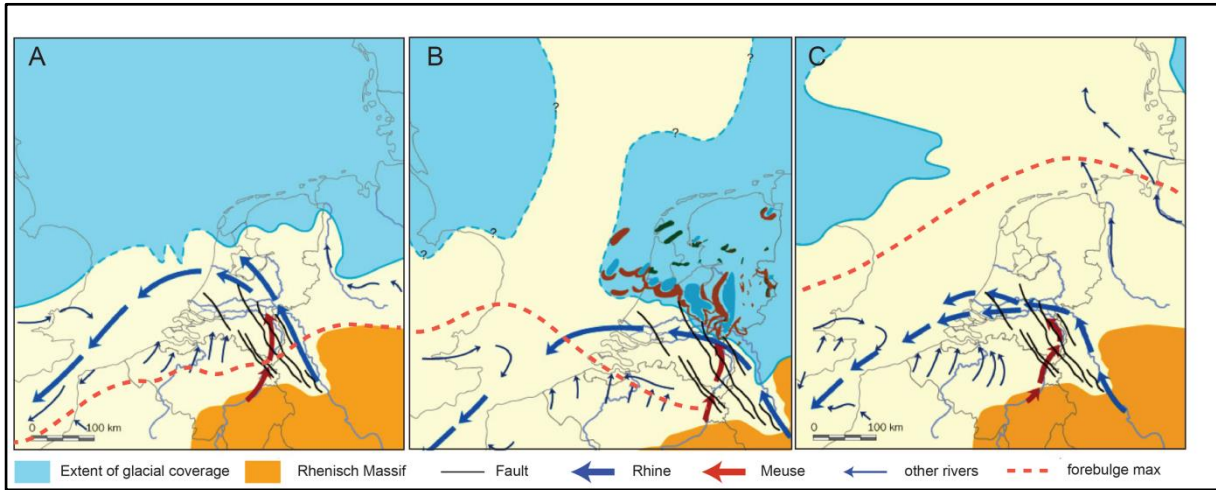
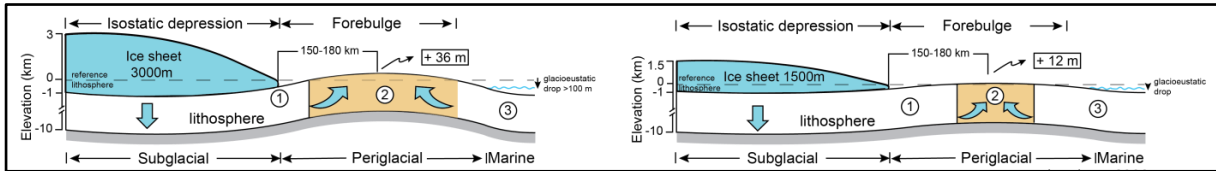


Figure 4-3 Upper: locations of isostatic depression, forebulge and non-affected areas in relation to ice-sheet thickness (3000 m vs. 1500 m). Note that with thinner ice both the distance from the ice margin and the width and elevation of the forebulge area decreases. Bottom: The position of these domains is illustrated for three different ice-advance scenarios with analogy to A) the Elsterian (475-410 kyr ago), B) Saalian (370-130 kyr ago) and C) Weichselian (115-10 kyr ago) ice-sheet configurations (Source: www.natuurinformatie.nl). During the Saalian, the Netherlands was partly ice covered, whereas during the Elsterian it was more or less at the forebulge position. During the Weichselian the ice sheet margin was >300 km away and the Netherlands only experienced permafrost conditions or marginal effects of forebulge uplift.

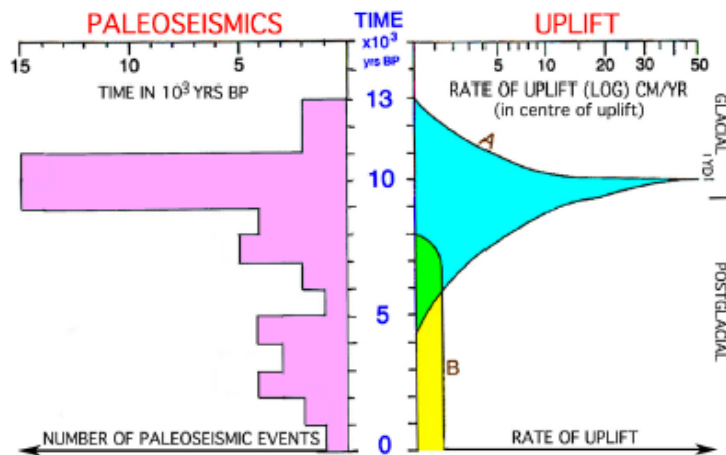


Figure 4-4 Frequency distribution of the 59 events in the Swedish Paleoseismic Catalogue (modified after Mörner, 2003, 2011). There is a distinct peak in the period 11000-9000 BP which is the time of the peak rate of glacial isostatic uplift of a once ice-covered regions.

Hampel et al. (2007) show that during deglaciation of areas that were once ice-covered fault slip accelerates by a factor of 6 with respect to the long-term rate. Their modeling results demonstrate that a significant fraction of slip occurred within a few thousand years after the last glaciation. Since a glacial cycle lasts only about 100 kyr (Shackleton et al., 1990; Marshall, 1998), the background tectonic stress regime for these kind of modeling exercises is assumed to be constant or stable on geological time scales (>1 Myr; e.g. Luttrell and Sandwell, 2010). Abrupt changes in seismic activity are presumably not to be explained by changes in tectonic stresses. This is furthermore demonstrated by modern glaciated areas that show almost no seismicity below the ice sheet (e.g. Munier and Fentont, 2004). Grollmund and Zoback (2003) plot the CFF (Coulomb Failure Function) against time for several existing faults in the Norwegian offshore, showing that during the last 110 kyr, during most of the Weichselian period when the ice sheet covered the area, the stress state did not favor fault slip on the studied faults. Because the reason for this observation is, that the direct overburden of the ice sheet tends to prevent fault slip. However, the stress field was periodically changed which led to repeated activation of reservoir-bounding faults during the course of the Pleistocene glaciations, especially during Weichselian interglacials. As a result, hydrocarbon fields in the Norwegian offshore appear to have been exposed to multiple periods of fault reactivation and potential hydrocarbon leakage.

4.2.2. Far field effects

Apart from vertical effects such as ice-loading and glacio-isostatic uplift after deglaciation, flexural behavior of the crust predicts a so-called glacio-isostatic forebulge to develop, approximately 150 km from the margin of the ice sheet. The vertical behavior of this bulge is proportional to ice thickness and further relies on rheological parameters of the crust. Using default rheological parameters, the forebulge uplift and subsidence is expected to be about 4% of the ice-loading effect and thus 1.2% of the ice thickness (Anderson and Anderson, 2010; Figure 4-3; Table 4-1). Geomechanical glacial rebound models predict significant influence of the ice-sheet (un)loading on stresses in the crust that can extend as far as 300-500 km from the ice-sheet margins (Johnston et al., 1998; Muir-Wood, 2000), however, the largest effects are located in the forebulge (see Figure 4-3).

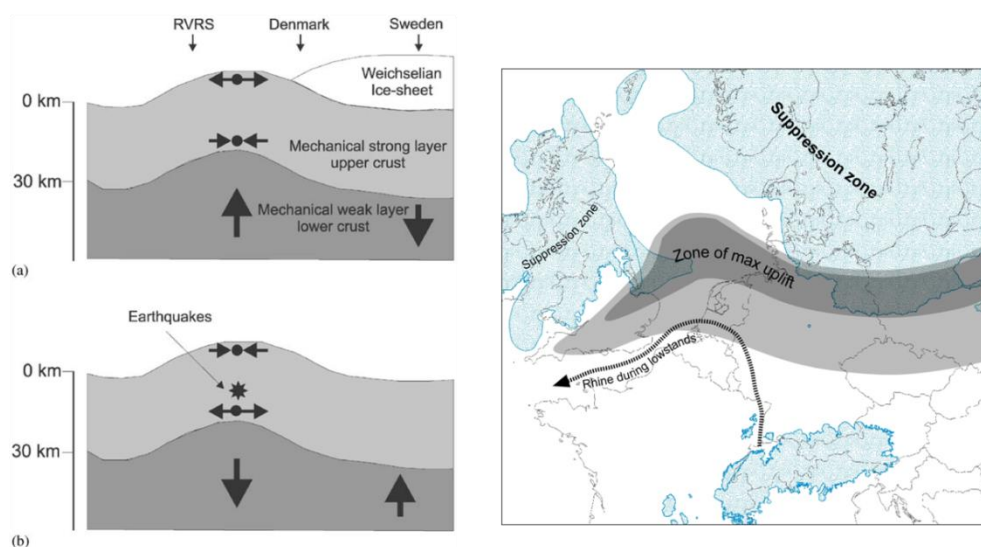


Figure 4-5 The left figure shows the state of stress in the forebulge during and after ice-sheet loading (modified after Houtgast et al., 2005). The right figure shows the extent of the ice cover during LGM, the area affected by stress change and the position of the forebulge (as zone of maximum uplift).

4.3. Assessment of glacio isostasy and -seismicity in the Netherlands

Kiden et al. (2002) showed based on Holocene relative sea-level curves that a forebulge was present in the coastal areas of the Netherlands, related to the ice sheet that covered the UK (Devensian glacier). Houtgast et al. (2005) extrapolated this observation parallel to the ice margin to conclude that the forebulge margin coincided with the Ruhr Valley Graben during the maximum extent of the Scandinavian ice-sheet, i.e., during the LGM (Figure 4-5).

Van den Berg et al. (2002) and Houtgast et al. (2005) suggest a link between faulting and crustal unloading due to melting of the Late Weichselian continental ice-sheets to explain the increase in fault activity at 10-15 ka BP in the Ruhr Valley Rift System. The present-day maximum horizontal stress direction in this rift system is approximately NW-SE oriented (Müller et al., 1992; Ziegler et al., 1995) and was established during the late Early Miocene (Bergerat, 1987; Becker, 1993; Hibsich et al., 1995; Van Balen et al., 2005). The main causes for this stress-field are the Mid-Atlantic ridge push and the Alpine collision (Gölke and Coblenz, 1996). There are no indications of changes in orientation nor magnitude for these far-field stresses on a 10^3 - 10^4 year time scale that could explain the possible increased fault activity around 15-10 ka BP along the main faults of the Ruhr Valley Graben. The timing of this increased activity and results from glacial rebound modeling indicate that glacial unloading of the crust can have triggered this increase in fault activity in the forebulge domain. This bulge started to collapse between 20-15 ka, i.e. after the LGM. The effects of forebulge collapse are superimposed on and more-or-less parallel to the long-term far-field stresses such that the faulting intensity in the Ruhr Valley Graben was temporarily increased. By using geodetically determined vertical movements, Kooi et al. (1998) showed that subsidence due to forebulge collapse still takes place in the Netherlands.

Also for northern Germany the far-field effects of glacial loading are postulated. Based on a seismic data set covering the glaciolacustrine Emme delta, an overall model for the Pleistocene reactivation of basement faults was developed by Brandes et al. (2011). Also, numerical simulations show that the seismicity can potentially be explained by the decay of the Scandinavian ice sheet after the Weichselian glaciation (Brandes et al., 2015). During the LGM, the advancing ice sheet caused far field extension, which might have reactivated pre-existing normal faults. Later, the fault activity was enhanced due to sediment and water loading. In addition, high pore pressures due to lake formation might have supported the slip processes along the faults. After glacial unloading and lake drainage, the fault activity stopped.

The relation between forebulge uplift and ice-sheet thickness depends on lithospheric strength (Young's Modulus, effective elastic strength), but in general amounts to ~4 % of the maximum deflection underneath the ice sheet (see explanation in Anderson and Anderson, 2010). Older estimates, proclaiming that the centre of the North Sea rose by about 170 m during the last Ice Age because of forebulging (Ehlers et al., 1979), are probably overestimating the flexural uplift component.

Steffen et al. (2014) estimate the sensitivity of fault throw and activation with respect to ice-sheet thickness for areas once covered by a continental ice sheets by applying a new finite-element approach. Variables in their modeling included lithospheric and crustal thickness, viscosity structure of upper and lower mantle, and fault location and angle. They conclude that the modelled fault slip magnitude, fault location and activation time are only slightly sensitive to a change in ice thickness (Figure 4-6). Ice-sheet thickness only affects fault slip by about 1 m for fault-slip along 45° faults directly below the ice sheet. Faults at different angles are far less sensitive. However, the ratio between vertical loading stress and GIA stress (Glacial Isostatic Adjustment or rebound stress) change with the thickness of the ice cover. An increase of vertical loading stress from 13 MPa to 31 MPa

is to be expected when the ice-sheet center thickness increases from 1500 m to 3500 m. This will also increase the flexure of the lithosphere. Thicker ice produces a large deflection and also the associated horizontal rebound stresses will increase. However, this change in horizontal stress is only 12 MPa at the same location during glacial maximum between 1500 m and 3500 m thick ice masses. Therefore, the difference between vertical loading and horizontal GIA stress grows with an increase in ice-sheet thickness. As such the differential stress increases, which favors fault reactivation and also the fault slip magnitude is non-linearly related to vertical glacial loading (e.g. Johnston, 1987).

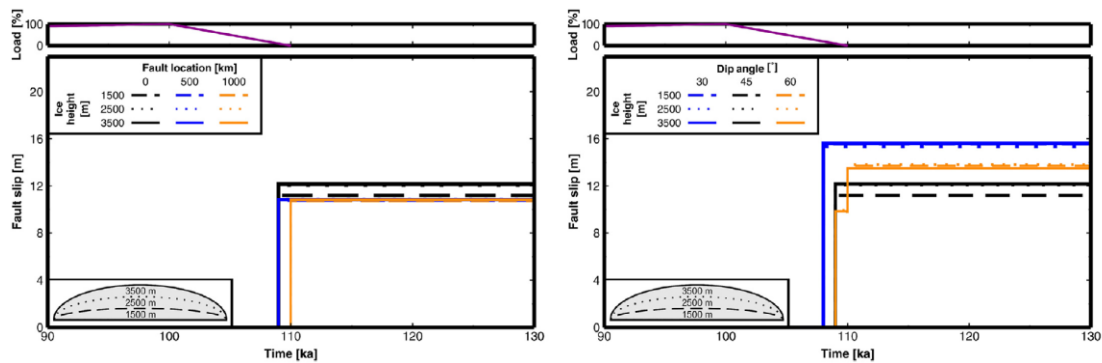


Figure 4-6 Fault slip for a variation of the ice-sheet thickness (load). The left side presents the specific variation with respect to different location, but a constant dip angle of 45°. The right side the specific variation with respect to the dip angle of the fault, but at a constant location at the centre of the load. The following additional parameters were used: crustal thickness 40 km; lithospheric thickness 160 km (modified after Steffen et al., 2014).

4.4. Summary of Dutch ice cover scenarios

4.4.1. Ice sheet extent

Various lines of geological evidence provide a detailed paleogeographic picture of ice-sheet distribution and ice-margin positions during some of the last glacial phases of the Pleistocene. During the Last Glacial Maximum of the Late Weichselian (MIS 2, Late Pleistocene) the southern margins of the Scandinavian Ice Sheet and the British Ice Cap remained well far away from the present Dutch territory (Figure 4-3C), affecting only the margins of the present Dutch offshore at distances of a few hundred kilometres from the modern coast. By contrast, during the preceding late Middle Pleistocene Saalian glacial phase (MIS 6, in the Netherlands also referred to as Drenthe glaciation), the margins of the Scandinavian Ice Sheet extended farther south and reached the central portions of the country (Figure 4-3B). During Pre-Elsterian glaciations such as the Early Pleistocene Tiglian and Menapian stages and the Middle Pleistocene Cromerian stage, the southwestern margins of the Scandinavian Ice Sheet did not reach farther than southern Denmark and northeastern Germany. This left the present Dutch onshore essentially unaffected by glacial deformation. However, in the Dutch northern offshore, seismic reflection data shows ample evidence for ice-berg scour marks throughout the Gelasian (Early Pleistocene) sequence, attesting to its close position relative to the southern ice margin during the Tiglian stage (Kuhlmann and Wong, 2008; Stuart and Huuse, 2012).

Stratigraphic, geomorphic and geochemical studies on Quaternary climatology and paleo-environments suggest that the volume and extent of ice sheets has been growing progressively over the Quaternary, towards maxima of the late Middle Pleistocene and Late Pleistocene (Ehlers et al., 2011). With the benefit of the doubt for predictions on global climate trends (see section 2.2), available information suggests that a next glacial cycle is not likely to trigger ice-sheet advance over the whole territory of the Netherlands. There

is however a fairly high probability for ice-sheet margins to reach down again to the northern and northeastern provinces of the Netherlands. The coincidence of maximum southward advance during several glacial stages may suggest another, possibly structural, control on ice extent rather than solely temperature and humidity. The main ice advance should be expected from a resurgent ice sheet nucleating over Scandinavia, where landmasses are of sufficient extent to sustain protracted accumulation of a significant ice volume. On the other hand, Great Britain and Ireland hosted only moderately thick ice caps unable to advance beyond a very few hundred kilometres from their spreading centres in north-central Britain.

4.4.2. Ice sheet thickness

Moreau et al., 2009 use the flow line model of Rea and Evans (2007) to estimate the thickness of the ice sheet in the Elsterain tunnel valleys. Bottomline of this approach is that all the input parameters could be found based on the subglacial topography. The model predicts an ice-surface between 800 and 1000m in altitude, representing thus the main relief in the area, 400 ky ago. The ice thickness is ranging between 0 m at the front to >1400m in the deepest valleys. This estimate of the altitude ignore the isostatic effect, and therefore underestimate the steepness of the ice front and consequently of the ice profile. Using the same flow line model and the position relative to the ice margin, the ice thickness in the norther part of the Netherlands (above the line Den Helder - Hoogeveen, Figure 4-3) can be estimated to be approximately 180 m (Figure 4-7). This is a very conservative estimate which heavily relies on the ice-sheet geometry adopted.

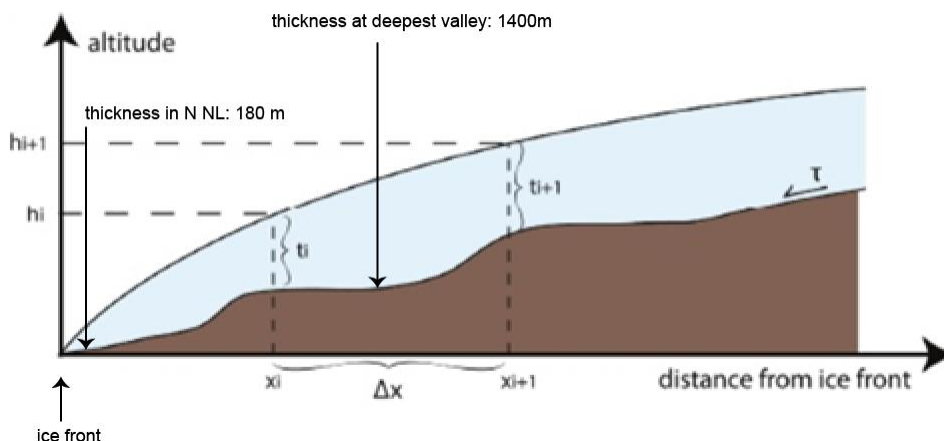


Figure 4-7 Parameters used for the ice thickness calculation along a flow line (Rea and Evans, 2007). Each altitude point of the ice sheet is calculated based on the former point values: x (distance from front, h (ice-surface altitude). Using the maximum ice-sheet thickness of 1400m in the deepest valley, a ice sheet thickness of ~100 m is estimated for the northernmost part of the Netherlands. Modified after Moreau et al., 2009.

Probably the best and only way to estimate the thickness of ice sheets that once covered the Netherlands is by finding a relationship between the degree of overcompaction of sediments that were hydrodynamically consolidated under an ice load. To this extend, Schokking (1998) used the lacutro-glacial “Pot Clay” of the Peel Formation, which was laid down in glacial channels (tunnel vales) during the Elsterian glaciation of the Late Pleistocene. The Pot Clay became overconsolidated by the load of the an ice sheet during the Saalian glaciation. Site investigation carried out for civil engineering constructions revealed changes with depth in the strength and overconsolidation ratio of the clays. From geotechnical and structural properties measured on core samples taken near Marum in the north of the Netherlands, a fossil overburden pressure of 2,1 MPa was estimated, which would have required an ice cover of at least 195 m. This thickness was likely to diminish to

near zero values at the margin of the Saalian ice-sheet margin, i.e. in the central part of the Netherlands.

For the Late Saalian glacial maximum, two recent model reconstructions of the Eurasian ice sheet have been performed: the isostatic reconstruction of Lambeck et al. (2006) and the dynamical ice sheet of Peyaud (2006). Using glacial rebound models Lambeck et al. (2006) inverted observations of crustal rebound and shoreline locations to estimate the ice thickness for the major glaciations over northern Eurasia. During the Late Saalian, the ice extended across northern Europe and Russia with a broad dome centered from the Kara Sea to Karelia that reached a maximum thickness of c. 4500 m and ice surface elevation of c. 3500 m above sea level. A secondary dome occurred over Finland with ice thickness and surface elevation of 4000 m and 3000 m, respectively. This ice thickness would account for a local deflection of ~1000 m.

The reconstruction of Peyaud (2006) has been computed using the GRISLI ice model. A comparison of the two models shows that both produce a Late Saalian ice sheet with almost similar shape. The mean elevation is also about 3000 m, and ~4000 m domes are located almost at the same place and ice volume is ~61 m equivalent to sea level (ESL). The only difference is that the Peyaud (2006) reconstruction links the British Isles ice cap to the huge Eurasian ice sheet. This concurs with the QUEEN ice sheet reconstruction (Ehlers and Gibbard, 2004), showing a Late Saalian ice sheet that did not extend over the southern part of the British Isles (Svendsen et al., 2004). During the Eemian interglacial (MIS-5d, 5b, 4) the maximum ice was centred over the Kara and Barents Seas with a thickness not exceeding c. 1200 m (Lambeck et al., 2006).

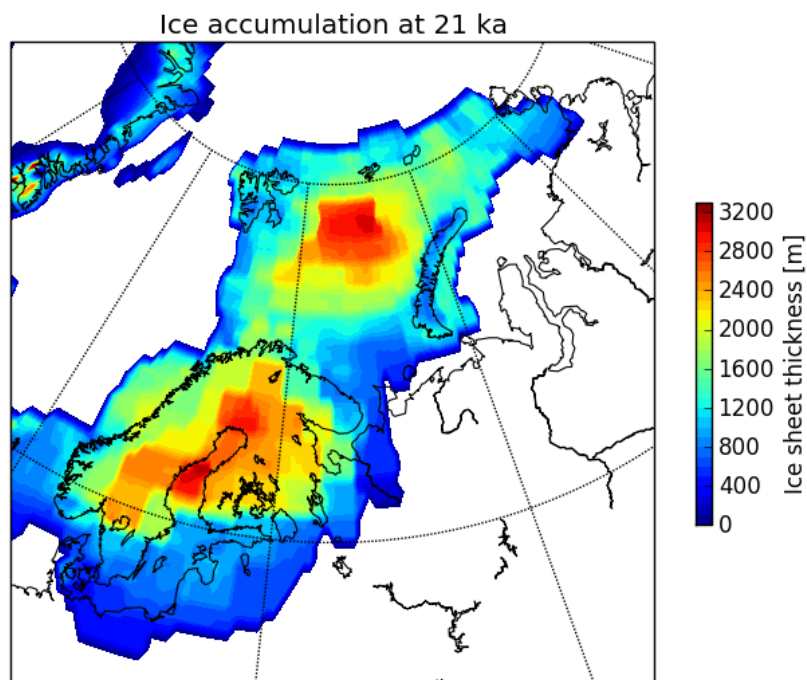


Figure 4-8 Ice sheet thickness at 21 ka (LGM) as modeled in ICE-5G. Two large domes are visible, one over the Baltic Sea and one over the Barents Sea, where the ice sheets only partially covers the Kara Sea and does not reach the Eurasian landmass (from IJpelaar, 2014)

Using an approach similar to that of Schokking (1998), Larsen et al., (1995) use the consolidation of bottomsets from glaciomarine deltas situated stratigraphically below and above the Weichselian maximum glaciation till at Skorgenes, western Norway, to quantify the ice thickness at the time of deposition of the till. The value of the preconsolidation pressure in the lower unit (15 ± 1 MPa), indicates an ice thickness over the site of some 1350 ± 90 m. This is, however, only considered a minimum because values of

preconsolidation pressures normally are lower than actual ice thickness would suggest due to incomplete drainage of the bed during consolidation. By mapping out ice marginal deposits Follestand and Fredin (2011) reconstruct the vertical extent and geometry of the Scandinavian ice sheet at the onset of the Younger Dryas deglaciation and propose average thicknesses of ~1500 m in the central inland areas of Norway.

The ICE-5G ice model (Peltier 2004), uses a-priory knowledge on the ice sheet and sediment history to model the Earth's response to ice loading and can be used to reconstruct ice-sheet thicknesses (see IJpelaar, 2014 for review). The maximum volume of the Fennoscandian ice sheet in this model is, in terms of sea level equivalent, 23,15m at 23ka. This is relatively small compared to the total modeled sea level rise of 129.9m, which also includes the ice sheets on Greenland, North America and Antarctica. The thickness of the southern domes over central Norway is ~2800 m (Figure 4-8), which is considerably larger than estimates that were made based on ice-marginal phenoma or sediment consolidation.

Based on this range of glacial advance deduced from previous glacial periods, four likely scenarios emerge, which are summarized in Figure 4-3 and Table 4-2. These scenarios describe the relationship between maximum ice-sheet loading (thickness) and far-field loading effects by analogy to past glacials and interglacials.

Table 4-2 Scenarios for ice coverage. Maximum (max) values apply to the location of the Scandinavian ice dome. Where possible estimates are given that apply to the Netherlands (NL).

Maximum ice load (m)	Ice load in the northern half of the Netherlands (m)	Glacial setting	Rebound stress increase (GIA in Mpa) in NL at forebulge	Vertical stress increase at 30 km (relative to hydrostatic, MPa)	Analogue
0	0	interglacial	0	0 at max, 0 in NL	Present day
2800	0	Glacial, only permafrost	no	25 at max, 0 in NL	Weichselian (LGM)
4000	195	Glacial, ice covered	>12	31 at max 2.1 in NL	Saalian
1400 (in tunnel valley)	180(?)	Glacial with forebulge	<12?	13 at max, -2.0 in NL	Elster

4.5. Relevance and synthesis for the safety case

Isolation

During ice loading a suppression of the ice-covered area will occur, whereas a glacio-isostatic forebulge will develop in front of the ice-sheet. With a postulated maximum ice-sheet thickness of ~4000 m (Saalian) the estimated ice coverage in the Netherlands amounts to ~200 m. The vertical isostatic loading and unloading effects (30% of ice-sheet thickness) would be in the order of 60-70 m. Forebulge uplift is in the order of 1.2 % of the ice sheet thickness, ie., maximally 48 m. Neither the forebulge uplift nor the isostatic rebound after ice loading will lead to an uplift and associated erosion that exceeds the thickness of the overburden such that the host rock will become exposed. The concentration of seismic activity in the forebulge area mainly concerns the localities of the main fault zones in the Netherlands. Estimated fault slip of several meters will also not lead to exposure of the host rock.

Delay & attenuation

Here we consider processes that, after ~10 kyr, affect the release and transport of radionuclides through the host rock and the geosphere due to diffusion, retention and retardation processes, and dilution and dispersion. The following applies:

- The release of consolidation water due to glacial loading enhances the transport of radionuclides into shallower groundwater systems both through the host rock but also in its overburden. So, after dissolution and transport through the host rock dilution and dispersion subsequently play a role in the geosphere.
- Increased stress during deglaciation (intensified seismicity and associated fluid flow).
- Exploratory calculations (Wildenborg et al, 2000) show that cyclic ice loading can lead to an acceleration of radionuclide migration in clay. The calculated contributions of dispersive transport to the total diffusion coefficient in clay amounts to 0.08 % under present-day conditions, 0.2 % under glacial conditions without ice loading and 14 % under glacial conditions with ice loading. The episodic occurrence of ice loading with an assumed duration of 20,000 years and a periodicity of 100,000 years increases the radionuclide mass fraction at the interface between the clay barrier and the upper aquifer. The increase of the mass fraction depends on the radio-isotope mass fraction and its maximum value is 2 to 9 times the mass fraction in the reference scenario (e.g., the current climate conditions). The increase probably falls within the uncertainty range of the estimated diffusive transport.

Engineered containment

The integrity of the engineered containment (the waste containers) only can be affected during the thermal stage (<~10 kyr). Anticipated future glaciations will not occur before ~55 kyr and therefore their predicted effects are irrelevant.

5. Permafrost

5.1. *Literature study on permafrost in NW Europe during the last ice age*

5.1.1. Motivation

This literature study serves as an appendix to SCK-CEN reports ER-138 and ER-148 dealing with phenomenological and numerical issues of permafrost development during the last ice age (Weichselian) in northern Belgium. More specifically, report ER - 138 is entitled "Permafrost in northwestern Europe during the Last Glacial" and deals with spatial and temporal patterns of permafrost aiming at deriving a temperature curve for the last glacial for the Mol site (Belgian Nuclear Research Center at Mol; <http://www.sckcen.be>). This temperature curve is subsequently taken as input data for report ER-148 which is entitled "Numerical simulation of permafrost depth at the Mol site". The studies were finished late 2010, early 2011, such that an update of relevant literature and new developments during the last 3 years is considered in this note.

5.1.2. New data on the stability of permafrost in Europe

In SCK-CEN report ER-138 evidence was shown from the literature indicating the existence of continuous and discontinuous permafrost in Belgium and the Netherlands throughout the Weichselian glacial. The evidence is mainly based on proxy data such as periglacial soil deformation phenomena (e.g., cryoturbations) and the link of these phenomena with the Mean Annual Air Temperature (MAAT in °C). During the LGM (Last Glacial Maximum; ca. 21 ka BP), the southern boundary of continuous permafrost would have been around 50° N (see references in Beerten, 2010 and Renssen and Vandenberghe, 2003).

In a new study on the (in)stability of permafrost in Eurasia by Vandenberghe et al. (2012), updated limits for the existence of continuous permafrost have been inferred, reaching 47° N i.e., central France. Interestingly the pattern of continuous and discontinuous permafrost is situated along a W - E axis, basically all over the Eurasian continent (Figure 5-1). This is in strong contrast with the distribution of the present-day permafrost extent, which runs from NW Russia to the large Asian mountain belts in SE Russia, where the permafrost pattern is disturbed. Earth system modeling with the LOVECLIM simulation tool also revealed that the distribution of LGM permafrost is determined by the presence of winter sea-ice in the Atlantic Ocean. Indeed, during the LGM, the penetration of temperate air masses from warmer oceans was hindered by sea ice, permafrost and cold ice-sheets in the north. Today, the permafrost pattern in Siberia is determined by the presence of winter sea-ice in the Arctic Ocean. Warmer air masses can more easily reach northern latitudes, especially those that are within the influence of the Atlantic Ocean (warm ocean currents). In a subsequent modeling study (Kitover et al., 2013), the evolution of the permafrost thickness over the last 21 kyr in Eurasia was calculated for different settings (Siberia, central Europe, western Europe).

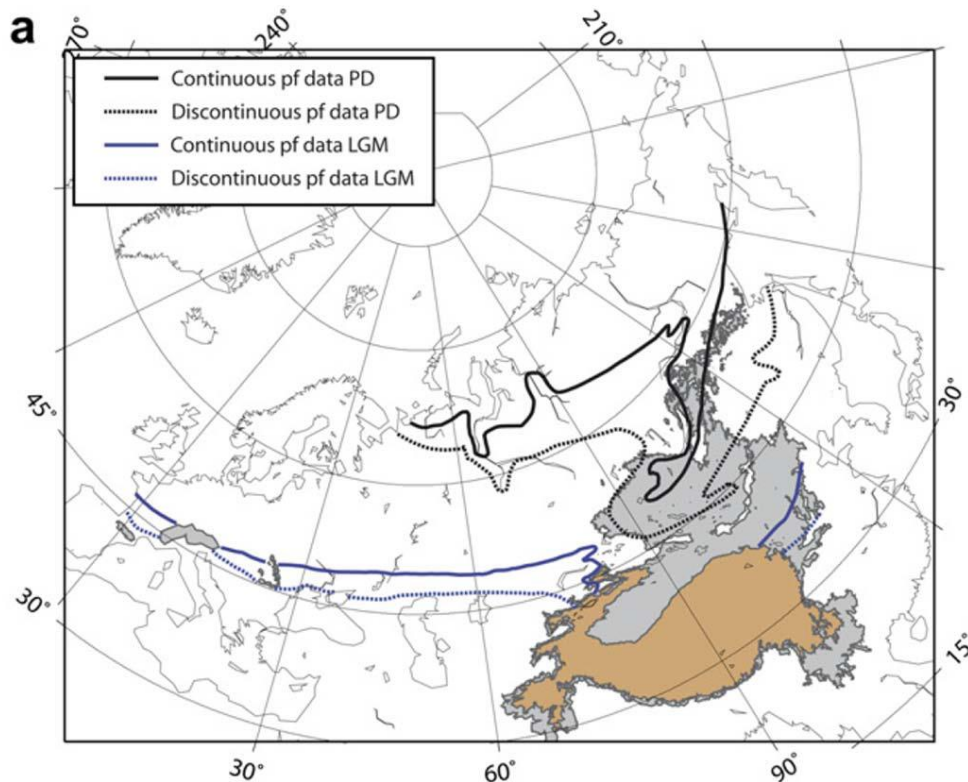


Figure 5-1 Reconstruction of permafrost extent, present-day (PD) and last glacial maximum (LGM) according to Vandenberghe et al. (2012).

The mean annual air temperatures were based on proxy data and were imposed on the western European surface, underlain by some standard European geology, reaching a MAAT of -8°C during the LGM. The modeling results are shown in Figure 5-2, indicating that permafrost during the LGM in the Netherlands would have reached thicknesses between 260-320 m, with full disappearance between 11-9 kyr BP. In this case, the linearised rate of thaw would be $2.2\text{-}3.2\text{ cm a}^{-1}$.

Kitover et al. (2013) also investigated the sensitivity of their model to the selected parameters. They calculated that an increase in porosity from 0.3 to 0.5 would decrease the depth of the permafrost base with ca. 50 m for a given set of parameters after 100 k model years. Changing the thermal conductivity from 2 W/m K to 3 W/m K would increase the permafrost depth with 100 m. The geothermal heat flux might have a great impact as for a given set of parameters the permafrost depth would increase from 250 m to 450 m while lowering the flux from 70 mW/m^2 to 40 mW/m^2 . Obviously, the sediment surface temperature (expressed as MAGST - Mean Annual Ground Surface Temperature) might have the greatest impact, since the permafrost base would reach a depth of 300 m after 100 k model years with a MAGST of -6°C , compared with a depth of 50 m with a MAGST of -2°C only.

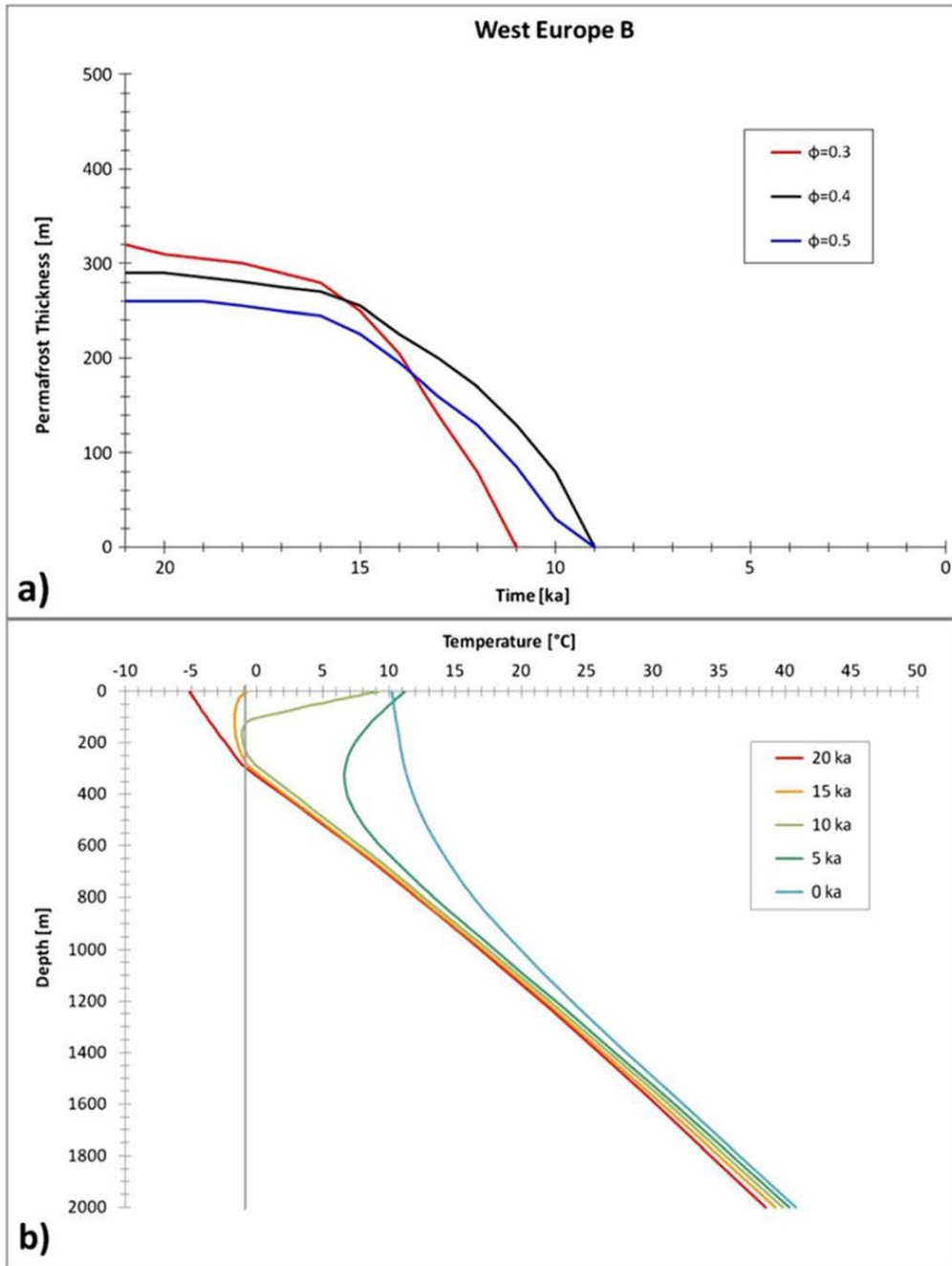


Figure 5-2 Permafrost simulation for western Europe. (a). The evolution of permafrost thickness with time for different porosities. (b). Temperature depth profiles for different time slices during the last 20 kyr. Modified after Kitover et al. (2013).

5.1.3. Comparison of permafrost depth modeling results for NW Europe

Here, we compare the permafrost depth modeling results for NW Europe during the LGM based on Delisle (1998), Grassmann et al. (2010), Govaerts et al. (2011) and Kitover et al. (2013). These four different modeling exercises revealed quite contrasting permafrost depths for the LGM, which is not surprising given different approaches were used with respect to parameters as glacial temperatures, duration of cold phases, thermal sediment properties, heat flux. The values derived from these four different studies range between ~100 m and ~300 m for a western European context, being site or non-site specific. The largest value is from Kitover et al. (2013) who used an extended cold period of unknown duration and a MAAT of -8°C to produce stable permafrost. The lowest value is from Delisle et al. (1998) who used a relatively high MAAT of -7°C for the LGM, a temperature which was reached only during an infinitesimal small time period at around 18 ka. Furthermore, this study uses the highest geothermal heat flux, 60 mW/m^2 , as is the case for the study by Govaerts et al. (2011). The latter however used a lower MAAT (-9°C) for the LGM, persisting for 2000 years and preceded by already very cold temperatures in the millennia before. Depending on the type of vegetation and the presence or absence of snow, permafrost depths between 200-250 m were calculated (Govaerts et al., 2011). Similar values were obtained in the study by Grassman et al. (2010) for northern Germany.

5.1.4. Implications for potential geological waste repositories in Belgium and the Netherlands

It is clear that the outcome of various permafrost modeling studies for NW Europe is highly variable, showing permafrost thickness between 100-300 m for the coldest period of the last glacial (Weichselian). Even if the model with the thickest permafrost would be regarded as an absolute maximum depth that is likely to be reached only during several millennia long and very cold (-8°C MAAT) glacial periods, it cannot be ruled out at this point that potential repository sites at depths of 300 m and less might be experiencing permafrost conditions at some point in the next 1 Myr.

In the absence of observations on paleo permafrost depths, this rather large range of modelled future permafrost depths calls for a better assessment of the input parameters. The discussed models cannot be regarded with confidence, as there is considerable uncertainty in the used input data. A better assessment of the input parameters also calls for renewed permafrost modeling. The parameter assessment will be covered in the following section of this chapter. The recent permafrost modeling performed by SCK-CEN and documented in report SCK-CEN-R-5848 is provided as Appendix to this report.

5.2. *Assessment of input parameters for Permafrost modeling*

5.2.1. Porosity prediction

Porosity is the essential parameter in modeling thermal perturbations, such as for hydrocarbon generation or permafrost development. Here, we aim to assign a porosity value to each of the lithostratigraphic units defined in TNO's Digital Geological Model (DGM) of the shallow Dutch subsurface, i.e. the model that includes all unit overlying the Rupel^c Formation (of which the Boom Clay is part). TNO's hydrogeological model REGIS provides a further subdivision and includes both aquifers (sand) and non-aquifers layers (clay). Using the REGIS information, a percentage of clay vs. sand for each of the DGM units can be calculated. Given the relatively small amount of porosity measurements of the sand and clay layers in the stratigraphic interval above the Rupel Fm., a best-fit, generally applicable porosity-depth relationship was established for all units using either a

^c Throughout this report the term Boom Clay is often used. However, Boom Clay is not an official stratigraphic unit in the Netherlands and is referred to as Rupel Clay Member. The latter is, together with the Rupel Sand Member, part of the Rupel Formation.

best-fit relationship that was calculated by the basin modeling package Petromod[®] or literature based curves

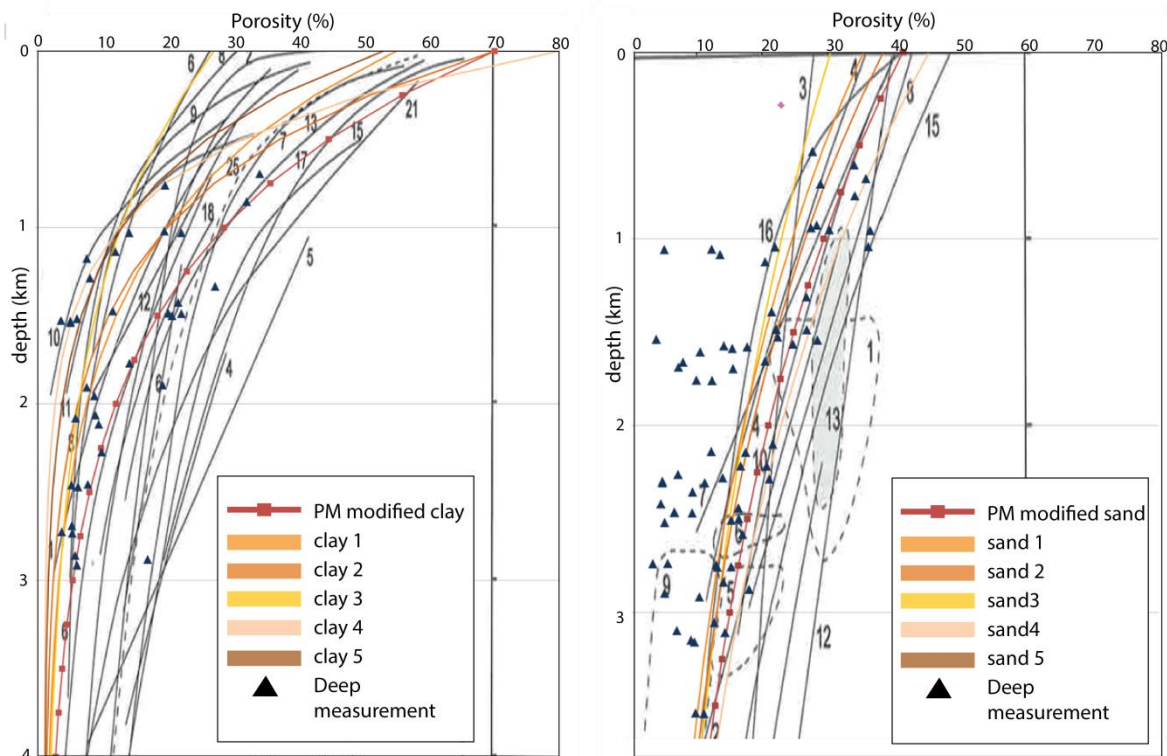


Figure 5-3). The latter allow to make porosity predictions for non-studied domains based on the layer depth alone and assuming that the maximum burial depth is at present. This is true if no tectonic uplift occurred after burial, which would make the porosity-depth relationship unusable.

For those units without any measurements, the porosity was determined using the best-fit relationship belonging to the lumped data for corresponding depositional facies (e.g., marine or fluvial). For instance, for the Breda Formation only porosity measurements of the sandy intervals exist. The Petromod best-fit (PM) appears to be the best-fit for these marine sands. Based on the cross plot of all marine clays, it appears that the clay 5 models gives the most representative porosity trend and was adopted for further modeling. In the end, for all sand and clay layers within DGM a best-fit porosity curve can be assigned (Table 5-1). It should be noted that the spread in the data is relatively large, i.e., up to ~20%.

Several units with complex lithologies exist. For instance, in highly heterogeneous fluvio-deltaic deposits single clay or sand layers cannot be readily identified. For these units a mixture of clay 1 and sand 2 (50/50 %) was adopted. Lithologies in ice-pushed ridges can be a mixture as well, but are less dominated by clay and are assumed to consist of sand 3 entirely.

Based on the selected porosity-depth trend a location-dependent mid-depth porosity of all DGM units was modelled using Athy's law (Athy, 1930) for mechanical compaction, which is based on hydrostatic pressure only and described by Equation 1. Each of the depth dependent (z in m) sand and clay compaction trends identified uses different input parameters for initial porosity (Q_0), minimum porosity (Q_1) and the porosity decay parameter or Athy factor (k in km^{-1})), as listed in Table 5-1.

$$\text{Equation 1: } Q(z) = Q_1 + (Q_0 - Q_1)e^{-kz}$$

5.2.1. Thermal parameters

For permafrost modeling the heat capacity, vertical thermal conductivity and thermal gradient are essential input parameters. In the used approach, these parameters depend on the surface and subsurface temperature. It should be noted that these thermal properties are regarded as lithological unit specific values but that they will change with changing boundary conditions. For instance, subsurface temperature is modelled using the basal heat flow and surface temperature as main input and will change as surface temperature changes. Gradients, conductivity and heat capacity will vary accordingly.

Heat capacity

The Waples model (Waples and Waples, 2004) was selected which uses temperature and heat capacity at 20°C (c_{20}) for reference. This value is 0.20 and 0.21 kcal/kg/K for sand and clay, respectively. The Waples Equation (2) can be applied to any mineral, lithology or rock value (except kerogen and coal).

The heat capacity is given by:

$$\text{Equation 2: } c_r = c_{20}(0.953 + 2.29 \cdot 10^{-3}T - 2.835 \cdot 10^{-6}T^2 + 1.191 \cdot 10^{-9}T^3)$$

Where T is measured in degrees Celsius.

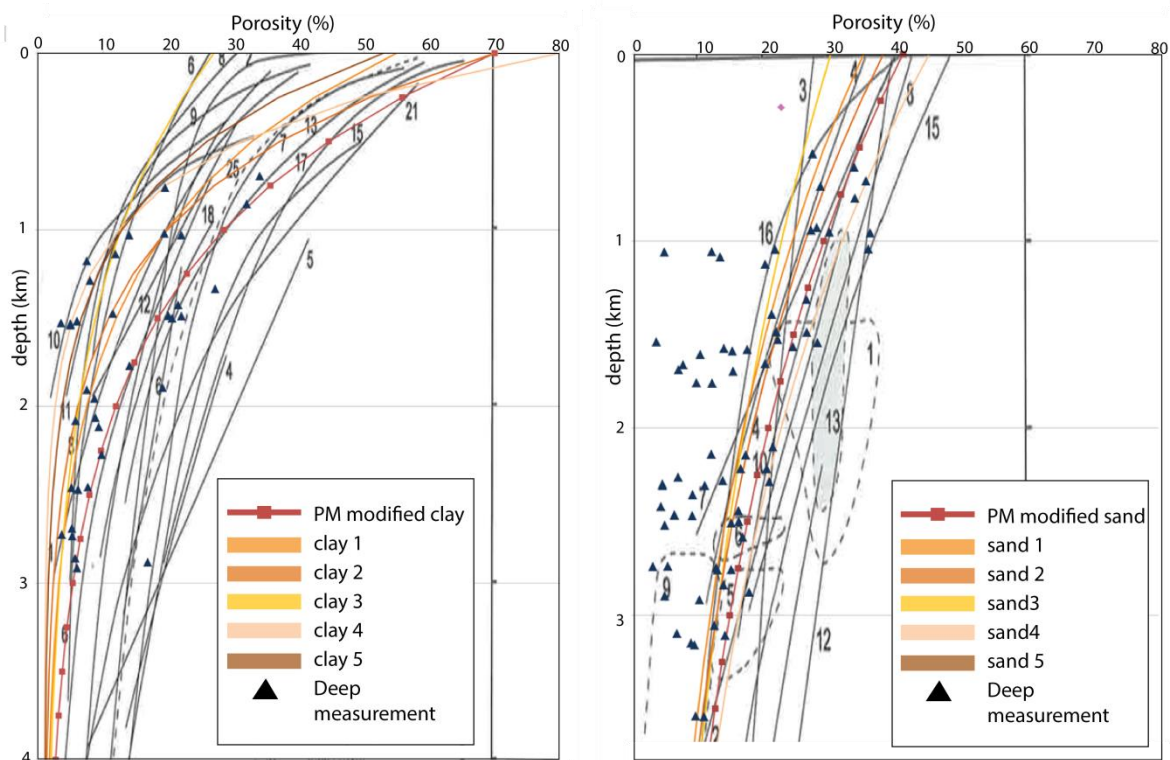


Figure 5-3 Literature based porosity-depth relationships in black lines (from Poelchau et al., 1997) and best-fit relationships based on actual porosity measurements (blue triangles) in colored lines. Left = clay porosities; Right - sand porosities.

Table 5-1 Input parameters for the estimating of porosity values for the lithostratigraphic zones above and including the Rupel Clay Member (Boom Clay).

Zones	Clay Φ	k (km^{-1})	Q0 (%)	Q1(%)	Sand Φ	K (km^{-1})	Q0(%)	Q1(%)	Complex Φ
Hl	clay1	1.06	55	1	sand2	-0.39	38	1	50/50

BX	clay5	1.48	53	1	sand3	-0.39	35	1	n.a.
BR	clay2	1.30	70	1	sand4	-0.36	45	1	n.a.
BE	clay5	1.48	53	1	sand2	-0.39	38	1	n.a.
EEWB	clay4	1.93	80	1	sandPM	-0.36	41	1	n.a.
KRZU	clay1	1.06	55	1	sandPM	-0.36	41	1	n.a.
DR	clay3	0.80	27	1	sand3	-0.39	35	1	n.a.
DT		n.a.	n.a.	n.a.		n.a.	n.a.	n.a.	sand3
DN		n.a.	n.a.	n.a.	sand3	-0.39	35	1	n.a.
URTY	clay4	1.93	80	1	sand3	-0.39	35	1	n.a.
PE	clay3	0.80	27	1	sand3	-0.39	35	1	n.a.
UR	clay1	1.06	55	1	sand2	-0.39	38	1	n.a.
ST	clay1	1.06	55	1	sand2	-0.39	38	1	n.a.
AP		n.a.	n.a.	n.a.	sand1	-0.29	30	0	n.a.
SY	clay1	1.06	55	1	sand3	-0.39	35	1	n.a.
PZWA	clay1	1.06	55	1	sandPM	-0.36	41	1	50/50
MS	clay5	1.48	53	1	sandPM	-0.36	41	1	50/50
KI	clay5	1.48	53	1	sandPM	-0.36	41	1	n.a.
OO	clay1	1.06	55	1	sand4	-0.36	45	1	50/50
BR	clay2	1.30	70	1	sand4	-0.36	45	1	n.a.
RU	clay1	1.06	55	1		n.a.	n.a.	n.a.	n.a.

Thermal conductivity

The Sekiguchi (1984) equation (3) is a very general equation that can be applied to any mineral, lithology, kerogen and coal, and uses temperature and thermal conductivity at 20°C for reference. These values are 3.95 and 1.64 W/m/K for sand and clay, respectively.

The thermal conductivity is given by

$$\text{Equation 3: } \lambda_r = 1.84 + 358 \cdot (1.0227\lambda_{20} - 1.8882)\left(\frac{1}{T} - 0.00068\right)$$

Where T is measured in degrees Celsius.

Thermal gradient

The thermal gradient is calculated based on the surface temperature, the mid depth and mid-depth temperature of each unit.

Salinity

The Cl-concentration of 1000 mg/l indicates the transition between brackish and saline groundwater. Where a stratigraphic unit is deeper than the 1000/mg/l plane conditions are assumed to be saline, where a stratigraphic unit is shallower, it contains fresh-brackish water. The brackisch/saline interface is obtained from DINoloket.

5.2.2. Area selection and data delivery

The depth of the subsurface units, affecting porosity and the thermal parameters, and their lithofacies distribution, affecting the average porosity of the unit, are considered relevant for area selection of permafrost modeling. Note that the depth to the top Rupel Fm. (Boon Clay) is representative for the total overburden depth, which is strongly affected by thick units such as the Breda Fm. The thickness distribution of the latter is strongly coupled to the tectonic setting i.e., it is thick in basins and relatively thin on structural highs. Also lithofacies, given as % of clay or sand, seems to be linked to certain structural elements, especially in the Ruhr Valley Graben. In the north, this correlation is less obvious. Area selection for permafrost modeling is based on the presence of 17 structural elements, including 6 highs, 5 basins and 6 platforms.

A geological property model was constructed based on the surfaces of the DGM shallow subsurface model. For each unit, vertical grid cells of 250x250 m and a height equal to unit thickness were constructed. These grid cells were populated with the parameters described before. Subsequently, all parameters were averaged over the vertical interval overlying the Rupel clay, the overburden, and assigned to the central point of the structural element. This forms the input for the permafrost modeling at these central points (see Appendix 1), which allows for an assessment of permafrost depth variation over the country.

Table 5-2 Example of input parameters and statistics for CNB element (see Figure 5-4 for locality).

Element	Item	Min	Max	Delta	No.	Mean	SD	VAR	Sum	Unit
CNB	average middepth porosity	0	70.1184	70.1184	82569	32.1894	11.9994	143.9847	2657846.845	%
CNB	Clay %	0	99.86	99.86	82835	7.41	14.76	217.97	614048.27	%
CNB	Heat capacity	0	0.2051	0.2051	82558	0.1768	0.0337	0.0011	14597.696	kJ/(m3.K)
CNB	mid depth T	10	11.24	1.24	82586	10.27	0.21	0.04	848084.29	°C
CNB	Thickness overburden	20.94	1213.09	1192.15	127563	656.18	317.44	100770.1	83704719.14	m
CNB	Depth of brackish-salt interface	-381.04	44.35	425.39	127554	-130.74	104.89	11002.93	-16675793.64	m
CNB	Thermal conductivity	0	4.0421	4.0421	82558	2.5396	0.6492	0.4214	209665.5013	kJ/(m.d.K)
CNB	Thickness of Rupel	-0.02	169.06	169.08	82835	28.25	25.76	663.52	2339897.92	m
CNB	Average depth	-1217.43	0	1217.43	127563	-646	321.21	103176.5	-82405449.85	m

5.3. Permafrost depth modeling

5.3.1. Results

Permafrost depth modeling using a best estimate temperature curve of the Weichselian as an analogue for the future indicates that the permafrost front (50 % ice and 50 % water) would point at permafrost depths between 140-180 m in the Netherlands. The permafrost depth modeling was applied only on single locations that represent the central point of identified structural elements in the Netherlands (see section 5.2.2). Using the same climatic data for the entire country, deepest permafrost is expected in the southern localities, due to the lower geothermal flux and higher average sand content of the overburden. Taking into account various sources of uncertainty - such as type and impact of vegetation, snow, air surface temperature gradients across the country, possible errors in palaeoclimate reconstructions, porosity, lithology and geothermal flux - stochastic calculations point out that permafrost depth during the coldest stages of a glacial cycle such as the Weichselian, for any location in the Netherlands, would be between 120-200 m at the 2σ level. The most conservative parameter combinations result in permafrost fronts going as deep as 270 m. The difference between the 5 % and 95 % - percentiles (2σ) is about 80 m, which is a relatively large interval given the low number of parameters. It is recommended to diminish the uncertainty on a number of important parameters in future analyses of permafrost evolution. The most sensitive parameters in permafrost development are the mean annual air temperatures and porosity, while the geothermal flux is the crucial parameter in permafrost degradation once temperatures start rising again. The uncertainty and sensitivity analysis are not performed for all localities and, to date, cannot be compared with the Boom Clay depth. For the localities that did undergo such a comparison the mean value and the 50-percentile overlap, indicating that the model behaves linearly.

5.3.2. Comparison with Boom Clay depth

Vis and Verweij (2014) constructed depth and thickness maps of the Boom Clay using the most recent publicly available data. All maps were made using a convergent gridding interpolation algorithm with a grid resolution of 250x250 m. In order to make a reliable comparison between the modelled permafrost depths at individual localities and the Boom Clay depth maps, the results were interpolated using the same convergent gridding method (Figure 5-4). Note that this interpolation of permafrost results is somewhat different than the Kriging method applied for the maps in Adendum 1 (Figures 11, 12, 13), but that the map results are underlain by the same data.

Permafrost depths are given using either the $+0.5^{\circ}\text{C}$, 0°C or -0.5°C isotherms, corresponding to respective depths above which $>0\%$ (PF_unf), $>50\%$ (PF_50), or 100% (PF_100) of the porewater is in solid phase thus frozen. Subsequently, these PF depth maps are compared with the depth of the Boom clay in order to identify zones that are affected by one of the freezing phase conditions of the porewater. Where the Boom clay is at shallower depths than the PF_unf depth, part of the porewater (0-100 %) is frozen, with increasing frost percentage going upward. Where the Boom clay is at shallower depths than PF_50, 50 % or more of the Boom Clay porewater is frozen. Where the Boom clay is at shallower depths than the PF_100, all pore water is frozen. For a permafrost front with 50 % ice and 50% water permafrost depths vary between 140-180 m in the Netherlands. This means that only in the northeastern and southwestern parts of the Dutch territory the top formation are at depths shallower than the permafrost depth (Figure 5-4E). If the permafrost front is taken where freezing starts, permafrost depths vary between 165-213 m and the affected domains are somewhat enlarged (Figure 5-4D). If the permafrost front is taken where 100% of the porewater is frozen, permafrost depths vary between 132-165 m consequently the affected domains are somewhat reduced (Figure 5-4F).

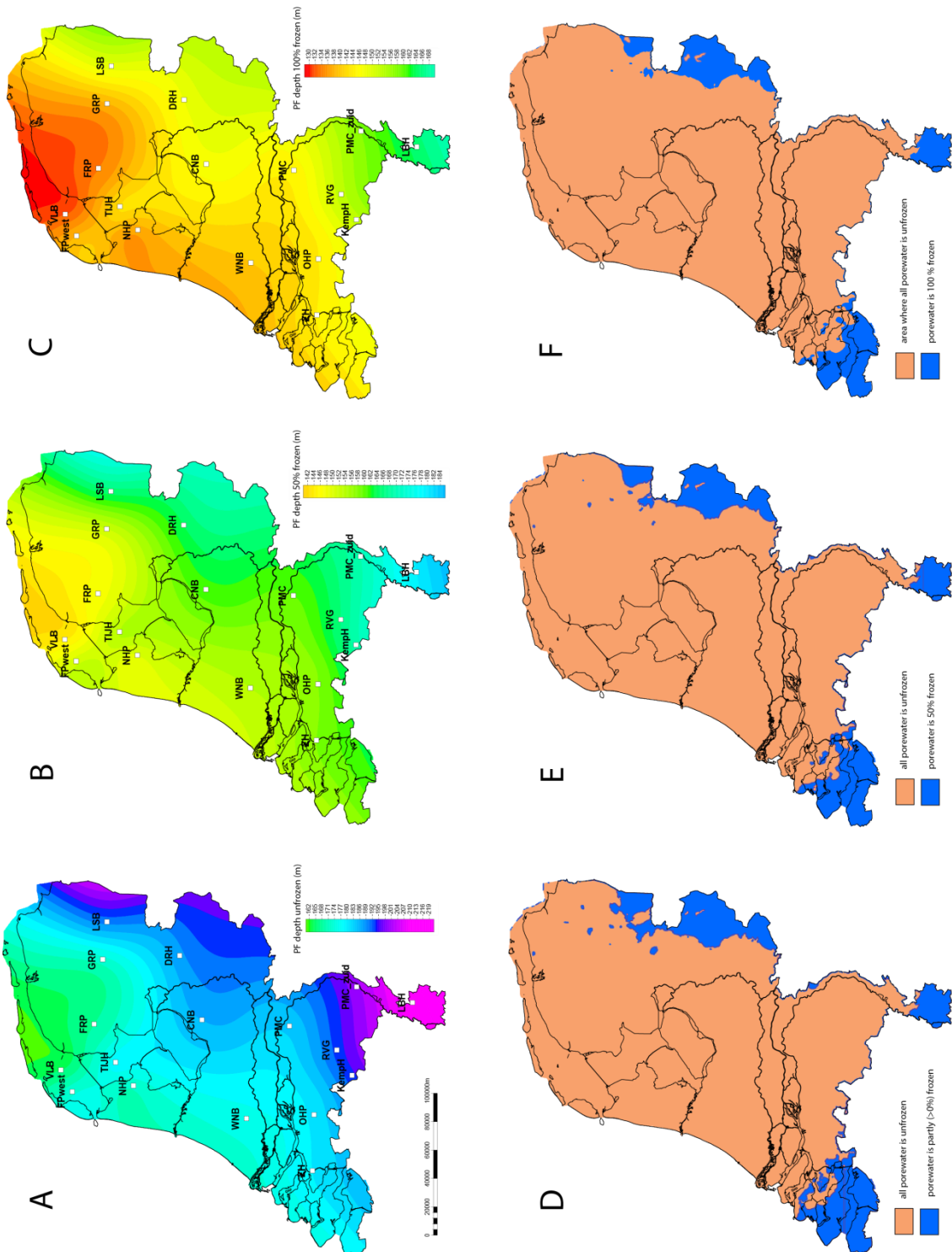


Figure 5-4 Maps showing interpolated permafrost (PF) depth modeling results with indication of the model localities: A) Maximum permafrost depths for the +0.5°C isotherm, representing the point at which the freezing process starts. Above this depth, the freezing process starts. B) Maximum PF depths for the 0°C isotherm. Above this depth 50 % percent of the pore water is frozen. C) Maximum PF depths for the -0.5°C isotherm. Above this depth, all porewater is frozen. In D), E), and F), the permafrost depth maps are compared with the depth of the top of the Boom Clay. Areas where the Boom Clay is shallower than the permafrost depth are indicated in blue. Depending on the used isotherm, these maps have a different meaning. D) Blue areas indicate domains where porewater starts to freeze. E) Blue areas indicate where pore water is 50% frozen. F) Blue areas indicate where pore water is 100% frozen. See text for discussion.

The 99 % percentile of a nation-wide stochastic simulation produces locally maximum permafrost depth of 270 m (see Appendix 1, Figure 19). Although the permafrost affected domains are considerably larger (Figure 5-5) such an assessment should be regarded as worst-case scenario, since the likelihood that permafrost depths are shallower are 99%.

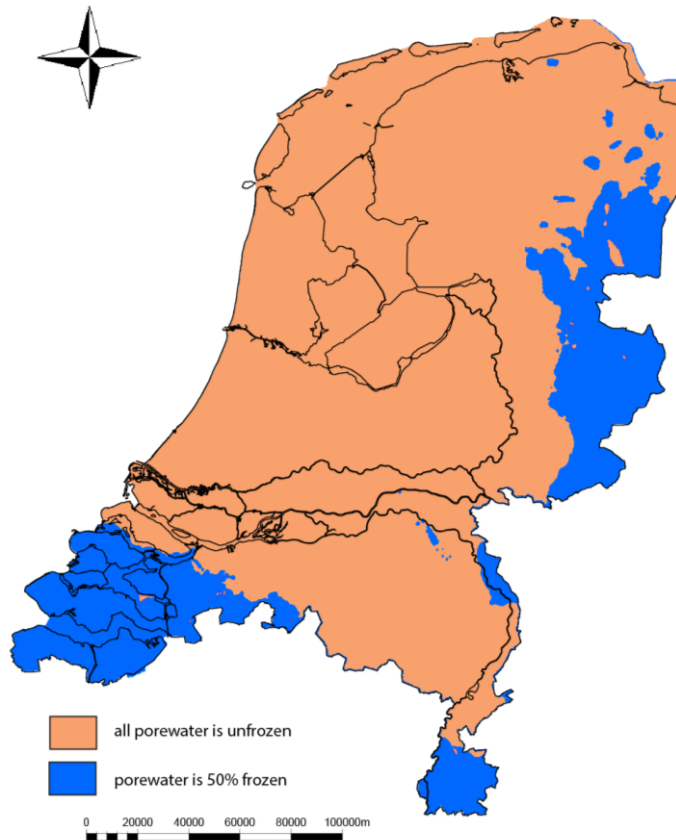


Figure 5-5 Maximum permafrost for the 50 % frozen isoline. The maximum, unlikely, permafrost depth of 270 m was considered constant over the entire country. The spatial variability of input parameters was not taken in to account.

5.1.Relevance and synthesis for the safety case:

Isolation

The stochastically derived maximum permafrost depth of 270 m, although highly unlikely, does not reach the top of the Boom Clay in most parts of the country. The outline of the few areas with predicted effect may be used to (re)define a minimum depth for site selection of disposal facilities.

Delay & attenuation

The permafrost depth assessment so far focused on the Boom Clay. The results, however, should also be applied to infer PF effects on the overburden. For instance the effects of permafrost on hydrogeology (groundwater flow, deep fluid flow, infiltration and recharge) specifically apply to the numerous lithologies in the overburden of host rocks.

Engineered containment

The integrity of the engineered containment (the waste containers) only can be affected during the thermal stage (<-10 kyr). Anticipated future permafrost will not occur before before ~55 kyr and, therefore, the predicted effects are irrelevant for this safety case.

6. Accommodation changes (sea level vs. supply)

6.1. Periodicities of global sealevel change

Long term global sea-level changes on the 10^7 to 10^8 year scale are created by tectonic and tectono-eustatic mechanisms and define the general frame for the development of first- and second-order depositional sequences. The causes for third-order sequences, which develop on the 10^6 -year scale (0.5-3 Myr; Haq et al., 1987), are often difficult to assess and are usually seen as the combined result of regional tectonics (e.g., Woodruff and Savin, 1989) and long period glacio-eustatic changes (e.g., Abels et al., 2005). In the latter case, sea-level cyclicity can be explained by a modulation of the shorter term Milankovitch-scale sea-level events (Miller et al., 2005). Fourth-, fifth- and sixth-order sequences are usually explained by climatically controlled glacio-eustatic sea-level fluctuations on the 10^4 to 10^5 year scale (e.g., Vail et al., 1991; Plint et al., 1992; Read, 1995; Abels et al., 2005). These sea-level changes are expected to have periodicities of 19/23 kyr, 41 kyr, and 100 kyr, i.e., corresponding to the Milankovitch frequency bands. Oligocene-Miocene sequence boundaries can be firmly linked with global $\delta^{18}\text{O}$ increases, demonstrating a causal relation between sea level and ice volume, as expected for the icehouse world of the past 33 Myr (Miller et al., 1991; 1996; Billups and Schrag, 2002). The term glacio-eustasy refers to changes in the amount of water in the oceans due to global climate change. When Earth's climate cools, a greater proportion of water is stored on land masses in the form of glaciers and snow. This results in falling global sea-levels relative to a land mass. The refilling of ocean basins by glacial meltwater at the end of ice ages is an example of eustatic sea level rise. A second significant cause of eustatic sea level rise is thermal expansion of sea water when Earth's mean temperature increases. Current estimates of global eustatic rise from tide gauge records and satellite altimetry is about 3 mm/yr (see IPCC report, 2007).

It thus appears that in assessing the effect of sea-level variation on the geosphere, the time-scale considered is very important. In this study, which focuses on a period of 1 Myr future evolution, emphasis will be on variation within that period i.e., on the 10^4 to 10^5 year scale, whereas lower-order processes are not considered.

6.2. Waterdepth change effects

Global sea-level change or eustasy, not to be confused with water depth or relative sea level, is a widely sought-after parameter, because it directly relates to its tectonic and climatic driving forces. Glacio-eustasy is a global change in sea level due to the uptake or release of water from glaciers and polar ice. Usually, however, the effects of global sea-level change are modulated by other processes in a way that a change in water depth at a certain location is affected by eustasy but not representing eustasy. Tectonic uplift and subsidence of the basin floor and the amount of sediment supplied to and accumulated in the basin may importantly alter the water depth. The effects of tectonics and sediment supply may even reverse the eustatic trends. The resulting waterdepth is what often is regarded as the local accommodation available (Figure 6-1). Based on the knowledge gained from the geological record, geoscientists are aware of the difficulties identifying the contributors to water depth changes. Accordingly, a prediction of future water depths and coast-line positions should not be based on predictions of glacio-eustatic variations solely since this neglects the effects of future tectonic and climate change on basin floor elevation and sediment budget, respectively.

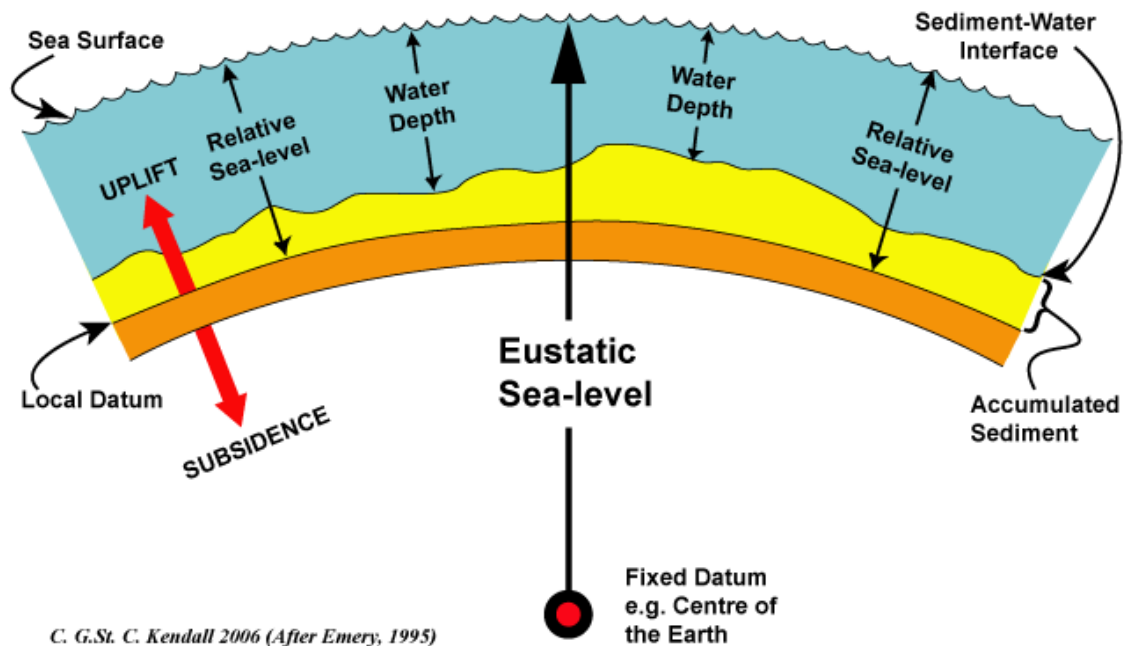


Figure 6-1 Explanation of terminology used in text (internet source: www.sepmstrata.org; from Kendall (2006), modified after Emery (1995).

This interplay of controls on accommodation is best described by a concept called “sequence stratigraphy” (Vail et al., 1977; Jervey, 1988; Posamentier et al., 1988; Posamentier and Vail, 1988) that describes how the available accommodation within a sedimentary basin is a function of glacio-eustasy and tectonics. Available sediment fills this accommodation, resulting in a depositional trend. Generally, a sequence-stratigraphic interpretation would outline characteristic depositional sequences that define a period of change in accommodation, whatever its cause Figure 6-2). A drop in relative sea level potentially leads to local erosion of the former subaqueous depositional areas as well as the continental realm, usually through the entrenchment or incision of river systems that develop a steeper gradient. This process is referred to as forced regression and results in a sea-ward and downward shift of the coastline. A rise in relative sea level potentially leads to the backfilling of the river-valley system and eventually results in the flooding of the subaerial domain such that the coastline repositions landward. This process is known as transgression. These generalities are used in the following discussion on the effects of future glacio-eustatic sea-level variations.

6.3. Water loading effects

Changes in waterdepth also have an isostatic response. Assuming only vertical isostatic adjustment occurs (the so-called Airy type isostasy), this amount is can be theoretically underbuild by equation 4:

$$\text{Equation 4: } \Delta h = \frac{\rho_w}{\rho_w - \rho_m} \Delta h_w$$

Taking a water density of 1000 kg m^{-3} and mantle density of 3300 kg m^{-3} the change in elevation (Δh) amounts to 23% of the change in water depth (Δh_w). Data on subsidence rates of the Rhône delta margin indicate that water loading during the last glacial-interglacial cycle is responsible for 20 m (20 %) of subsidence for a water column of ~100 m (Jouet et al., 2008). Thus, 80 m can be attribute to sea-level rise and 20 m (25%) to its isostatic response. This value is in line with the theoretical expectation of 23%.

6.4. Interplay between eustatic sea-level change and sediment budget

Both sediment supply (rate) and glacio-eustatic sea-level changes can be regulated by the same orbital periodicity as suggested by Perlmutter (1985) and Perlmutter and Matthews (1989). Leeder et al. (1998) proposed that during ice ages, feedback processes reinforce the underlying climate signal and as a result affect sediment discharge either positively or negatively. Thus, ups and downs of base level can be accompanied by rise or fall in sediment supply from the catchments. According to numerical catchment models of Leeder et al. (1998), which take into account climate-related vegetation coverage and buffering capacity, sediment discharges can either be at peak (out-of-phase, OP) or at minimum (in-phase, IP) level during full glacial climates, i.e. glacio-eustatic low stands. Almost simultaneously, Perlmutter et al. (1998) and later Perlmutter and Plotnick (2003) modelled climate-controlled sediment supply using the forward modeling package SEDPAK to evaluate phase relationships. They suggest that for the present icehouse world, an opposite supply-sea level phase relationships exists between northern and southern hemispheres that is determined by the antipodal character of Earth's insolation. The exact way, in which climatic steering of sediment delivery operates, is determined by the nature of the regional climate, vegetation type in the catchment area, and the size, relief and temporal storage capacity of the catchment area (see reviews in Leeder, 1997; Van der Zwaan, 2002). Climate also determines sediment volume, type, and texture, whereas the succession of the climates over an insolation cycle ("direction of change") determines the phase relationships between supply and glacio-eustacy (Perlmutter and Plotnick, 2003). Without doubt, many other factors are essential for a proper evaluation of the climate-supply relationship and indirectly for climate-related accommodation changes in specific settings.

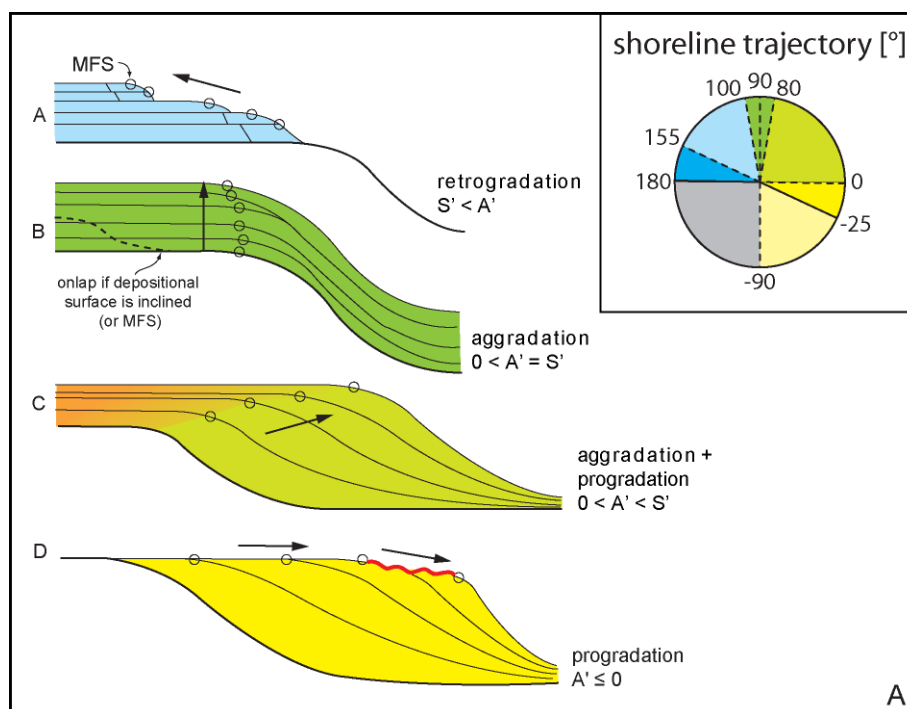


Figure 6-2 Depositional sequence types vs. the ratio between accommodation change and sediment supply. Inset shows how the position of the shoreline throughout the sequence (the shoreline trajectory cf. Helland-Hansen and Martinsen, 1996) is indicative for the depositional behavior.

For several specific cases the accommodation-supply relationship, which is the basis for water-depth changes, will be considered for the climate scenarios presented in Chapter 11. In view of the previous glacio-eustatic lowstand during the Last Glacial Maximum at ~120 m

below present sea level, it should be expected that a forthcoming, more intense glacial cycle with greater ice accumulation would possibly lower sea levels further by a very few tens of metres. Even considering the resulting river profile adjustments within major drainage systems (the Rhine-Meuse system crosses several countries), the range of expected fluvial incision over Dutch territory remains very far from subcrop depths for the Boom Clay top.

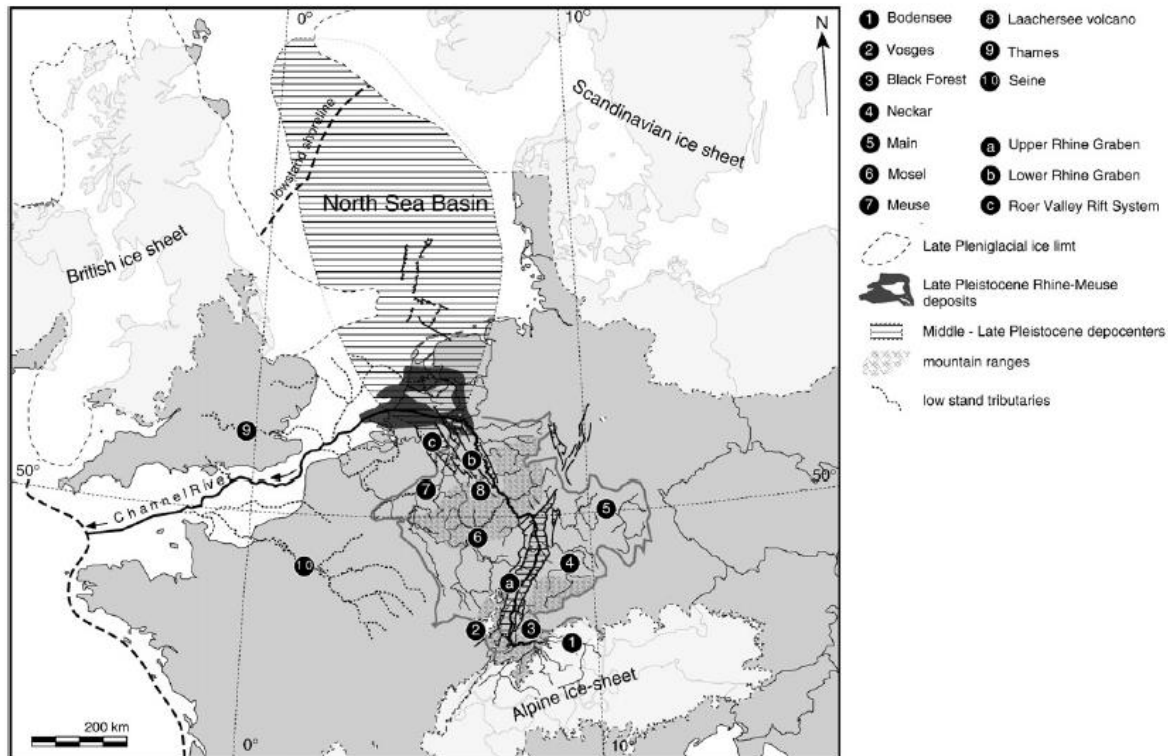


Figure 6-3 The setting of the Rhine catchment (after Van Balen et al., 2010). Structural data were taken from Ziegler (1990, 1994). Late Pleniglacial ice limits are based on maps compiled for the QUEEN project (Ehlers and Gibbard, 2004).

Using a simple linear approach, the change in river profile and the expected amount of fluvial incision at a certain position along this profile can be estimated. For instance, the Rhine drainage from the inlet at Rheinfelden (southern Germany; Figure 6-4) is ~600 km long. A sea-level drop of 120 m will be accompanied by a westward shift of lowstand coastlines onto the far Atlantic margin (Figure 6-3), which would lengthen the lowstand river profiles by several hundred kilometres (e.g. Törnqvist et al., 2003). This would lower the potential for incision considerably and explains why the 120 m sea-level is not represented by fluvial incision depths. The strong tendency for fluvial systems to alternate degradation with strong aggradation during lowstand stages, in response to increased available bedload in a glacial climate is another important factor for reducing fluvial incision potential (e.g. Törnqvist et al., 2000, 2006; Busschers et al., 2007; Blum et al., 2013; Figure 6-5). Moreover, climatically induced changes in sediment transport, river profile changes, sea-level drop and morphological adjustment are processes that take a different amount of time and pronounced time lags may exist between cause in the upstream part and effect in the downstream part of fluvial systems (e.g. Bull, 1991; Törnqvist, 2007). For a more extensive discussion on non-linear response of fluvial systems to climate change see Van Balen et al. (2010).

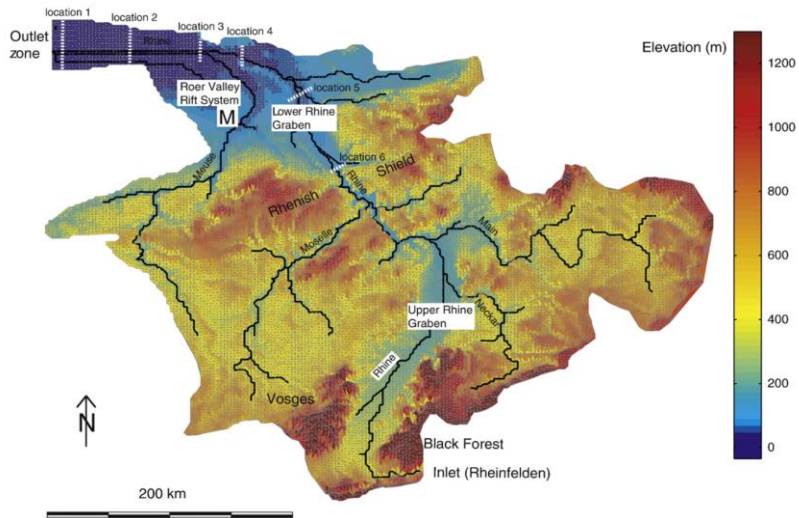


Figure 6-4 Topography of the present Rhine catchment (after Van Balen et al., 2010).

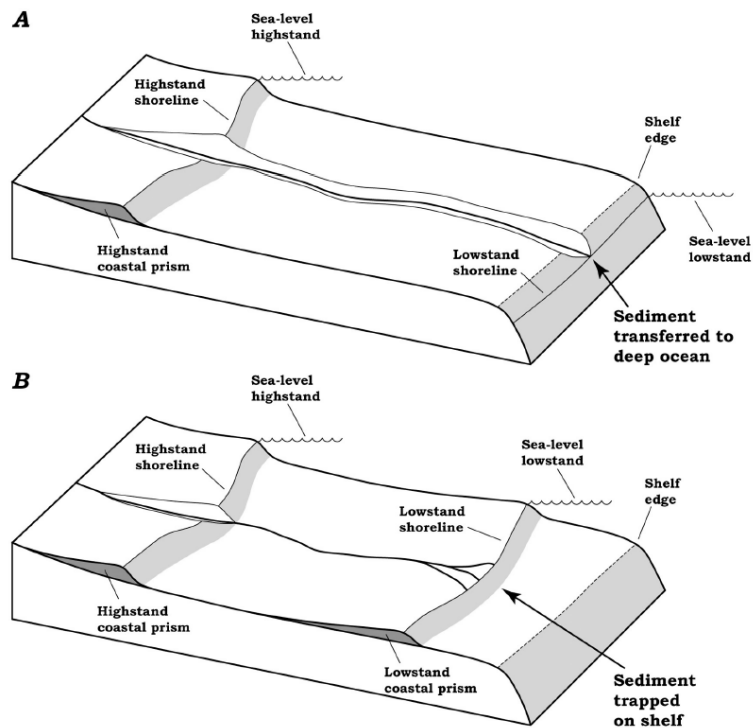


Figure 6-5 Contrasting scenarios of relative sea level fall and fluvial response (after Posamentier and Allen, 1999 and Törnqvist et al., 2006). (A) Lowstand shoreline below the shelf edge triggers headward erosion and the development of a cross-shelf valley that provides a direct connection between the hinterland and the deep marine realm. (B) Lowstand shoreline that remains on the shelf limits fluvial incision and valley formation to the highstand coastal prism and traps the majority of terrigenous sediment updip of the shelf edge.

6.5. *Relevance and synthesis for the safety case:*

Isolation

The expected maximum amount of fluvial incision in case of 120 m (or more) fluvial incision is not likely to affect the Boom Clay. In such an assessment, changes in the actual depth position of the Boom Clay are not taken into account. Only a combined uplift of more than 100 m and a fluvial incision of 120 m have a small effect in the eastern part of the Netherlands. Submergence of the Netherlands is not relevant for the isolation safety case

Delay & attenuation

A change in river profile, either induced by a sea level rise or drop, will influence the topographic effect on hydraulic heads and alters hydrology in general. The effects of such changes are studied in OPERA tasks 4.2.1. task 6.2.1.

Engineered containment

The integrity of the engineered containment (the waste containers) only can be affected during the thermal stage (<~10 kyr). Anticipated future glaciation and sea-level drops will not occur before before ~55 kyr and, therefore, the predicted effects are irrelevant for this safety case. A sea-level rise will not affect this safety function.

GEOLOGY SECTION

|

7. Effects of seismicity and faulting

7.1. *First assessment of effects*

Here, only natural seismicity is concerned, either induced by tectonic forces or triggered or enhanced by glacial unloading (see Chapter 4). There are two ways in which tectonic movements can have an effect on the safety functions of the host rock and the geosphere (Figure 2-1):

1. Exposure / exhumation of the unit under scrutiny, such that the isolation function will be affected by exposure of radionuclides to surface waters and air.
2. Hydrological changes through changes in pore water pressure and fluid flow effects along discontinuities in the crust.

7.2. *Relevance and synthesis for the safety case:*

Isolation

As a first best estimate, the documented displacements along active faults in the Netherlands provide a bandwidth of natural tectonic processes. For the Netherlands, based on historical records, large seismic events are not expected to have more than a limited effect on the regional landscape. However, it is possible for fault scarps of a few meters to occur as a consequence of repeated large-scale fault movements associated with multiple seismic events of varying magnitude. The possibility of exposing the Boom Clay can easily be discarded if the total expected vertical offset does not exceed the depth position of the Boom Clay in the Netherlands within the next 1 Myr. Also, the accumulated effect of multiple seismic events in a seismically active area resulting in, for example, modified drainage patterns, may not be particularly significant from a geological perspective.

Delay & attenuation

Seismic events potentially have an effect on the delay and/or attenuation of radionuclides transport due to possible changes in groundwater flow patterns through faults and fractures. These groundwater flows, if reaching the surface, might have a contaminating effect at the location of the geosphere-biosphere interface. This is a complex process that is relatively unpredictable although it can be generalized by stating that the only way for upward transport of deep fluids is through permeable faults. Renewed fault movement tends to increase the permeability of a damage zone parallel to the fault core (Caine et al., 1996), which may facilitate the deep circulation of fluids.

It is also important to realize that fault activity can be enhanced by loading and unloading of the lithosphere by sediment, water or ice. For instance, small changes in pore water volume occurring when a porous medium is mechanically compressed (loaded) or expanded (unloaded), both result in changes in pore water pressure (e.g., Domenico and Schwartz, 1998). In highly permeable rock these transient changes in fluid pressure will quickly dissipate. However, in low-permeability units like shale or clay the effects of loading and unloading can induce anomalous fluid pressures that require thousands of years to return to equilibrium conditions (e.g., Neuzil, 1993).

Engineered containment

For a specific waste repository site, the problems of locating all faults present and to estimate their fault slip rates appears to be much more crucial to evaluate future performance than estimating the rate of formation of new faults (Trask, 1982). The rationale is that faults that have moved under the current stress field, even at low rates, are likely to move again during the time the waste will remain toxic. New faults only form in response to changes in the pattern of tectonic stress. Such changes appear to occur very slowly and can be discarded for the future 1 Myr times span considered.

8. Salt tectonics

8.1. Introduction

Salt structures, i.e. salt walls and diapirs, are key features in defining the deep subsurface structure, especially in the northern part of the Netherlands. The salt structures are, almost without exception, related to one or more basement faults i.e., faults in the underburden of the salt. Movements along these faults enabled the upward flow of salt because it weakened the overburden and creates a differential stress field due to the differential loading. The buoyancy force related to the density inversion alone seems insufficiently strong to deform the overburden. The faulting is the trigger mechanism for the salt movement and the larger the throw on the fault, the better the salt structure will be developed.

The OPLA study (Remmelts, 1993) gave insight into the structural development of the salt structures in the northeastern part of the Netherlands. An important conclusion is that salt structures are formed in relation to basement faulting and that accelerated growth occurs in periods of enhanced tectonic activity. Salt structures rose mainly in response to the main Mesozoic tectonic phases. Less important Cenozoic activity can be deduced from the uplift and thinning of stratigraphic units above and around salt structures. It should be realized however, that the latter processes take place on a smaller time scale (millions of years) than the Mesozoic structuration (tens of millions of years).

A large number of studies addressing the potential of nuclear waste storage in salt structures studied the dynamic behavior of salt, both in the past and future. Many of these studies focus on internal deformation of the salt and provide information that is not necessarily relevant for the safety functions of nuclear waste disposal in the Boom Clay. Salt flow processes that affect the depth position of the Boom Clay or its overburden (geosphere) after their deposition, however, are considered herein. These occur later and on a smaller time-scale in a period without large tectonic events. Thus, fault trigger mechanisms are less important and any change in differential loading of the salt is more likely to induce salt flow rather instantaneously. The main sources for differential loading are accumulated sediment wedges and ice sheets. The latter process was central in the OPLA study that focused on the past and future (100 kyr) evolution of shallower salt structures (<1 km) that are in the depth range of (peri-)glacial processes.

8.2. Ice-sheet loading and salt structures

Lang et al (2104) use a finite-element method approach (ABAQUS) to simulate the reaction of salt structures to ice-sheet loading. Their results unambiguously indicate that salt structures respond to ice-sheet loading and that an ice advance towards the diapir causes flow of salt from the source layer below the ice sheet towards the diapir. The diapir rises as long as the load is applied to the source layer but not to the crest of the diapir. When the diapir is transgressed by the ice sheet, the diapir is pushed down, resulting in a depression at the surface and slight broadening of the diapir. During ice-sheet retreat the downward displacement is partially reversed due to the renewed rise of the diapir. Hseinat and Hübscher (2014) propose glacio-isostasy being the key factor for reactivation and upward propagation of the sub-salt fault. Moreover, they propose a causal link between ice-load induced tectonics, the generation of near-vertical faults in the upper crust above an inherited deep-rooted fault and the evolution of tunnel valleys. Faulting and folding beneath the ice sheet creates a weakness zone that facilitates erosion by pressurized glacial and subglacial meltwater, which is the primary explanation for tunnel valley evolution (Piotrowski,1994,1997; Huuse and Lykke-Andersen, 2000; Jørgensen and Sandersen, 2004). Based on seismic data, the Kossau tunnel valley (in the southeastern Bay

of Kiel, Germany) is considered to have resulted from such interplay between the underlying fault system and subglacial meltwater erosion. Plastic deformation of the overburden is restricted to the area directly above the salt diapir. Ice-induced salt flow is observed in depths of up to 5000 m. Besides affecting the depositional architecture of glaciogenic and interglacial deposits, ice-induced salt movements may affect hydrocarbon reservoirs in the vicinity of salt structures. The distribution of deformation in the overburden suggests a reactivation of faults along and above the salt structure. The vertical and lateral displacement of a salt structure changes the stress state within the adjacent rocks and may also affect the pore pressure. The long-term effect of these perturbations, which will take very long to dissipate (Nikolinakou et al., 2012), may thus cause deviations from the expected stress state and elevated pore pressures near salt structures and may pose a problem during drilling operations. See also see chapter 10 on fluid migration pathways associated with salt structures.

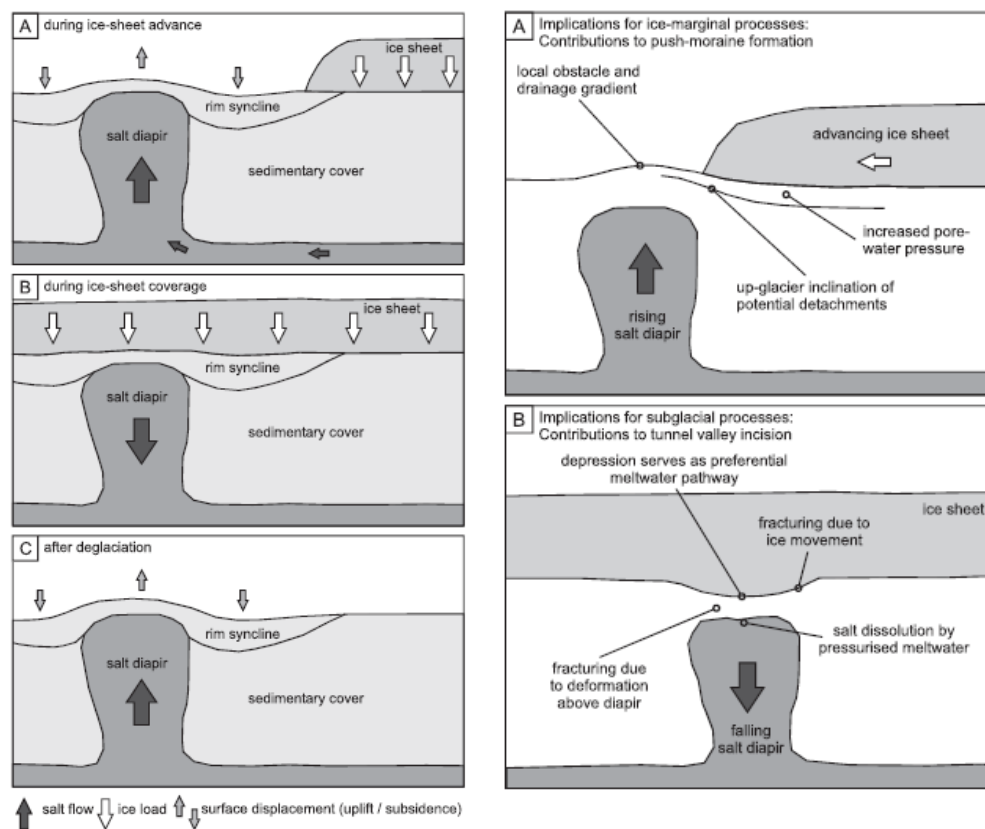


Figure 8-1 LEFT: Conceptual model of the interaction of salt diapirs and ice sheets (compiled from Liszkowski, 1993; Lehné and Sirocko, 2007; Sirocko et al., 2008). A) During ice advance the diapir rises. (B) Push down during ice coverage. C) Diapir rise after deglaciation. RIGHT: Implications of the modeling results for ice-marginal and subglacial processes (not to scale). A) Potential contribution of proglacial ice-induced rise of a salt structure to the formation of push-moraines by creating a topographic obstacle and inclining potential detachments (after Lang et al., 2014) . According to their model results, the uplift is up to 4 m in a distance of ~1 km to the ice margin. B) Potential contribution of the subglacial fall of a salt structure to subglacial erosion and tunnel-valley formation by providing a preferential drainage pathway and fracturing of the overburden of the salt structure. The subglacial depression is up to 36 m deep and has the same width as the salt diapir.

8.3. Quantifying growth rates from Dutch subsurface data

The OPLA study (Remmelts, 1993) presents an improved methodology to calculate growth rates of salt structures based on the present-day anomalous depth position of stratigraphic layers above and around salt structures. Growth rates are divided into two categories i.e., the external growth rate (section 8.3.1), which is the rate at which the top of the salt structure (including its caprock) rises with reference to the top of the mother salt layer, and the internal growth rate (section 8.3.2), which represents the volume of salt that passes a certain horizontal section of the salt structure per unit of time. During salt rise, dissolution of salt is likely to occur and will lead to subsidence, a process referred to as subsrosion. Theoretically it is possible to estimate subsrosion rates from the comparison of the average internal growth rate and the average external growth rate. An assumption which has to be made is that without subsrosion these two figures should be the same. Accordingly, the difference indicates the rate of subsrosion, which can be translated into the volume of subroded salt. In executing these calculations the inverse process of overburden compaction ("decompacting") has proven to be very important.

8.3.1. Average external growth rate

It is assumed here that under normal conditions and without salt movement, sedimentation will result in a layer of constant thickness over the whole region. When a salt structure rises, it disturbs the uniform sedimentation by local uplift of the area directly above the structure and the development of a rim syncline directly around it (Figure 8-2). Away from the salt structure this anomaly will dissipate. As a result, above some of the salt structure, it appears to be the case that the Boom Clay is at shallower depths and also thinner compared to the average regional trends (Figure 8-4). This is also observed in seismic sections of the salt domes. This difference in thickness equals (after compaction corrections) the rise of the salt structure. When divided by the time represented by the sedimentary interval under investigation, it yields the average external growth rate. This method has successfully been applied by Hospers and Holte (1984), Sørensen (1986), Rijks Geologische Dienst-30.010 (1989) and Petersen (1991).

For OPLA (Remmelts et al., 1993), the calculations were executed for a number of salt structures in the northeastern Netherlands and the M-blocks offshore. The calculated values of the average external growth rates vary between -0.04 and 0.06 mm/yr. The Schoonlo salt structure shows an anomalously high growth rate of 0.11 mm/yr. In general the average internal growth rates of the onshore structures are 3 to 5 times higher during the Early and Middle Oligocene related to the Pyrenean tectonic phase (35-29 Ma) than in the Late Tertiary and Quaternary (20-0 Ma), with enhanced compression in the Quaternary. This supports the above mentioned relationship between accelerated growth and occurrence of tectonic phases. Actual growth rates of salt structures will however, have deviated significantly from calculated values.

8.3.1. Average internal growth rate

The average internal growth rate is the volume of salt which passes per time unit through an arbitrarily chosen horizontal section of the salt structure (Figure 8-3). The main assumption made for the calculation of the average internal growth rate is that the volume of salt accumulated in the salt structure equals the excess volume of the sediments in the rim synclines (c.q. depletions areas) after the volume has been corrected for compaction effects (Sørensen, 1986; Remmelts, 1993).

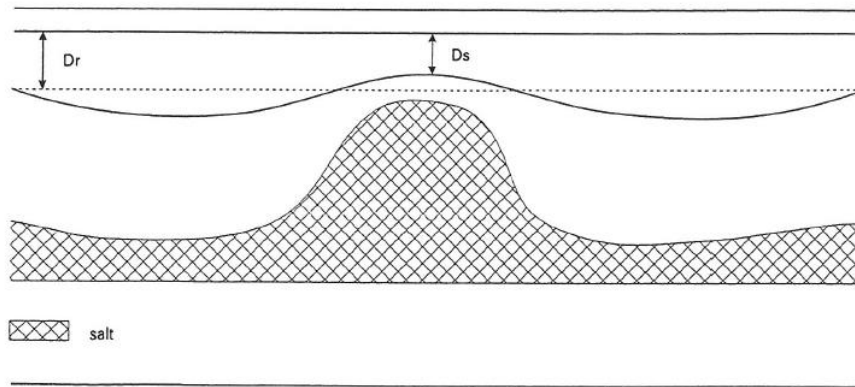


Figure 8-2 Schematic representation of the calculation of the external growth rate. D_r is the regional thickness of a unit. D_s is the thickness of this unit above the salt structure. $D_r - D_s$ is a measure for the external growth rate (modified after Remmelts et al., 1993).

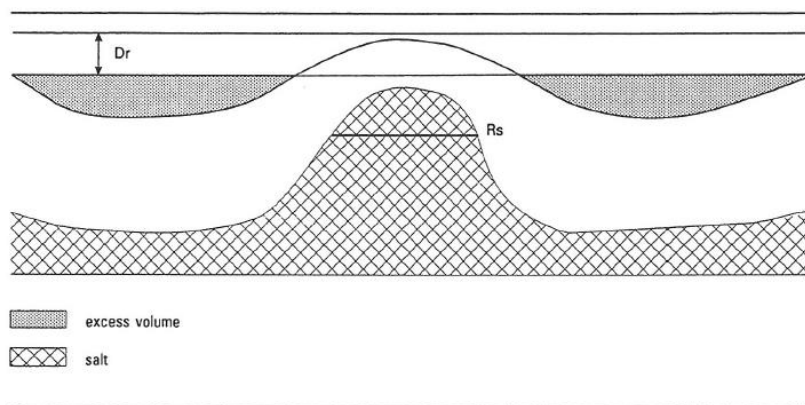


Figure 8-3 Schematic representation of the calculation of the internal growth rate (modified after Remmelts et al., 1993).

8.4. Suggestion for alternative approach to estimate salt induced uplift

Whereas previous studies (e.g., the OPLA study; Remmelts, 1993) focused on the understanding of the processes underlying the growth of salt structures for predicting future evolution, a more empirical approach is suggested here. This approach needs to focus on documenting the Boom Clay depth position above salt structures in great detail. Currently, basin modeling software is able to integrally incorporate the decompaction procedure, which at times of the OPLA project was still a troublesome part of the calculation methodology. It is suggested to use basin modeling software (for instance Petromod[®]) that is able to perform burial history analysis on 3D geomodels and to incorporate lateral and vertical salt flow as well. Such analysis requires a 3D age-constrained layer model, which currently is publically available for the Dutch subsurface. Also, porosity-depth relations for the stratigraphic units should be determined, either based on actual measurements or library default values. Furthermore, values for paleo-water depth and heatflow should be used. The output i.e., the changing depth position of the stratigraphic units through time, can be used to derive uplift and subsidence rates. The most recent vertical motion rates at each locality in the 3D model can then be extrapolated to make predictions for the future. Such an approach is empirical and implicitly takes all geological processes into account that underlie the vertical motion, rather than focusing on the underlying processes. The burial history also gives information

on accumulation rates for the stratigraphic intervals. In extrapolating future uplift and subsidence scenarios for the Boom Clay, accumulation rates can be extrapolated as well to account for future accumulation of sediment.

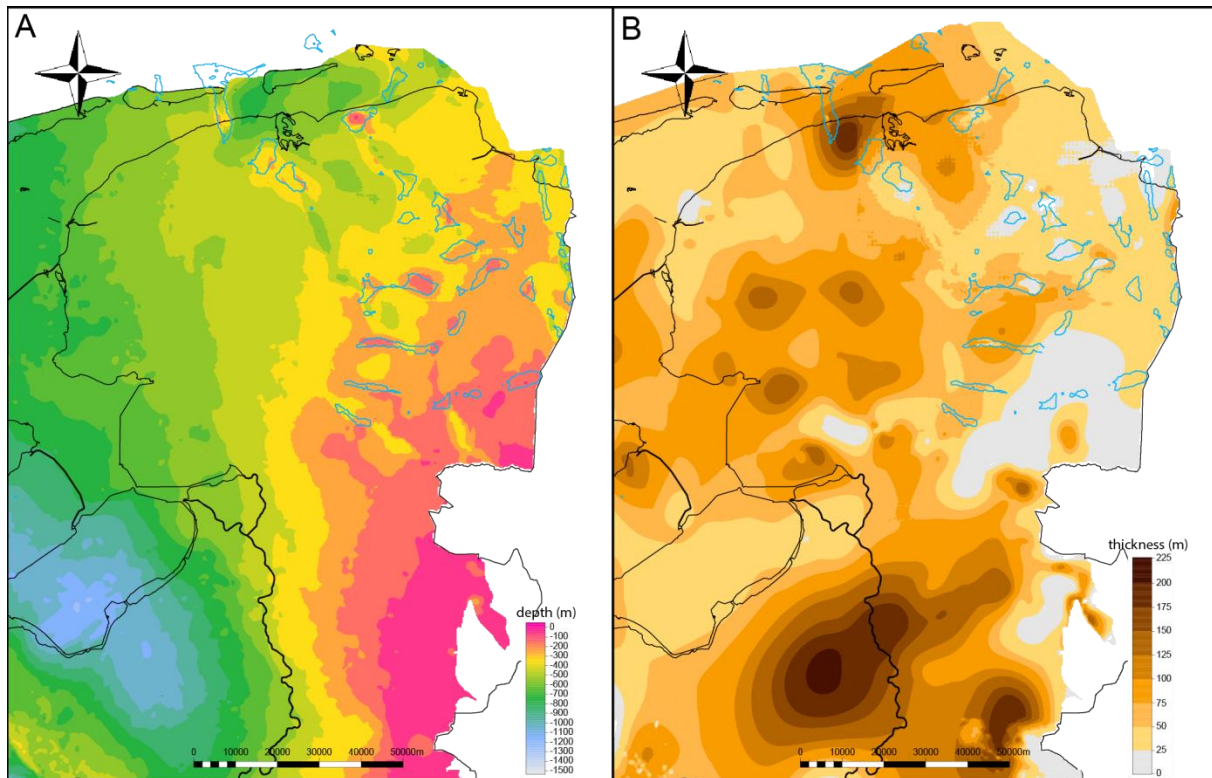


Figure 8-4 Depth (A) and thickness (B) maps of the Boom Clay Fm. in the northeastern region of the Netherlands (adopted from Vis and Verweij, 2014). Above salt structures (indicated by blue polygons) the unit is thinner and at shallower depths.

8.5. Relevance and synthesis for the safety case

Isolation

The highest calculated external growth rates are 0.11 mm/yr. Assuming that this extreme rate continues for 1 Myr, this would result in an uplift of 110 m. This would result in exposure of the Boom Clay above some salt domes. If however, the uplift is less continuous and future deposition takes place, the likelihood of exposure is reduced. On the 1 Myr timescale it is not expected that a reorganization or intensification of the stress field occurs that intensifies the salt growth rates.

Delay & attenuation

In case of a future glaciation, the causal link between ice-load induced tectonics, the generation of near-vertical faults in the upper crust above an inherited deep-rooted fault and the evolution of tunnel valleys related to preferential drainage pathway would dramatically influence the delay and attenuation of safety functions of the Boom Clay and its overburden. The vertical and lateral displacement of a salt structure also changes the stress state within the adjacent rocks and leads to changes in pore pressure and consequently affects deep fluid and groundwater flow. Seals of existing hydrocarbon reservoirs, and aquifers in general, may become breached.

Engineered containment

Not affected on the time scale considered.

9. Compaction and subsidence

9.1. Introduction

An understanding of the relief and shape of the surface environment is clearly relevant to determining groundwater recharge and flow on a regional scale. On the local scale, there may be topographic effects on surface drainage that are relevant to describing near-surface hydrological pathways. A description of topography is however normally not incorporated directly in a biosphere assessment model. Instead, its influence is incorporated in the parameterization of specific processes such as interflow.

The change of topography in the Netherlands is mainly determined by exogenic processes including tectonics, isostatic responses and compaction (Kooi et al., 1998).

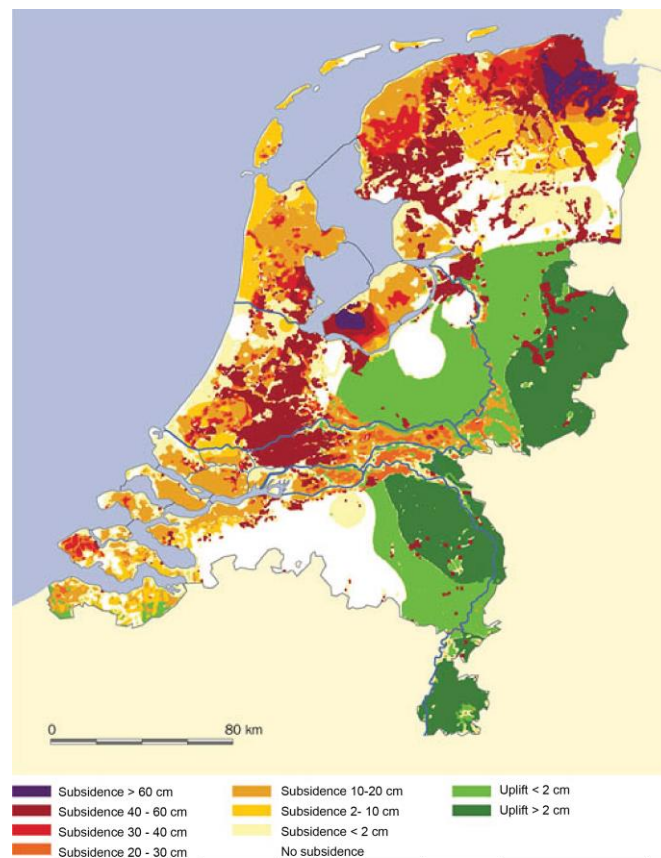


Figure 9-1 Expected subsidence and uplift for 2050 relative to the situation in 1964. In this map the effects of natural processes and human activities (e.g., oil- and gas extraction) are combined. (Source: <http://www.natuurinformatie.nl>).

The main processes that contribute to subsidence of the surface (here regarded as sub-process) are:

- Peat compaction of which the amount and rate is strongly dependent on the water table. This compaction is not ever lasting, if it continues at the present rate all peat will be oxidized in 2700 AD, with an associated subsidence of -7m (see Caro Cuenca et al., 2007).
- Tectonic crustal deformations (uplift/subsidence), including salt tectonics (see Chapters 9 and 10, respectively).

- Isostatic adjustment to loading/unloading of the lithosphere including glacio- and hydro-isostasy and isostatic subsidence of the crust caused by the changes in surface load due to deposition of Holocene sediments, the deglaciation of Fennoscandia, the filling of the North Sea with meltwater from the melting global ice sheets (Kooi et al., 1998). For a more extensive overview the reader is referred to Chapter 4.
- It may be assumed that only natural processes play a role on the 1 Myr timescale. However, the effects of currently induced subsidence have to be taken into account. The subsidence prediction for 2050 AD may serve as a base scenario in which all contributing processes are taken into account.

The levelling results of the Netherlands point to a significant tilting of the country with the coastal regions subsiding relative to the inland areas. Differential movements at scales up to 100 km are most likely a consequence of isostasy and tectonic activity whereas the contribution from compaction is most significant for the coastal provinces. Evaluation of the isostasy and compaction processes show that these can explain only part (30-45 % and <5 %, respectively) of the observed phenomena and the levelling results imply surprisingly large rates of recent tectonic activity.

Through the interplay of these processes, it is expected that the larger part of the Netherlands will continue to subside except for its most eastern and south-eastern parts (

9.2. Relevance and synthesis for the safety case:

Note that the compaction component does not change the depth position of the Boom Clay, whereas isostatic and tectonic processes do. The effects on the safety functions of these processes are dealt with in previous Chapters. The changing depth position of the Boom Clay is important to consider in modeling the effect of processes with a clear depth function e.g., groundwater flow (and the fresh/salt water interface) or permafrost development. Soil compaction result in changing porosities and may therefore affect the penetration of permafrost depths. It is suggested that this effect should be incorporated in alternative permafrost modeling scenarios.

10. Fluid migration pathways

10.1. Introduction

There are several indications for both past and active fluid flow that likely to have affected the safety function of the Boom Clay and its overburden. A study by Judd et al. (1997) shows that the British Continental Shelf has an average yearly methane flux of 0.2-5.6 10^6 g/km², which contributes to about 40 % of the total UK methane emission. If a correction is made for the dissolution of methane in seawater, the flux approximates to 5-38 10^6 g/km² per year, which is a good estimate of the amount of gas expelled at the seafloor (Hovland et al, 1993). These numbers suggest that sea-floor gas venting must be a widely present phenomenon in the North Sea. Indeed, deep seismic and sea-floor acoustic data show many expressions of both active and past fluid or gas seepage, migration and sea-floor venting. These expressions include:

- seabed and paleo pockmarks
- seepage plumes in the water column
- acoustic blanking
- seismic acoustic anomalies (e.g., bright spots indicative for gas accumulations)
- shallow seismic chimneys

Many of these features give evidence that Boom Clay has been affected by vertical venting systems that have been active for a long time in geological history. Note that these features are well expressed in offshore seismic data, while the Cenozoic shallower strata in general are badly expressed in onshore data. This precludes the interpretation of fluid flow phenomena in onshore seismic data. This is one reason that, to date, shallow gas accumulations were never identified onshore. Another explanation is that the absence of a water column and associated hydrostatic pressure leads to insufficient sealing capacity of Cenozoic clays and as a result buoyancy drives the gas to the Earth's surface where it will vaporize. Thus, absence of gas accumulations and the seismic data quality may falsely suggest that gas and fluid migration do not occur onshore the Netherlands.

10.2. Shallow gas accumulations

The inventory of bright spots (Direct Hydrocarbon indicator (DHI) for shallow gas) in sedimentary units above the Mid Miocene unconformity in the northern offshore area has shown that many of the potential shallow gas accumulations occur in the Southern North Sea (SNS) Delta sedimentary units, either in stratigraphic traps or in multiple stacked structural traps above salt structures (Schroot et al., 2005; Van den Boogaard and Hoetz, 2011; Ten Veen et al., 2011, 2013). Seismic attribute analysis suggests that the salt structures are important, or were important in the past, in conducting fluids and gas from deeper levels (Ten Veen et al., 2011; 2013). At present migration and charging of gas within the SNS delta still takes place under normal (hydrostatic) to close-to-normal pore pressure conditions (Verweij et al., 2012).

The migration of gas (and/or fluids) and the charging and leakage of the reservoirs in the delta deposits during Pliocene to recent times developed under highly dynamic pressure, stress and temperature conditions that resulted from the combined influence of rapid sedimentary loading of the delta deposits, waxing and waning of ice sheets, and glacial-interglacial temperature fluctuations. The current presence of gas in intra-delta reservoirs is a result of gas charging and leakage of the traps in the Plio-Pleistocene delta under these highly dynamic conditions. Current gas column heights reflect different trapping conditions, such as:

1. Trap filled to capillary seal capacity of the mudstone caprock.
2. Trap not filled to capillary seal capacity of the mudstone caprock, because:
 - a. Trap is filled to structural spill point.
 - b. Lack of charge.
 - c. Leakage after charging stopped through breaching of permeable mudstone caprock.
 - d. Leakage during charging due to hydraulic failure induced by fluid pressures exceeding seal strength.
 - e. Leakage along permeable fault zones penetrating the reservoir.
3. Trap filled to more than capillary seal capacity of the mudstone caprock, because charging exceeded the capillary seal capacity of mudstone caprock, while the ongoing charging rate was higher than the leakage rate through the mudstone caprock.

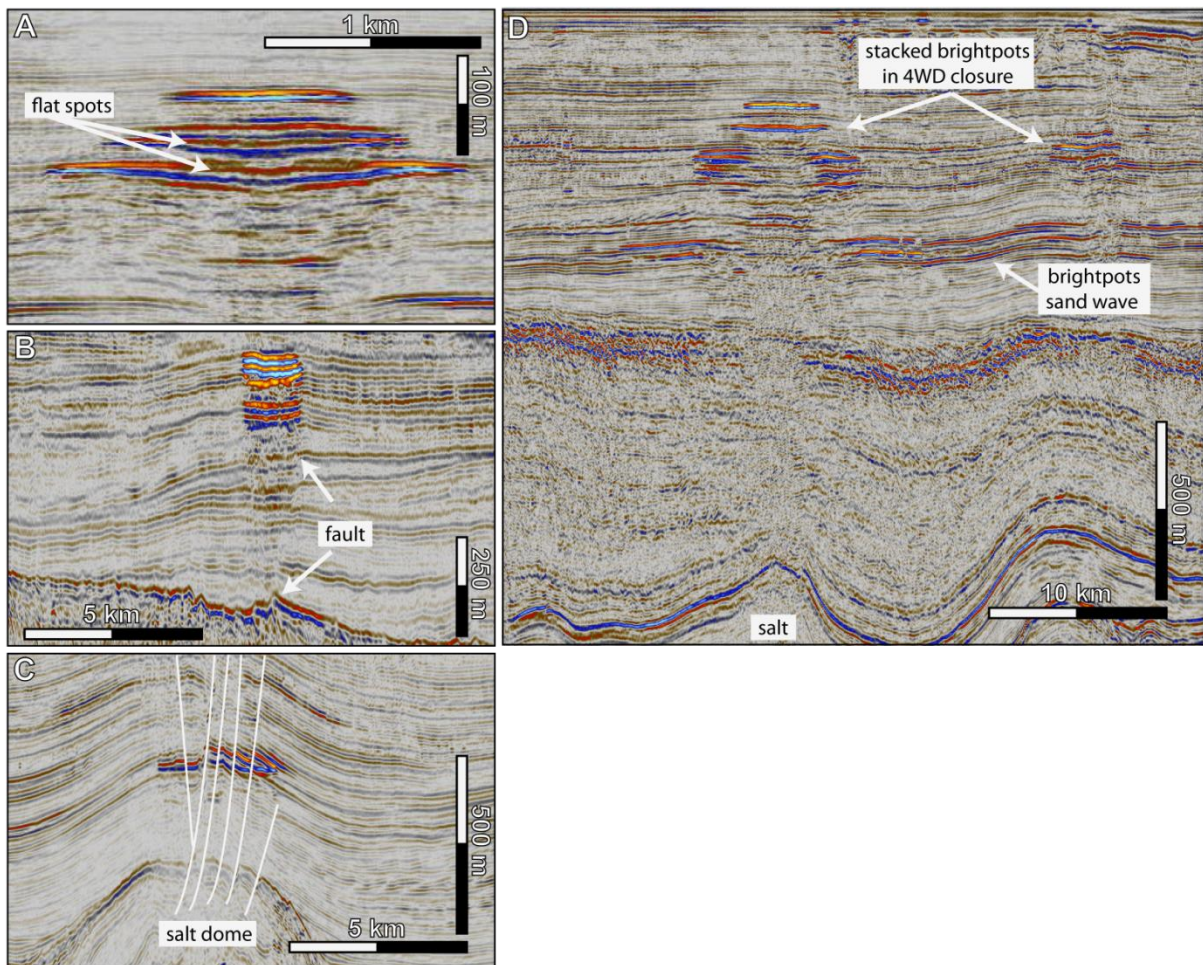


Figure 10-1 Seismic sections of the Dutch Northern offshore with various types of Bright Spots . A) Stacked bright spots indicative of multilayered gas fields, each with their own gas-water contact (seen as flat spots). B) Multilayered bright spots above acoustic turbulence zone that hint at gas expulsion from faulted zone below. C) Bright spots with lateral fault seal. D) Stacked bright spots in anticlinal (four-way dip closures) closure above salt domes. In all examples shown, gas migrates through the Ruper Clay Mb interval (modified from Ten Veen et al., 2014).

10.3. Seabed pockmarks

Seabed pockmarks are concave, crater-like depressions, which are commonly associated with the release of gas or fluids from the subsurface (King and MacLean, 1970; Hovland and Judd, 1988). The first report of these morphological features was by King and MacLean (1970) from muddy parts of the Scotian Shelf. The pockmarks encountered range in diameter from 15 to 45 m and have depths of 5 to 10 m. On seafloor echograms they appear as V-shaped notches. During the 1970's and 1980's pockmarks were also reported in large quantities from the North Sea (Hovland and Judd, 1988; McQuillin and Fannin, 1979). At that time it was thought that pockmarks did not occur in the shallower Southern North Sea. Later on, however, closer line spacing and better observation techniques led to the discovery of some pockmarks in the south as well. In the Netherlands sector pockmarks have been found on archive 3.5 kHz sub-bottom profiler records at two locations, in blocks A5 and F10 respectively (e.g. Schroot et al., 2005; Figure 10-2, 12-3). These features are typically about 40 m in diameter and 2 m deep.

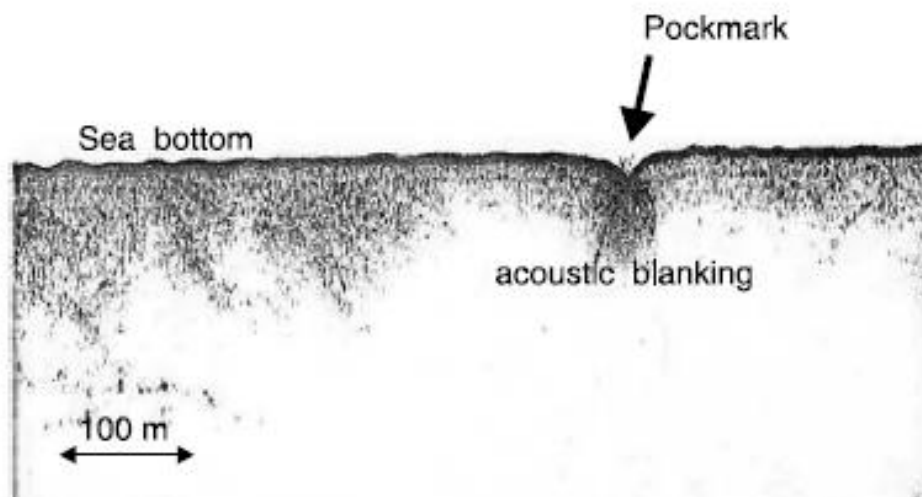


Figure 10-2 A 3.5 kHz sub bottom profiler record showing a seabed pockmark in block A5; diameter about 40 m and depth 2 m. Acoustic blanking suggests the presence of gas in the shallowest sediments. (Modified after Schroot et al., 2005).

Palaeo-pockmarks

Pockmarks are common features throughout the Southern North Sea (SNS), Plio-Pleistocene delta sequence and are key in understanding the fluid and gas venting throughout geological history. Occasionally, the vertical vents led to gas accumulations that are seen on seismic data as bright spots (Figure 10-4). Some occur stacked Figure 10-5, but the fact that most of them are vertically isolated suggests that they are the expression of older seafloor pockmarks. High concentrations of pockmarks are also very common in younger stratigraphic units (Figure 10-4). Through the westward progradation of the delta, they occur farther west i.e., where they vertically are less separated from the Mid Miocene unconformity (MMU), due to the progradational westward onlap onto this surface. The downward extent of seismic chimneys indicates that fluid escape originated as deep as the MMU and may be linked to polygonal fault patterns at this level. Occasionally, the vertical vents led to gas accumulations that are seen on seismic data as bright spots (Figure 10-4). Some small gas accumulations are related to salt structures.

There is a marked difference between pockmarks in older vs. younger strata: the latter are associated with vertical chimneys and are stacked, indicating that fluid escape at the seafloor continued for a long period.

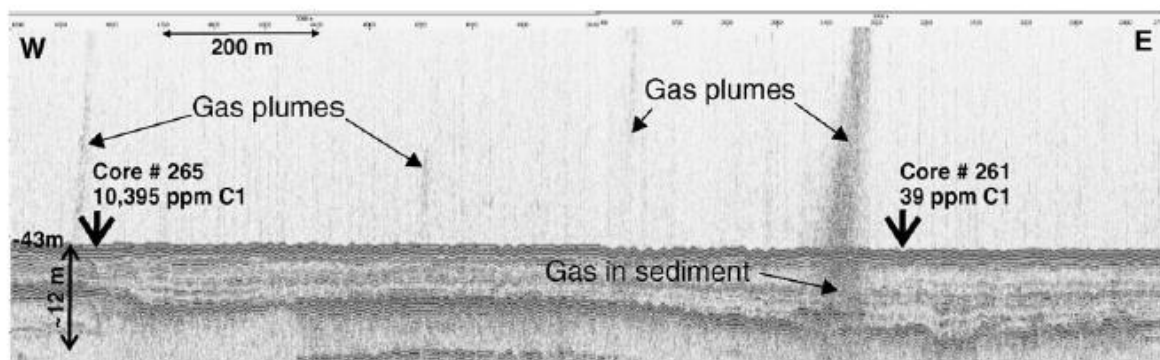


Figure 10-3 High frequency sub-bottom profiler record running W-E across the B13 gas accumulation and showing gas plumes in the water column (Modified after Schroot and Schüttenhelm, 2003).

Pockmarks in the oldest strata show no vertical stacking. Thus the pockmarks in the delta sequence and the polygonal fault in the MMU are crucial for understanding that:

- 1) Fluid (water and gas) escape occurred already during the deposition of the first progradational delta units of Latest Miocene - Pliocene age.
- 2) The gas source is (predominantly) thermogenic in origin.
- 3) Gas venting occurred at the seafloor i.e., no sealing capacity existed initially.
- 4) None of the pockmarks in the oldest strata is associated with Bright Spots indicative of gas accumulations. This suggests that only some time after deposition the pockmarks might have become sealed off. Also the fact that they are not vertically continuous supports this interpretation.

In the SNS delta pockmarks also occur as elongated features with dimensions up to 300 m wide, 15 m deep and as long as 1.25 km. Andresen et al. (2008) describe similar features (type B pockmarks) from the Oligocene and Miocene delta sequence of Denmark that also parallel the strike of the identified shelf clinoforms. These elongated pockmarks are thought to develop due to fluid expulsion and subsequent erosion by sea-bottom currents. In Denmark the pockmarks occur above gas-mature Jurassic source rocks and thermogenic gas is suggested as the main fluid involved in the pockmark formation. The timing of gas expulsion from the Jurassic source rocks in combination with loading imposed to the basin by the progradational Miocene clinoforms are interpreted as the main factors controlling the timing and location of the pockmarks. The pockmarks observed in the Plio-Pleistocene succession in the Netherlands likely also tell a story of thermogenic gas venting to the surface and palaeocurrents scouring of the seabed. In one particular case, the pockmarks occur right above the F3-FB gas-condensate field in reservoirs of the Upper Jurassic Scuff Group. The severely faulted nature of the Cretaceous and Lower Cenozoic deposits above the reservoir might form the pathway for upward fluid expulsion. The orientation of the elongated pockmarks agrees with that of the sand waves in higher units and are likely formed and modulated by a similar bottom-current system. Also in the Netherlands, progradational clinoforms formed the necessary loading that might have triggered the fluid expulsion. Moreover, the MMU consist of a vast network of polygonal faults that might be caused by fluid escape due to sediment loading. Westward, where the thicknesses of the onlapping units onto the MMU diminish, this fault pattern and the pockmarks are absent.

10.4. Acoustic Chimneys

Typically when fluids (gas is usually a fluid at depths of several 100s of meters) migrate upwards from deep thermogenic sources or reservoirs, connate gas stays behind and in seismic data generates vertical noise trails (Conolly and Garcia, 2014; Figure 10-6). On seismic data these vertical migration paths are generally recognized as vertically aligned zones of chaotic, often low amplitude reflectivity, described variously as gas chimneys, seepage pipes, blowout pipes, or gas clouds. The paths are often associated with other seismic seepage-related features such as mud volcanoes, fault related pockmarks, hydrocarbon related diagenetic zones (HRDZ's), and actual gas accumulations. Figure 10-6 shows an example from the A18-02 block in the Dutch northern offshore, where gas migration is highlighted by a so-called chimney cube made visible using functionality of OpenDtect (courtesy dGB). Approximate position of the Boom Clay is indicated to illustrate that this unit is vulnerable to fluid migration as well.

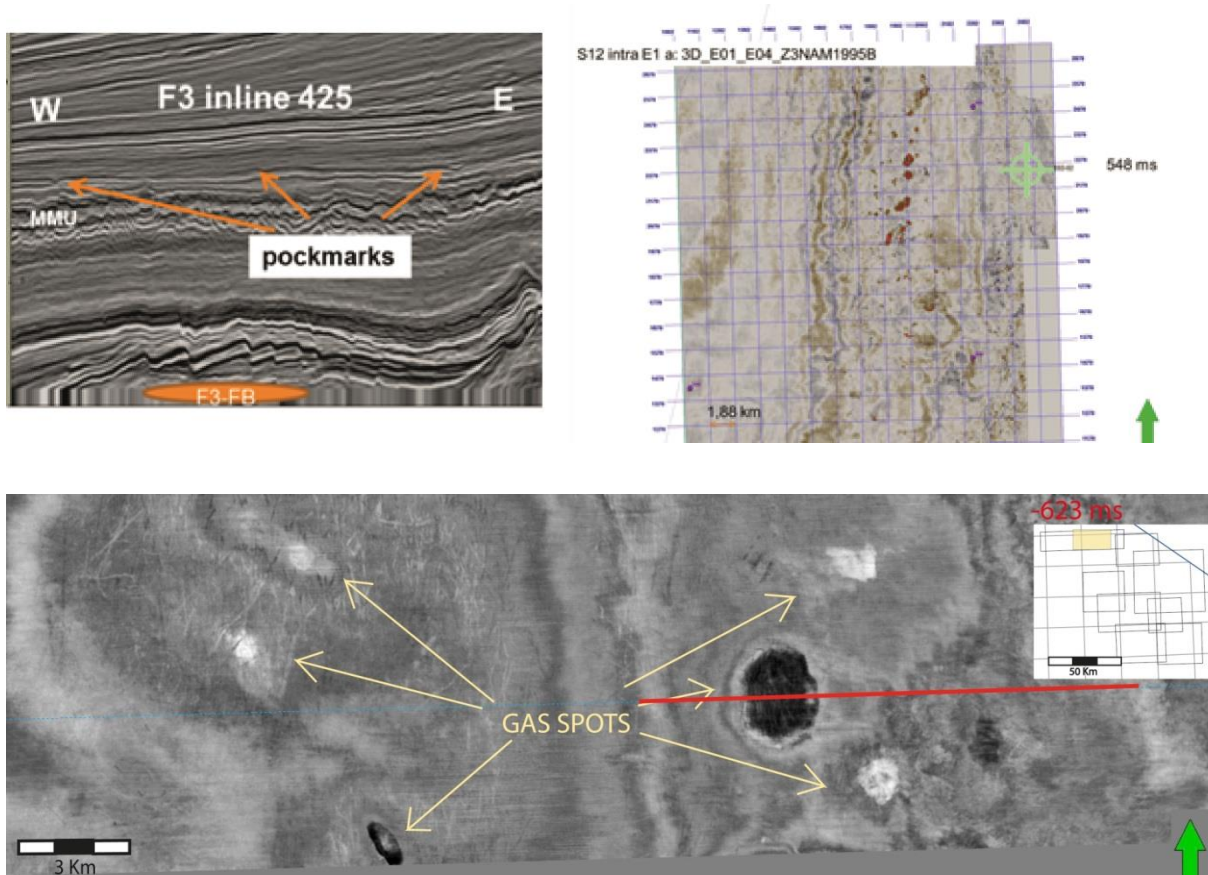


Figure 10-4 Paleo pockmarks in the base of the Plio-Pleistocene delta succession seen in seismic section (upper left) and pockmarks on seismic timeslice (upper right) in westernmost part of the study area (Elbow Spit Platform). Detail of gas spots (gas-filled) that appear as bright features in seismic data (bottom).

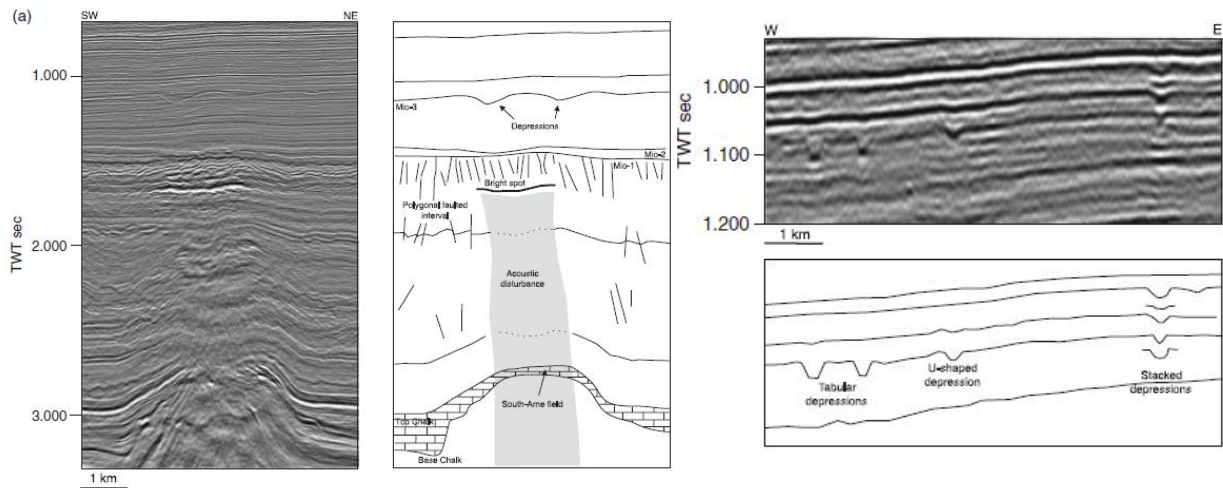


Figure 10-5 Example from South Arne Field Denmark showing the relation between zones of deeper HC reservoirs and acoustic disturbance zone, pockmarks and gas accumulations above. The stacked pockmark depressions suggest a preferred location for the formation of the depressions i.e., suggesting the existence of long-lasting fluid/gas migration pathways (modified after Andresen et al., 2008).

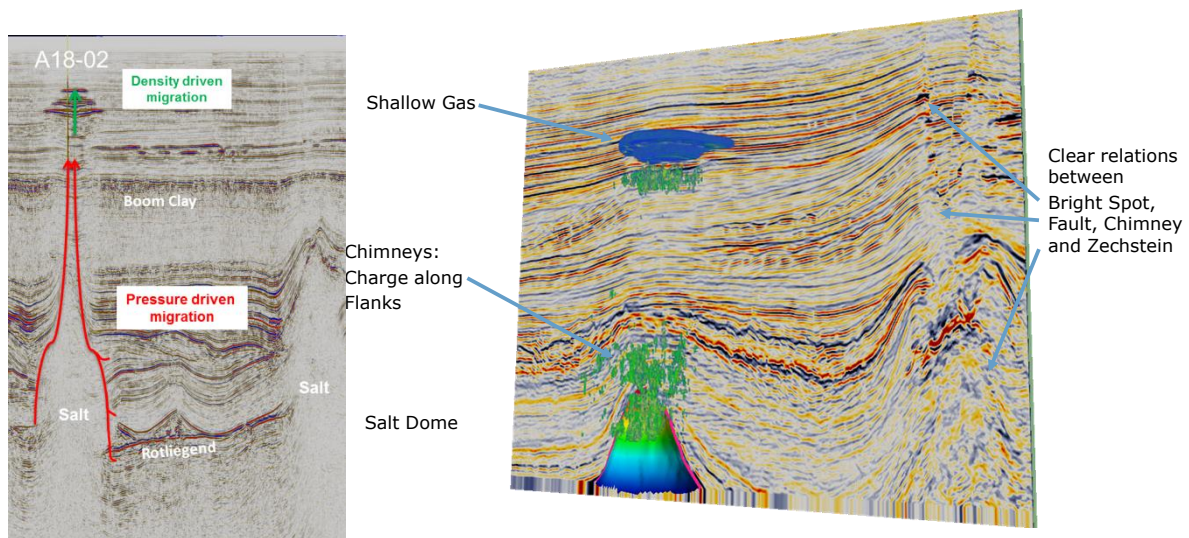


Figure 10-6 Indications of seismic blanking (left) and acoustic chimneys (right) in seismic data around well A18-02 in the Dutch northern offshore. In the deeper subsurface the fluid flow is pressure driven (red arrows); high up in the sequence, the pressure drive gives way for the buoyancy drive (green arrows). Approximate depth position of the Boom Clay is indicated.

10.5. Combination of explosive methane venting and deglaciation

Methane occurs in nature in the form of gas or, in sediments and bedrock, in the form of ice methane hydrate or clathrate. The volumetric relation between the ice and gas phases is 1 : 168, which implies a very large expansion when ice transform into gas. The transition is phase-boundary controlled by temperature and pressure (Mörner, 2011, Figure 10-7). During periods of permafrost, the geothermal gradient adapted to colder conditions allowing for shallow gas accumulations in the bedrock to be transformed into methane ice. During ice ages, the vertical pressure is strongly deformed and methane ice may be formed all the way up to the surface wherever there are voids. During the postglacial period after

an ice age, not only a temperature increase is expected, but also a decrease due to land uplift (see Chapter 4). These processes will affect the stability of an accumulation methane ice in the bedrock. Since the ice/gas transition is instantaneous, chances are high that this transition will lead to an explosive venting of methane gas (Figure 10-7). Note that this will not occur at greater depths where methane ice is not likely to form.

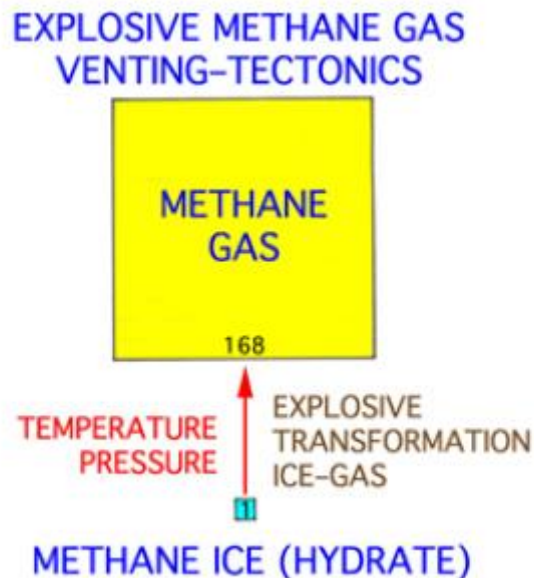


Figure 10-7 When methane ice in the bedrock transforms into gas, the increase in volume is 1 : 168, which leads to an explosive venting of methane gas. This venting may severely deform the bedrock (“methane venting tectonics”) as recorded in Sweden (modified after Mörner, 2013).

10.6. Relevance and synthesis for the safety case:

Isolation

The physical isolation function will not be affected by enhanced fluid flow processes since they do not lead to exposure.

Delay & attenuation

The increased fluid flow release is a process that enhances the transport of radionuclides into shallower groundwater systems both through the host rock but also into its overburden. So, after dissolution and transport through the host rock, dilution and dispersion are processes that can be significantly influenced.

Engineered containment

Not likely to become affected.

11. Combined scenarios - a synthesis

11.1. Introduction

In assessing the combined effects of future climate and tectonic processes and their effect on the geosphere, the time-scale considered is very important. In this study, focusing on a period of 1 Myr of future evolution, low-order processes with periodicities of several millions of years are not considered. Starting point are future climate scenarios as described in Chapter 2.2. The range of likely future climate scenarios in the Netherlands for a normal evolution scenario are: 1) the present-day temperate maritime climate, 2) the Mediterranean climate, 3) the boreal climate, and 4) the periglacial climate. Glacial conditions i.e., ice sheet coverage in the Netherlands is assessed here as well although considered an alternative evolution scenario.

11.2. Periglacial conditions

11.2.1. Sea-level change

To form the ice sheets of the last Ice Age, water from the oceans evaporated, condensed as snow and was deposited as ice in high latitudes. Thus global sea level fell during glaciation (see Chapter 2 for a full explanation). Inspired by the existing fear and awareness of near future sea-level rise numerous internet sources predict the relocation of the shoreline during sea-level rise, but fail to include the effects of sea-level fall. Similarly, by applying the present-day land and sea topography, a prediction of emergence due to glacio-eustatic lowering is easily made. In view of the previous glacio-eustatic lowstand during the Last Glacial Maximum at ~120 m below present sea level (-123 ± 2 m for the Sunda Shelf; Hanebuth et al., 2009), it should be expected that only a more severe glacial cycle with greater ice accumulation would lower sea level beyond this level. Whether the glacio-eustatic lowering actually results in a sea-level lowering depends on 1) the effects of glacial climate on sediment supply (see chapter 11.2.2) and 2) if present, the near- and far-field isostatic effects of ice loading (see chapter 11.2.3).

11.2.2. Sediment budget

In estimating the contribution of sediment budget on accommodation change, the periglacial Pleistocene SNS delta is used as an analogue. A sea-level/sediment supply scenario is proposed for the last northern hemisphere glaciations (Ten Veen et al., 2011; Donders et al., 2015 in prep.) that predicts that warmest intervals or interglacials are coupled to the coarser-grained sediments, and the coldest intervals or glacials are linked to the finer-grained sediments. During glacial conditions, supply of coarse grained sediment to the marine basin is reduced, since permafrost conditions and the continental glacial cover impede the long-distance transport of sediments. As a result, in the marine realm (condensed) clay deposition will prevail. The relatively sediment-starved shelf seas will be typified by ice rafts that plough the sea floor. It is reasonable to assume that such a scenario with an in-phase sea-level/sediment supply relationship is likely to exist for future northern hemisphere glaciations as well, since they are still part of the same Quaternary ice-house period.

Whereas this mechanism may account for the lack of marine deposition during interglacials and glacials, respectively, the overall geometry of the SNS delta is strongly progradational and aggradational. This means that coastlines are rapidly westward translating by infill of the remaining accommodation (formation of a lowstand coastal prism), but that sea-level fall will not reach beyond the shelf edge, which (at present) is positioned southwestward of the Channel.

Fluvial incision phenomena in the SNS delta are multiple, but never exceed ~20 m. This westward shift of lowstand coastlines onto the far Atlantic margin, would lengthen

lowstand river profiles by several hundred kilometres (e.g., Törnqvist et al., 2003; 2006) considerably increasing aggradation potential along active channel belts. This tendency for strong aggradation is also referred to in several studies of regional Quaternary sedimentology that describe how in periglacial fluvial systems degradation alternates with strong aggradation during lowstand stages, in response to increased available bedload in a glacial climate (e.g. Törnqvist et al., 2000; Busschers et al., 2007; Blum et al., 2013)

11.2.3. Glaciotectonic effects

For the 1 Myr time period considered, it is safe to assume that major tectonic events leading to amounts of subsidence or uplift - sufficient to affect the safety function of the Rupel Clay Mb. - can be disregarded (see chapter 7). Far-field isostatic adjustment to ice loading or unloading does play a role on the time scale considered although the rate and timing of vertical adjustment compared to that of actual ice-sheet loading is, at least partly, different. Flexural behavior of the crust predicts a so-called glacio-isostatic forebulge to develop, approximately 150 km from the margin of the ice sheet. The vertical elevation of this bulge is related to the downwarp of the lithosphere by ice-sheet loading (it amounts to ~1.2 % of maximum ice sheet thickness; see Table 4-1), and the rheological parameters of the crust. The vertical behavior of this bulge thus affects sea level in periglacial areas, i.e. in front of the ice sheet. In addition to this, the retraction of water causes an isostatic rebound or uplift due to water unloading in the order of ~20 % of the change in water depth. The effects of forebulge uplift and water unloading would thus add up (max 20 % of 120 + 1.2 % of 3000 = 54 m). At this stage it is unknown if these two isostatic processes occur at the same rate. Also the effects of gravitational attraction of water masses by the ice sheet may in fact lead to a local sea-level rise just in front of the ice sheet (Tamisiea et al., 2003) During the Weichselian - here used as analogue for periglacial conditions - the summit of the forebulge was positioned just northward of the Netherlands (see Figure 4-3). Marginal effects of forebulge uplift - and later collapse - are inferred for the Netherlands which add up to effects of water loading (Kiden et al., 2002).

11.2.4. Permafrost

The permafrost modeling presented in this report (Chapter 5.3) uses climate data (MAAT curve) from the Weichselian, including Marine Isotopic Stages 2-5, porosity, density and thermal parameters. The maximum permafrost depth changes across the Netherlands, depending on lateral changes in the percentage of sand in the overburden and geothermal gradient. Maximum depth in the north is ~140 m, whereas in the southernmost part permafrost reaches a depth of ~185 m. These depths are above the minimum depth of the top Boom Clay and predicted future permafrost likely only affects the formation's overburden. The degree to which this occurs depends on the MAAT. For the assessment here it would be convenient to consider a relationship between ice-sheet proximity and permafrost depth. However, during LGM temperatures were lower than during the relatively milder Saalian ice age, however land-ice reached further south during latter period. This suggests that high aridity during the Weichselian played an important role in the potential for build-up of the northern hemisphere ice sheet and, therefore, the suggested relationship probably does not exist.

11.2.5. Hydrogeological and geochemical changes

Sea level lowering or lowering of the salt-fresh water interface would have a negative effect on permafrost depth. This is described in WP 4.2.1 and WP6.

11.2.6. Scenario synthesis

Based on the glacio-eustatic, glacio-tectonic and sediment budget scenarios sketched above, a scenario matrix can be designed that is applicable to periglacial conditions with changing thickness and proximity of a (remote) ice sheet and varying permafrost depth.

Sea-level lowstand (far below present day situation; exact numbers are not relevant for that location of the disposal facility), minimum sediment supply and various scenarios for ice coverage as far as proximity and thickness of the ice sheet are concerned. Considering the resulting profile adjustments of major drainage systems, the range of expected fluvial incision over Dutch territory will be a few tens of metres at most and thus remains very far from subcrop depths of the Boom Clay top.

Table 11-1 Scenarios for ice loading and advance using the analogy with past glacial and periglacial periods.

Ice thickness NL (m)	Ice proximity (m)	climate	Vertical trend at position NL	Depositional setting	Analogues
0	Remote	periglacial with permafrost	minor	Continental to coastal marine	Weichselian
195	Ice margin in north NL, forebulge in south NL	Glacial/ ice covered	Subsidence in N NL; Uplift in southern NL	Glaciotectonic in north/ continental in far south	Saalian
180	Far field, forebulge south of NL	periglacial/permafrost	Uplift in south NL, suppression in north	Glaciotectonic in north/ continental in south	Elster

11.3. Glacial conditions

11.3.1. Sea level

For the maximum southward land ice coverage the Saalian stage is taken as analogue (Table 11-1). The land-ice is reaching half-way the Netherlands. The global eustatic sea level drop resulting from the Late Saalian glaciation (MIS 6) is still not constrained accurately, but seems to have been of the same order as during the LGM (Rabineau et al., 2006) i.e., 120 m. In terms of ice volume, Bintanja et al. (2005) estimate that the Late Saalian only had the sixth largest global ice volume (LGM is seventh). This does not interact with the fact that the Late Saalian Eurasian ice sheet was the largest in Fennoscandia. This suggests that the ice distribution over the various continental ice sheets varied for each glacial period (Colleoni, 2009).

11.3.2. Sediment budget

As a direct consequence of the presence of land ice, north flowing rivers will be deflected westward, whereas the already westward-flowing Rhine-Meuse system will become the pathway for fluvio-glacial drainage. Through fluvial aggradation, this river system will importantly contribute to the infill the shelf that becomes exposed after sea-level lowering.

11.3.3. Glaciotectonic effects

At glacial maxima, sea level is expected to be minimum and if the exposed land becomes covered by glaciers, the isostatic compensation results in a lowering of the land surface beneath the ice sheet (see chapter 4). With an ice sheet thickness of 195 m this loading effect will amount to ~60-70 m. The area just in front of the ice load, due to its flexural behavior, will also subside. The uplifting forebulge will be positioned south of or in the southernmost part of the Netherlands.

11.3.4. Glaciotectonic deformation and erosion

Due to the ice-sheet advance glaciotectonic deformation will affect both ancient deposits and glacial outwash deposits newly deposited in front of the ice sheet. The maximum depth of these structures does not reach the depth of the Boom Clay, although overlying aquifers and aquitards may become affected.

11.4. *Present Temperate - Interglacial conditions*

Here we consider a situation where the climate is comparable with the present-day interglacial climate. It is also assumed that the interglacial is preceded by a glacial period and thus includes the deglaciation stage as well as the rise in sea level. Such a situation is not likely to occur earlier than within ~70 kyr, assuming the next glacial period will start at 55 kyr from now.

11.4.1. Sea level (change)

During interglacial conditions, global sea-level is expected to rise due to melting glaciers (see Chapter 2 for full explanation). For matters of simplicity, it is assumed that a “new” interglacial (after the next glacial) will result in re-establishment of normal (present-day) glacio-eustatic sea level. Whether or not this glacio-eustatic rise is expressed as an actual increase of water depth, depends on 1) the sediment budget, that fills the newly added marine accommodation space and 2) the glaciotectonic isostatic response to deglaciation.

11.4.2. Glaciotectonic effects

The initial stages of deglaciation are characterized by an elastic response to ice-sheet unloading. This will result in an uplift of the once ice-loaded areas and subsidence (or collapse) of the forebulge region. Table 4-1 summarizes the expected vertical amounts of uplift and subsidence for various ice-sheet thicknesses. Especially the post-elastic response period is of relevance, since it predicts that a period of >10 kyr is needed before a full rebound of the lithosphere has taken place. This applies to both the ice-loaded area and the forebulge.

11.4.3. Sediment budget

In analogy with the Plio-Pleistocene SNS delta, a transitional glacial-interglacial period would favor the development of thick sediment wedges. Especially, during melting of the glaciers, the sediment load of rivers is high and will cause a situation where the raise in accommodation due to glacio-eustatic rise is outpaced by sediment input which would favor the formation of a prograding deltas. After deposition of such a delta, the loading of the sediment wedge may enhance deep fluid flow (see Chapter 10) as occurred during deposition and loading of the SNS delta wedge as well. If such a delta would form landward of the present-day coastlines it might induce deep fluid flow that can also affect the Boom Clay and its overburden.

11.5. *Global warming related sea-level rise - Mediterranean type*

11.5.1. Sea level

Beerten et al., 2011 consider two scenarios for global warming: one with and one without a marine transgression. Here, we only consider the first scenario with sea-level rise up to 60 m, which would be the response when all ice on Earth will melt (see De Craen, 2009 and references therein). Several attempts to illustrate the effects of a rising sea-level exist on the internet (e.g. Google - floodmap; Figure 11-). However, these simulations use the present-day topography as reference and do not consider other contributors to changes in accommodation, such as isostatic and sediment effects.

Using the Mediterranean climate as a predicted future conditions, the associated sea-level scenarios from +20 m onward result in a complete drowning of the Netherlands due to global warming and melting of part of the continental ice sheets.

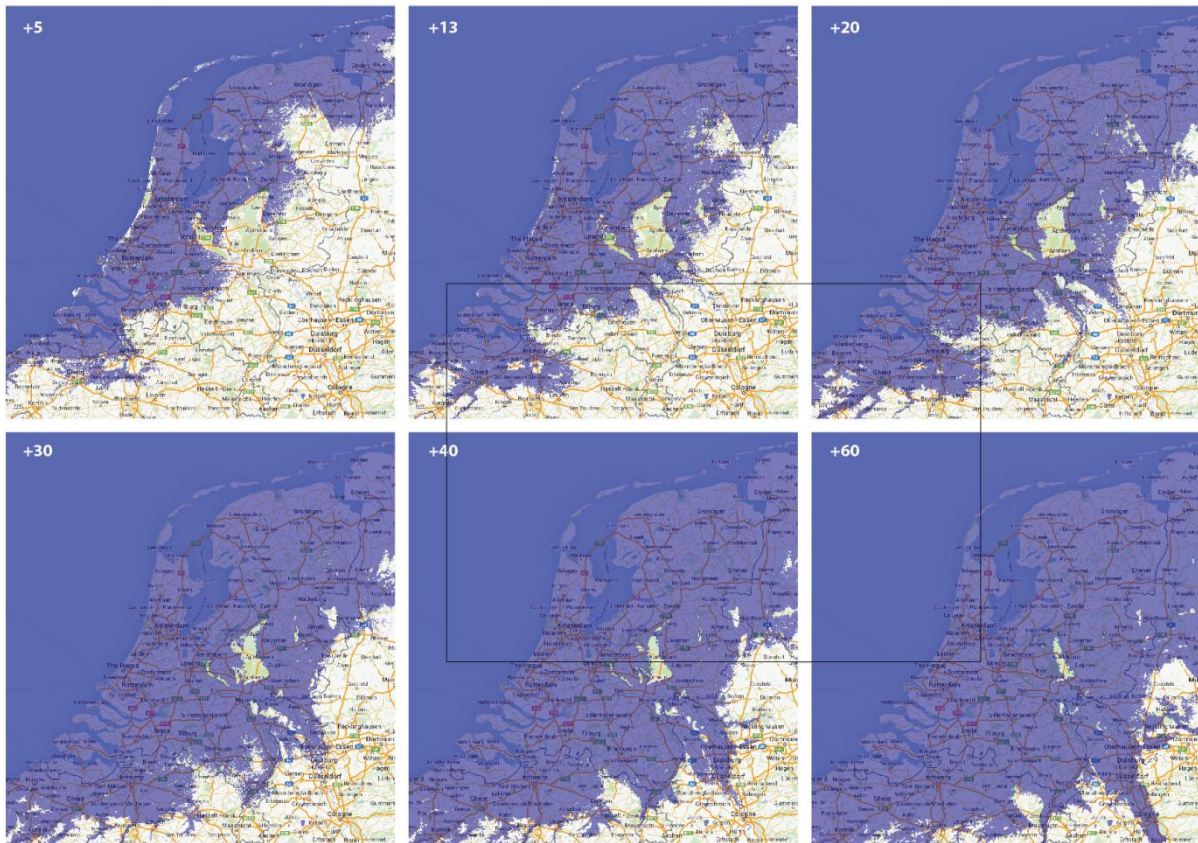


Figure 11-1 Predicted effects of sea-level rise on the position of the shore line (from internet source <http://flood.firetree.net>, consulted in February, 2015).

Also of importance is the effect of water loading. In the extreme case of melting of all ice on Earth, a sea-level of ~ 60 m will be increased by 14 m. This implies that the +60 m situation as depicted in Figure 11- underestimates the water depth and thus the accommodation. Following the theory of vertical (“Airy”) isostatic compensation, the coast line is not expected to reposition as a consequence of loading and the coastline scenarios depicted in Figure 11- are, in that respect, representative. Flexural isostatic compensation, however, assumes that the earth’s lithosphere will bend under a (water) load. Such a mechanism would reposition the coastline further landward.

The duration of a future marine transgression is extremely difficult to predict because it not only depends on climate change but also on vertical movements of the Earth’s crust (uplift and subsidence). Analogues from the Neogene and Quaternary geological record in the Southern North Sea Basin (Vandenberghe et al., 2004) indicate that “natural” marine conditions may last for several tens of thousands of years (Pleistocene and Holocene transgressions) up to more than 4 Ma (Late Miocene sand transgression). In case of anthropogenic sea-level effects, the duration of marine conditions becomes even more speculative.

11.5.1. Sediment budget

Due to flooding, lagoonal to shallow marine environments may be created. Wave actions and currents will level the existing topography and river systems will bring their sediment load to form delta bodies covering present-day land. After deposition of such a delta, the loading of the sediment wedge may enhance deep fluid flow (see Chapter 10) as occurred during deposition and loading of the SNS delta wedge as well. Shifting the area of

maximum sediment load, as can be expected to be associated with sea-level variation, may thus affect areas that were previously unaffected by deep fluid flow processes.

11.5.2. Glaciotectonic effects

Although the postulated sea-level rise is an effect of global warming it still coincides with the current interglacial period. It is therefore assumed that current post-glacial rebound processes will continue for at least 10 kyr. These effects are about 0,6 mm per year and will exponentially decrease. In case of a far future sea-level rise following a future glacial period it is reasonable to assume that the same processes of post-glacial isostatic readjustment play a role.

11.6. *Boreal Climate*

11.6.1. Sea level

A boreal climate under oceanic influence can be seen as a transitional state between the present day temperate climate and a full periglacial climate with no or at most discontinuous permafrost developed. With regard to this climate type transition it should also be acknowledged that the sea-level will be lower than at present. If, using a linear approach, it is assumed that the Boreal climate is half-way the transition to a full glacial, sea-level lowering of maximum 60 m can be expected which is 50 % of the 120 m sea-level drop of the Weichselian.

11.6.2. Sediment budget

Precipitation and run-off are not changing dramatically if the Murmansk climate is taken as analogue for a boreal climate.

11.6.3. Glaciotectonic effects

Assuming that current post-glacial rebound processes will continue for at least 10 kyr, it is not expected to take place during a future change towards glacial conditions, which under natural circumstances are expected to occur in 55 kyr and even much later if anthropogenic influence is taken into account. However, if the Boreal climate scenario is considered a transitional stage, a time in between the present and 55 kyr needs to be taken, i.e, ~22 kyr. This estimate is still beyond the duration of current rebound processes which can thus be neglected.

12. Concluding Remarks

This report summarizes the results of a study carried out in the context of OPERA. It attempts to describe the future 1 million year evolution of the geological and geohydrological properties of the geosphere. By using the two main natural driving forces climate and tectonics as starting point, the effects of a wide range of associated processes are elucidated. In such an assessment, it is common practice to translate or extrapolate observations of past behavior to the future. This practice is based on the assumptions that past and current trends in driving forces can be safely extrapolated over the next 1 million years and that the ensuing processes act in the same mode as they do in the past and present. Since the validity of this assumption can be questioned the future is difficult to predict. However, in the absence of better alternative it often is the current best practice. Also this work assumes to be thorough in the sense that all relevant geological and geohydrological processes were considered. This is purely according to the viewpoints and best knowledge of the authors.

Considering the huge amount of previous studies that address the effects of single processes, either in academic or applied context (radioactive waste disposal, CO₂ and gas storage, HC exploration) this work only refers to them, rather than redoing them. This study, however, focuses on the interaction of geological and geohydrological future processes by defining future scenarios that are importantly driven by the climatic evolution. As such, the focus shifts from individual processes to the interaction of multiple processes. Although the predictability of the climate scenarios is unsure, the process interaction is better predictable since it derives from our knowledge and observations of the geological past and present.

13. Recommendations

By describing the future scenarios some boundary conditions are given for the interacting processes and their mutual effects. The fact that these are difficult to quantify and that dependencies and phase lags between these processes are relatively unknown, requires more in-depth studies of process interaction. More specifically, the following issues should be addressed:

- Future water-depth predictions can be improved by studying the interrelationship between climatically steered sea-level changes, changes in sediment supply and the isostatic response to the different loads. Such studies also help to understand why fluvial incision in the Netherlands is seemingly unrelated to sea-level drops, which is more directly of relevance for the safety functions isolation and delay & attenuation
- Whereas many studies focused on the isostatic and fluid dynamic effects associated with glacial loading, the role of advancing sediment loads, as being common with delta progradations, is less well studied. This report summarizes several lines of evidence that such effects played a role in the geological past, but that these are only qualitatively assessed.
- The permafrost modeling performed for this study, is sophisticated in so far that a detailed assessment of input parameters of the overburden of the Boom Clay has been carried out. This enabled to highlight an unexpected spatial variation in predicted permafrost depths over the Netherlands. This permafrost modeling used the present day geology as reference point. For the near future, and even more so, for the far future periglacial conditions it might be more appropriate to assume that additional sediment is deposited. It is therefore recommended that permafrost modeling takes these effects into account. Moreover, changes in compaction through time, the effect of groundwater flow, the role of salt content and vegetation should also be addressed.
- Although future seismicity will not be considerable and the impact on the safety functions is expected to be minimal, the effects of fluid flow along Dutch faults that have a tendency to be reactivated is relatively unknown. Especially, far-field relaxation after glacial unloading may lead to enhanced faulting intensity and seismicity by superposing stresses on the regional stress field. Fluidization phenomena have been reported for faults just outside the Ruhr Valley Graben (pers comm. Van Balen, 2015) and are suggested to be related to deglaciation after the LGM. This hints at higher fluid pressures during seismic events. The depth and severity of such pressure changes is less well studied. In other words, it is unknown to what extent the Boom Clay and its overburden are affected by. In the light of enhanced seismicity related to deglaciations, also the reactivation potential of faults outside the known active systems, such as the Ruhr Valley Graben, should be studied.

14. Acknowledgements

A multidisciplinary inventory of possible future geological evolution scenario's requires an open mind towards the opinion of many researchers that address the issues raised in this report. The NAC workshop in April 2014 was a first initiative to gather Dutch experts from several disciplines who were challenged to give their view on the Earth's future evolution from the perspective of their own expertise. We highly appreciate the contributions to this workshop of Ronald van Balen, Roderik van de Wal, Henk Kooi, Danielle Kitover, Wim Westerhoff, Bert Vermeersen, Kim Cohen, and Salomon Kroonenberg. Some of their relevant published work is referred to in this report, but it should be acknowledged that the time span of prediction studied in this project is much longer than most of these colleagues feel comfortable with. However, much of what is assumed in this report is based on their inspiring stories told on the NAC conference and later discussions.

15. References

- Al Hseinat, M. and Hübscher, C., 2014. Ice-load induced tectonics controlled tunnel valley evolution - instances from the southwestern Baltic Sea, *Quaternary Science Reviews*, Volume 97, 1 August 2014, Pages 121-135., ISSN 0277-3791, <http://dx.doi.org/10.1016/j.quascirev.2014.05.011>.
- Andersen, B. G., 1981. Late Weichselian ice sheets in Eurasia and Greenland, in G. H. Denton and T. J. Hughes, eds., *The last great ice sheets*: New York, Wiley, p. 1-65.
- Archer D., Ganopolski A., 2005. A movable trigger: fossil fuel CO₂ and the onset of the next glaciation. *Geochemistry, Geophysics, Geosystems*, 6, doi:10.1029/2004GC000891.
- Athy, L.F., 1930. Density, porosity, and compaction of sedimentary rocks. *AAPG Bulletin*, 14:1-24.
- Beerten, K., 2010. Permafrost in northwestern Europe during the Last Glacial. External Report of the Belgian Nuclear Research Centre, Mol, Belgium: SCK·CEN - ER - 138.
- Bense, V.F., and M.A. Person, 2008. Transient hydrodynamics within intercratonic sedimentary basins during glacial cycles, *J. Geophys. Res.*, 113, F04005, doi:10.1029/2007JF000969.
- Berger A., 1978. Long-term variations of daily insolation and Quaternary climatic changes. *Journal of Atmospheric Science*, 35, 2362-2367.
- Berger A., Tricot C., Galleé H., Loutre M.F., 1993. Water vapour, CO₂ and insolation over the last glacial-interglacial cycles. *Philosophical Transactions of the Royal Society*, London, B341, 253-261.
- Berger A., Yin Q., 2012. Modeling the past and future interglacials in response to astronomical and greenhouse gas forcing. In: Henderson-Sellers A. and McGuffie K. (eds.), *The Future of the World's Climate*, 2nd ed., Elsevier, 437-462.
- Björnsson, H., 1996. Scales and rates of sediment removal: a 20 km long, 300 m deep trench created beneath Breiðamerkurjökull during the Little Ice Age. *Annals of Glaciology*, 22, 141-146.
- Blum, M., Martin, J., Milliken, K., Garvin, M., 2013. Paleovalley systems: insights from Quaternary analogs and experiments. *Earth-Science Reviews*, 116, 128-169.
- Booth, D.B., Hallet, B., 1993. Channel networks carved by subglacial meltwater: observations and reconstructions in the eastern Puget Lowland of Washington. *Geological Society of America Bulletin*, 105, 671-683.
- Boulton G.S. et al., 1993. Deep circulation of groundwater in overpressured subglacial aquifers and its geological consequences. *Quaternary Science Reviews*, 12, 739-745.
- Boulton, G.S., Hagdorn, M., Maillot, P.B., Zatzepin, S., 2009. Drainage beneath ice sheets: groundwater-channel coupling and the origin of esker systems from former ice sheets. *Quaternary Science Reviews*, 28, 621-638.
- Brandes, C., Polom, U. and Winsemann, J., 2011. Reactivation of basement faults: interplay of ice-sheet advance, glacial lake formation and sediment loading. *Basin Research*, 23: 53-64. doi: 10.1111/j.1365-2117.2010.00468.
- Brandes, C., Steffen, H., Steffen, R. and Wu, P., 2015. Intraplate seismicity in northern Central Europe is induced by the last Glaciation. *Geology*, 43(7), 611-614.
- Broecker W.S., 1998. The end of the present interglacial: how and when? *Quaternary Science Reviews*, 17, 689-694.
- Bull, W.B., 1991. *Geomorphic Responses to Climatic Change*. Oxford University Press, Oxford. 326pp.
- Bungum, H., Lindholm, C., Faleide, J.I., 2005. Postglacial seismicity offshore mid-Norway with emphasis on spatio-temporal-magnitudal variations. *Marine and Petroleum Geology*, 22, 137-148.
- Busschers, F.S., Kasse, C., Van Balen, R.T., Vandenberghe, J., Cohen, K.M., Weerts, H.J.T., Wallinga, J., Johns, C., Cleveringa, P., Bunnik, F.P.M., 2007. Late Pleistocene evolution of Rhine-Meuse system in the southern North Sea Basin: imprints of climate

- change, sea-level oscillation and glacio-isostasy. *Quaternary Science Reviews*, 26, 3216-3248.
- Caine, J. S., J. P. Evans, and C. B. Forster, 1996. Fault zone architecture and permeability structure, *Geology*, 24, 1025-1028.
- Cohen, K.M. and Hijma, M.P., 2008, Het Rijnmondgebied in het Vroeg Holoceen: inzichten uit een diepe put bij Blijdorp (Rotterdam), *Grondboor & Hamer*, 62, pagina 64-71.
- Colleoni, F., 2009. On the Late Saalian glaciation (160 - 140 ka): a climate modeling study. *Climatology*. PhD. thesis Université Joseph-Fourier - Grenoble I; Stockholm University, 184 pp.
- Caro Cuenca, M., Hanssen, R. and Van Leijen, F. 2007. Subsidence due to peat decomposition in the Netherlands kinematic observations from radar interferometry , *Fringe 2007*, Frascati, Italy).
- Cochelin A.-S., Mysak L., Wang Z., 2006. Simulation of long-term future climate changes with the green McGill paleoclimate model: the next glacial inception. *Climatic Change*, 79, 381-401.
- Cox, S. F., 1995. Faulting processes at high fluid pressures: An example of fault valve behavior from the Wattle Gully Fault, Victoria, Australia, *J. Geophys. Res.*, 100(B7), 12,841-12,859, doi: 10.1029/95JB00915.
- De Crook, Th., 1996. A seismic zoning map confirming to Eurocode 8, and practical earthquake relations for the Netherlands. *Geologie en Mijnbouw* 75, 11-18.
- Dehls, J.F., Olesen, O., Olsen, L. & Blikra, L.H., 2000. Neotectonic faulting in northern Norway; the Stuoragurra and Nordmannvikdalen postglacial faults. *Quat. Sci. Rev.*, 19, 1447-1460.
- Delisle, G., 1998. Numerical simulation of permafrost growth and decay. *Journal of Quaternary Science* 13, 325-333.
- Demant, D., Evers, L.G., Teerlynck, H., Dost, B. & Jongmans, D., 2001. Geophysical investigation across the Peel boundary fault (The Netherlands) for a paleoseismological study. *Netherlands Journal of Geosciences / Geologie en Mijnbouw* 80, 119-127.
- Renssen, H., Vandenberghe, J., 2003. Investigation of the relationship between permafrost distribution in NW Europe and extensive winter sea - ice cover in the North Atlantic Ocean during the cold phases of the Last Glaciation. *Quaternary Science Reviews* 22, 209-223.
- Domenico, P. A., and F. W. Schwartz, 1998). *Physical and Chemical Hydrogeology*, 2nd ed., John Wiley, New York. dormant normal fault in the northern North Sea, *Geology*, 28, 595.
- Ehlers, D., Gibbard, P., and van Weering, Tj.C.E., 1979, Glacial deposits of Britain and Europe: general overview, by: in *Glacial Deposits in Britain and Ireland*, edited by J.Ehlers, P.Gibbard, & J.Rose, pp 493-501, Rotterdam: Balkema.
- Ehlers, J., Gibbard, P.L., Hughes, P.D., 2011, *Quaternary Glaciations - Extent and Chronology*. Elsevier, the Netherlands.
- Eyles, N., De Broekert, P., 2001. Glacial tunnel valleys in the Eastern Goldfields of Western Australia cut below the Late Paleozoic Pilbara ice sheet. *Palaeogeography, Palaeoclimatology, Palaeoecology*, 171, 29-40.
- Fjeldskaar, W., Lindholm, C., Dehls, J.F. & Fjeldskaar, I., 2000. Postglacial uplift, neotectonics and seismicity in Fennoscandia. *Quat. Sci. Rev.*, 19, 1413-1422.
- Follestad, B. and Fredin, O., 2011. Geometry and vertical extent of the late Weichselian ice sheet in northwestern Oppland County, Norway. *Norges geologiske undersøkelse Bulletin*, 451, 1-19.
- Gasson, E., M. Siddall, D. J. Lunt, O. J. L. Rackham, C. H. Lear, and D. Pollard, 2012. exploring uncertainties in the relationship between temperature, ice volume, and sea level over the past 50 million years. *Rev. Geophys.*, 50, RG1005, doi:10.1029/2011RG000358

- Glasser, N.F., Sambrook-Smith, G.H., 1999. Glacial meltwater erosion of the Mid-Cheshire Ridge: implications for ice dynamics during the Late Devensian glaciation of northwest England. *Journal of Quaternary Science*, 14, 703-710.
- Govaerts, J., Weetjens, E., Beerten, K., 2011. Numerical simulation of permafrost depth at the Mol site. External Report of the Belgian Nuclear Research Centre, Mol, Belgium: SCK·CEN - ER - 148.
- Grassmann, S., Cramer, B., Delisle, G., Hantschel, T., Messner, J., Winsemann, J., 2010. pT - effects of Pleistocene glacial periods on permafrost, gas hydrate stability zones and reservoir of the Mittelplate oil field, northern Germany. *Marine and Petroleum Geology* 27, 298-306.
- Grauls, D., (1999). Overpressures: Causal Mechanisms, Conventional and Hydromechanical Approaches. *Oil & Gas Science and Technology*, 54, 667-678.
- Grollmund, B., and M.D. Zoback, 2003. Impact of glacially-induced stress changes on fault seal integrity offshore Norway, in: Davies, R., Handschy, J. eds., *AAPG Bull.* 87, 493-506.
- Grollmund, B., Zoback, M.D., 2001. Did deglaciation trigger intraplate seismicity in the New Madrid seismic zone? *Geology*, 29 (2), pp. 175-178.
- Hampel, A., Hetzel, R., Densmore, A.L., 2007. Postglacial slip-rate increase on the Teton normal fault, northern Basin and Range Province, caused by melting of the Yellowstone ice cap and deglaciation of the Teton Range? *Geology*, 35, 1107-1110.
- Hansen J.E., Sato M., 2012. Paleoclimate implications for human-made climate change. In: Henderson-Sellers A. and McGuffie K. (eds.), *The Future of the World's Climate*, 2nd ed., Elsevier, 21-47.
- Hays J.D., Imbrie J., Shackleton N.J., 1976. Variations in the Earth's orbit: pacemaker of the ice ages. *Science*, 194, 1121-1132.
- Herrero C., García-Olivares A., Pelegrí J.L., 2014. Impact of anthropogenic CO₂ on the next glacial cycle. *Climatic Change*, 122, 283-298.
- Imbrie J., Berger A., Boyle E.A., Clemens S.C., Duffy A., Howard W.R., Kukla G., Kutzbach J., Martinson D.G., McIntyre A., Mix A.C., Molino B., Morley J.J., Peterson L.C., Johansson, J.M. et al. (2002). "Continuous GPS measurements of postglacial adjustment in Fennoscandia. 1. Geodetic results". *Journal of Geophysical Research*, 107, 2157.
- Ijpelaar, M.P., 2014. The effects of late Weichselian sediment redistribution on post-glacial isostasy in the Fennoscandian and Barents Sea region, MSc. Thesis, TU Delft.
- Johnston, P., Wu, P., Lambeck, K., 1998. Dependence of horizontal stress magnitude on load dimension in glacial rebound models. *Geophysical Journal International*, 132, 41-60.
- Jørgensen, F., Sandersen, P.B.E., 2006. Buried and open tunnel valleys in Denmark - Erosion beneath multiple ice sheets. *Quaternary Science Reviews*, 25, 1339-1363.
- Judd, A., G. Davies, J. Wilson, R. Holmes, G. Baron and I. Bryden, 1997. Contribution to atmospheric methane by natural seepage on the UK continental shelf. *Marine Geology*, 137, 165-189.
- Kehew, A.E., Kozłowski, A.L., 2007. Tunnel channels of the Saginaw Lobe, Michigan, USA. In: Johansson, P., Sarala, P. (eds.), *Applied Quaternary Research in the Central Part of of Glaciated Terrain*. Geological Society of Finland Special Paper, 46, 69-78.
- Kehew, A.E., Piotrowski, J.A., Jørgensen, F., 2012. Tunnel valleys: concepts and controversies - A review. *Earth-Science Reviews*, 113, 33-58.
- Kidder D.L., Worsley T.R., 2012. A human-induced hothouse climate? *GSA Today*, 22, 4-11.
- Kiden, P., Denys, L., Johnston, P., 2002. Late Quaternary sea-level change and isostatic and tectonic land movements along the Belgian-Dutch North Sea coast: geological data and model results, *Journal of Quaternary Science*, 17(5-6), 535-546.
- Klemann, V., Wolf, D., 1998. Modeling of stresses in the Fennoscandian lithosphere induced by Pleistocene glaciations. - *Tectonophysics*, 294, 3-4, 291-303, Kitover, D.C., Van Balen, R.T., Roche, D.M., Vandenberghe, J., Renssen, H., 2013. New estimates of

- permafrost evolution during the last 21k years in Eurasia using numerical modeling. *Permafrost and Periglacial Processes* 24, 286-303 Kleinberg, R., and D. Griffin, 2005). NMR measurements of permafrost: Unfrozen water assay, pore-scale distribution of ice, and hydraulic permeability of sediments, *Cold Reg. Sci. Technol.*, 42, 63-77.
- Knight, J., 1999. Geological evidence for neotectonic activity during deglaciation of the southern Sperrin Mountains, Northern Ireland. *J. Quat. Sci.*, 14, 45-57.
- Kooi, H., Johnston, P., Lambeck, K., Smither, C., and Molendijk, R., 1998. Geological causes of recent (100 yr) vertical land movement in the Netherlands. *Tectonophysics*, 299, 297-316.
- Kuhlmann, G., Wong, T.E., 2008. Pliocene palaeoenvironmental evolution as interpreted from 3D-seismic data in the southern North Sea, Dutch offshore sector. *Marine and Petroleum Geology*, 25, 173-189.
- Lambeck, K., Purcell, A., Funder, S., Kjaer, K.H., Larsen, E., and Moller, P. 2006. Constraints on the Late Saalian to early Middle Weichselian ice sheet of Eurasia from field data and rebound modeling. *Boreas*, 35, 539-575.
- Lang N., Wolff, E.W., 2011. Interglacial and glacial variability from the last 800 ka in marine, ice and terrestrial archives. *Climate of the Past*, 7, 361-380.
- Larsen, E., Sandven, R, Heyerdahl, H. and Hernes, S., 1995. Glacial geological implications of preconsolidation values in sub-till sediments at Skorgenes, western Norway. *Boreas*, 24 (1), 37-46.
- Ledley T.S., 1995. Summer solstice solar radiation, the 100 Kye ice-age cycle, and the next ice age. *Geophysical Research Letters*, 22, 2745-2748.
- Lemieux, J.-M., E. A. Sudicky, W. R. Peltier, and L. Tarasov, 2008). Simulating the impact of glaciations on continental groundwater flow systems: 2. Model application to the Wisconsinian glaciation over the Canadian landscape, *J. Geophys. Res.*, 113, F03018, doi:10.1029/2007JF000929.
- Lisiecki, L. E., and Raymo, M. E., 2005. A Pliocene-Pleistocene stack of 57 globally distributed benthic $\delta^{18}\text{O}$ records, *Paleoceanography*, 20, PA1003, doi: 10.1029/2004PA001071.
- Lorius C., Jouzel J., Raynaud D., 1993. Glacial-interglacials in Vostok: climate and greenhouse gases. *Global and Planetary Change*, 7, 131-143.
- Loureaux M.F., Berger A., 2000. Future climatic changes: are we entering an exceptionally long interglacial? *Climatic Change*, 46, 61-90.
- Lowe, A. L., Anderson, J.B., 2003. Evidence for abundant subglacial meltwater beneath the paleo-ice sheet in Pine Island Bay, Antarctica. *Journal of Glaciology*, 49, 125-138.
- Lundqvist, J., 1986, Late Weichselian glaciation and deglaciation in Scandinavia: *Quaternary Science Reviews*, 5, 269-292.
- Luttrell, K. and Sandwell, D., 2010. Ocean loading effects on stress at near shore plate boundary fault systems. *J. Geophys. Res.* 115, B08411. <http://dx.doi.org/10.1029/2009JB006541>.
- Mangerud, J., E. Larsen, O. Longva, and E. Sonstegaard, 1979, Glacial history of western Norway 15,000-10,000 B.P.: *Boreas*, v. 8, p. 179- 187.
- Marshall, S.J., 1998. Dynamics of the Pleistocene ice sheets. In: Wu, P.P. (Ed.), *Dynamics of the Ice Age Earth: A Modern Perspective*. In: *GeoRes. Forum Series*. Trans. Tech. Publications, Zürich, pp. 217-248.
- McPherson, B., and G. Garven, 1999). Hydrodynamics and overpressure mechanisms in the Sacramento Basin, California, *American Journal of Science*, 299, 429-466.
- Moreau, J., Huuse, M., Gibbard, P.L. and Moscariello, A., 2009. 3D Seismic Megasurvey Geomorphology of the Southern North Sea - Tunnel Valley Records and Associated Ice-sheet Dynamics. 71st EAGE Conference & Exhibition – Amsterdam, The Netherlands.
- Mörner, N.A., 1978. Faulting, fracturing, and seismicity as functions of glacio-isostasy in Fennoscandia. *Geology*, 6, 41-45.

- Mörner, N.A., Tröfthen, P.E., Sjöberg, R., Grant, D., Dawson, S., Bronge, C., Kvamsdal, O. & Siden, A., 2000. Deglacial paleoseismicity in Sweden: the 9663 BP Iggesund event. *Quat. Sci. Rev.*, 19, 1461-1468.
- Muir-Wood, R., 2000. Deglaciation seismotectonics: a principal influence on intraplate seismogenesis at high latitudes. *Quat. Sci. Rev.*, 19, 1399-1411.
- Muir-Wood, R., 2000. Deglaciation seismotectonics: a principal influence on intraplate seismogenesis at high latitudes? *Quaternary Science Reviews*, 19, 1399-1411.
- Munier, R., Fenton, C., 2004. Review of post glacial faulting - Current understanding and directions for future studies. In: *Respect Distances - Rationale and Means of Computation*, Swedish Nuclear Fuel and Waste Management Co., Stockholm, Report R-04-17. 62pp.
- Neuzil, C., 1993. Low fluid pressure within the Pierre Shale: A transient response to erosion. *Water Resour. Res.*, 29, 2007-2020.
- O'Cofaigh, C., 1996. Tunnel valley genesis. *Progress in Physical Geography*, 20, 1-19.
- Oerlemans J., Van der Veen C.J., 1984. *Ice Sheets and Climate*. Reidel, Dordrecht, pp. 217.
- Oppo D.W., McManus J.F., Cullen J.L., 1998. Abrupt climate events 500,000 to 340,000 years ago: evidence from subpolar North Atlantic sediments. *Science*, 279, 1335-1338.
- Osborne, M. J., and R. E. Swarbrick, 1997). Mechanisms for generating overpressure in sedimentary basins: a reevaluation, *AAPG bulletin*, 81, 1023-1041.
- Paillard D., 2001. Glacial cycles: toward a new paradigm. *Reviews of Geophysics*, 39, 325-346.
- Pedersen, S.A.S., 2014. Architecture of Glaciotectonic Complexes *Geosciences*. 2014, 4, 269-296.
- Peltier, W., 2004. Global glacial isostasy and the surface of the ice-age earth: The ice-5g (vm2) model and grace. *Annu. Rev. Earth Planet. Sci.*, 32, 111-149.
- Persson, P.O.G., C.W. Fairall, E.L. Andreas, P.S. Guest and D.K. Perovich, 2002. Measurements near the atmospheric surface flux group tower at SHEBA: Near surface conditions and surface energy budget. *Journal of Geophysical Research*, 107(C10), doi:10.1029/2002JC000705.
- Petit, J. R. and 18 others, 1999. Climate and atmospheric history of the past 420,000 years from the Vostok ice core, Antarctica. *Nature*, 399, 429-436.
- Peyaud, V. 2006. Role of the Ice Sheet Dynamics in major climate changes. Ph.D. thesis, Laboratoire de Glaciologie et de Géophysique de l'Environnement, Université Grenoble .
- Piotrowski, J.A., 1994. Tunnel-valley formation in northwest Germany - Geology, mechanisms of and subglacial bed conditions for the Bornhöved tunnel valley. *Sedimentary Geology*, 89, 107-141.
- Pisias N.G., Prell W.L., Raymo M.E., Shackleton N.J., Toggweiler J.R., 1993. On the structure and origin of major glacial cycles. 2. The 100,000-year cycle. *Paleoceanography*, 8, 699-735.
- Poelchau, H.S., Baker, D.R., Hantschel, T., Horsfield, B., Wygrala, B., 1997. Basin Simulation and the Design of the Conceptual Basin Model. In: Welte, D.H., Horsfield, B., Baker, D.R. (eds.) *Petroleum and Basin Evolution*, Springer Verlag Berlin Heidelberg, pp. 3-70.
- Rabineau, M., Berne, S., Olivet, J.L., Aslanian, D., Guillocheau, F., and Joseph, P. 2006. Paleo sea levels reconsidered from direct observation of paleoshore-line position during glacial maxima (for the last 500,000 yr). *Earth Planet. Sc. Lett.*, 252, 119-137.
- Rea, B.R., Evans, D.J.A. [2007] Quantifying climate and glacier mass balance in north Norway during the Younger Dryas. *Palaeogeography, Palaeoclimatology, Palaeoecology*, 246, 307-330.
- Rommelts, G., Muyzert, E., van Rees, D.J., Geluk, M.C., de Ruyter, C.C., and Wildenborg, A.F.B., 1993. Evaluation of salt bodies and their overburden in the Netherlands for the

- disposal or radioactive waste, b. Salt Movement. Report 30.012B-ERB, Rijks Geologisch Dienst.
- Renssen, H., Vandenberghe, J., 2003. Investigation of the relationship between permafrost
- Richmond, G.M.; Fullerton, D.S., 1986. Summation of Quaternary glaciations in the United States of America. *Quaternary Science Reviews* 5: 183-196. doi:10.1016/0277-3791(86)90184-8.
- Ritter, J.R.R., Jordan, M., Christensen, U.R. & Achauer, U., 2000. A mantle plume below the Eifel volcanic fields, Germany. *Earth and Planetary Science Letters*, 186, 7-14.
- Roberts, S. J., and J. A. Nunn, 1995. Episodic fluid expulsion from geopressed sediments. *Marine and Petroleum Geology*, 12, 195-202.
- Rubel, F., and M. Kottek, 2010. Observed and projected climate shifts 1901–2100 depicted by world maps of the Köppen–Geiger climate classification, *Meteorol. Z.*, 19, 135–141.
- Schokking, F., 1998. Anisotropic geotechnical properties of a glacially overconsolidated and fissured clay. PhD thesis, TU Delft.
- Sekiguchi, K., 1984. A method for determining terrestrial heat flow in oil basinal areas, *Tectonophysics*, 103, 67-79.
- Shackleton, N.J., Berger, A., Peltier, W.R., 1990. An alternative astronomical calibration of the lower Pleistocene time scale based on ODP Site 677. *Trans. R. Soc. Edinb. Earth Sci.* 81, 251-261.
- Sibson, R. H., (1995). Selective fault reactivation during basin inversion: potential for fluid redistribution through fault-valve action, Geological Society, London, Special Publications, 88(1), 3-19, doi: 10.1144/GSL.SP.1995.088.01.02.
- Sibson, R. H., (2007). An episode of fault-valve behavior during compressional inversion? The 2004 MJ6.8 Mid-Niigata Prefecture, Japan, earthquake sequence. *Earth and Planetary Science Letters*, 257, 188-199.
- Steffen, R., Wu, P., Steffen, H. and Eaton, D.W., 2014. The effect of earth rheology and ice-sheet size on fault slip and magnitude of post glacial earthquakes. *Earth, Plan., Sci., Letters*, 388, 71-80.
- Stuart, J.Y., Huuse, M., 2012. 3D seismic geomorphology of a large Plio-Pleistocene delta - 'Bright spots' and contourites in the Southern North Sea. *Marine and Petroleum Geology* 38, 143-157.
- Svendsen, J.I., Alexanderson, H., Astakhov, V.I., Demidov, I., Julian, A.D., Funder, S., Gataulling, V., Henriksen, M., Hjort, J., Houmark-Nielsen, M., Hubberten, H.W., Ingulfsson, O., Jakobsson, M., Kjer, K.H., Larsen, E., Lokrantz, H., Lunkka, J.P., Lys, A., Mangerud, J., Matiouchkov, A., Murray, A., Muller, P., Niessen, F., Nikolskaya, O., Polyak, L., Saarnisto, M., Siegert, C., Siegert, M.J., Spielhagen, R.W., & Ruedige, S., 2004. Late Quaternary ice sheet history of Northern Eurasia. *Quaternary Sci. Rev.*, 23, 1229-1271.
- Tamisiea M E, Mitrovica J X, Davis J L, Milne G A, 2003. Long wavelength sea level and solid surface perturbations driven by polar ice mass variations: Fingerprinting Greenland and Antarctic ice sheet flux. *Space Science Reviews*, 108, 81-93.
- Ten Veen, J.H., Geel, C.R., Kunakbayeva, G., Donders, T.H., Verreussel, R.M.C.H., 2011. Property prediction of Plio Pleistocene sediments in the A15 shallow gas system. TNO Report TNO-060-UT-2011-01184/C12.
- Ten Veen, J. H., Verweij, J. M., de Bruin, G., and Donders, T., 2014. First Steps Toward Maturing the Shallow Gas Play - Results of an Integrated Exploration Workflow. International Petroleum Technology Conference. doi:10.2523/IPTC-17563-MS.
- Thorson, R.M., 1996. Earthquake recurrence and glacial loading in western Washington. *GSABull.*, 108, 1182-1191.
- Törnqvist, T.E., 2007. Fluvial environment/response to rapid environmental change. In: Elias, S.A. (Ed.), *Encyclopedia of Quaternary Science*. Elsevier, Amsterdam, pp. 686-694.

- Törnqvist, T.E., Wallinga, J., Busschers, F.S., 2003. Timing of the last sequence boundary in a fluvial setting near the highstand shoreline - Insights from optical dating. *Geology*, 31, 279-282.
- Törnqvist, T.E., Wallinga, J., Murray, A.S., De Wolf, H., Cleveringa, P., De Gans, W., 2000. Response of the Rhine-Meuse system (west-central Netherlands) to the last Quaternary glacio-eustatic cycles: a first assessment. *Global and Planetary Change*, 27, 89-111.
- Tzedakis P.C., Channell J.E.T., Hodell D.A., Kleiven H.F., Skinner L.C., 2012. Determining the natural length of the current interglacial. *Nature Geoscience*, 5, 138-141.
- Tzedakis P.C., Raynaud D., McManus J.F., Berger A., Brovkin V., Kiefer T., 2009. Interglacial variability. *Nature Geoscience*, 2, 751-755.
- Van Balen, R., and S. Cloetingh, 1995. Neural network analyses of stress-induced overpressures in the Pannonian Basin. *Geophysical Journal International*, 121, 532-544.
- Van Balen, R.T., Busschers, F.S., and Tucker, G.E., 2010. Modeling the response of the Rhine-Meuse fluvial system to Late Pleistocene climate change. *Geomorphology* 114, 440-452.
- Van den Berg, M., Vanneste, K., Dost, B., Lokhorst, A., Van Eijk, M. & Verbeeck, K., 2002. Paleoseismic investigations along the Peel Boundary Fault: geological setting, site selection and trenching results. *Netherlands Journal of Geosciences / Geologie en Mijnbouw* 81: 39-60.
- Van der Vegt, P., Janszen, A., Moscariello, A., 2012. Tunnel valleys: current knowledge and future perspectives. In: Huuse, M., Redfern, J., Le Heron, D.P., Moscariello, A., Craig, J. (eds.), *Glaciogenic Reservoirs and Hydrocarbon Systems*, Geological Society of London Special Publication, 368, 75-97.
- Van Dijke, J. J. and Veldkamp, A., 1996. Climate-controlled glacial erosion in the unconsolidated sediments of northwestern Europe, based on a genetic model for tunnel valley formation. *Earth Surf. Process. Landforms*, 21, 327-340.
- Van Eck, T., Goutbeek, F., Haak, H., Dost, B., 2006. Seismic hazard due to small-magnitude, shallow-source, induced earthquakes in The Netherlands, *Engineering Geology*, Volume 87 (1-2), 105-121.
- Vandenberghe, J., Renssen, H., Roche, D.M., Goosse, H., Velichko, A.A., Gorbunov, A., Levavasseur, G., 2012. Eurasian permafrost instability constrained by reduced sea - ice cover. *Quaternary Science Reviews* 34, 16 - 23.
- Van Weert, F.H.A., van Gijssel, K., Leijnse, A. and Boulton, G.S., 1997. The effects of Pleistocene glaciations on the geohydrological system of Northwest Europe. *Journal of Hydrology*, 195, 137-159.
- Verweij, J.M., ten Veen, J.H., De Bruin, G., Nelskamp, S.N., Donders, T., Kunakbayeva, G., Geel, K., 2012. Shallow gas migration and trapping in the Cenozoic Eridanos delta deposits, Dutch offshore. Extended abstract. 74th EAGE Conference & Exhibition Copenhagen, Denmark, June 2012.
- Vettoretti G., Peltier W.R., 2004. Sensitivity of glacial inception to orbital and greenhouse gas climate forcing. *Quaternary Science Reviews*, 23, 499-519.
- Vis, G.-J., Verweij, J.M., 2013. Geological and geohydrological characterization of the Boom Clay and its overburden. Report OPERA-PU-4-1-1-TNO.
- Visser, H., (2005). De significantie van klimaatverandering in Nederland. Een analyse van historische en toekomstige trends (1901-2020) in het weer, weersextremen en temperatuurgerelateerde impact-variabelen. Rapport nr 550002007, Milieu- en natuurplanbureau, Bilthoven.
- Waples, D.W. and Waples, J.S., 2004. Review and Evaluation of Specific Heat Capacities of Rocks, Minerals, and Subsurface Fluids. Part 1: Minerals and Nonporous Rocks. Kluwer Academic Publishers-Plenum Publishers, p. 97-122.
- Wildenborg, A.F.B., Orlic, B., de Lange, G., de Leeuw, C.S., Zijl, W., van Weert, F., Veling, E.J.M., de Cock, S., Thimus, J.F., Lehen-de Rooij, C., and den Haan, E.J., 2000. Transport of Radionuclides disposed of in clay of Tertiary ORigin (TRACTOR), NITG 00-223-B.

- Wingfield, R.T.R., 1990. The origin of major incisions within the Pleistocene deposits of the North Sea. *Marine Geology*, 91, 31-52.
- Yin Q.Z., Berger A., 2010. Insolation and CO₂ contribution to the interglacial climate before and after the Mid-Brunhes Event. *Nature Geoscience*, 3, 243-246.

|

Appendix 1

Report SCK-CEN-R-5848 - Numerical simulation of Permafrost depth in the Netherlands

|

OPERA

Meer informatie:

Postadres
Postbus 202
4380 AE Vlissingen

T 0113-616 666
F 0113-616 650
E info@covra.nl

www.covra.nl

